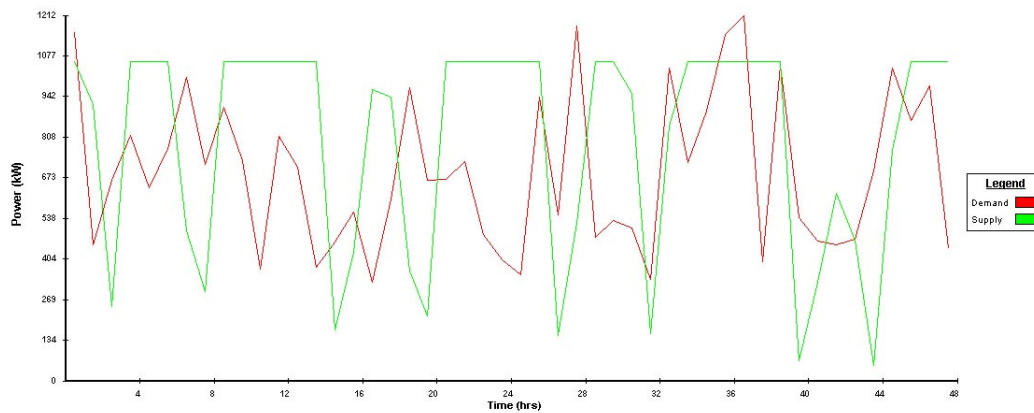


# Tidal Current Turbine Farms in Scotland:

## A Channel Model Approach to Determine Power Supply Profiles and the Potential for Embedded Generation

By Scott Love



A Thesis for the Degree of MSc in Energy Systems  
& the Environment

Department of Mechanical Engineering  
University of Strathclyde

2005

### **Copyright Declaration**

The copyright of this dissertation belongs to the author under the terms of the United Kingdom Copyright Acts as qualified by University of Strathclyde Regulation 3.49. Due acknowledgement must always be made of the use of any material contained in, or derived from, this dissertation.

## **Acknowledgements**

Primarily I would like to thank Dr Paul Strachan for his supervision of this thesis and for his sound guidance throughout the entire process. His help in the differentiating my use of the “astronomical” from the “astrological” and the “complimentary” from the “complementary” was invaluable at times.

My thanks also go to Dr Andrew Grant and Mr. Cameron Johnstone for their insight into all matters marine and renewable, as well as for an invaluable experience gained from the 2005 EWTEC Conference.

Gary Connor was also a source of help at various times, with knowledge from the developer’s perspective as well as from a policy stance.

I owe Jun Hong and Jae-min Kim a great debt of gratitude for their immense help with the MERIT implementation phase.

Not least, I would also like to thank my family and friends for their help and continued support during the writing of this thesis.

Finally I would like to thank Janet Harbidge for all her great help throughout the course.

## **Abstract**

Tidal Current Turbines make use of largely proven technology from the vast experience of wind power. Much research has been carried out to provide methods for estimating the potential energy resource of wind farms. However, to date there has been a distinct lack of simple and accessible models for the appreciation of energy output from tidal current turbine farms.

This thesis presents a simple working model for determining the output of farms of these devices operating in open channels, in a bid to assess their potential or otherwise for matching local demand either autonomously or in parallel with other forms renewable generation.

There are many different software packages currently available with the ability to perform supply demand matching for the well established renewable forms of generation such as wind, hydro, CHP\*, biomass and solar heating and solar PV. However, none of those existing packages provides an option for tidal current turbines.

This thesis utilised a basic hydrodynamic channel approach in conjunction with a harmonic method for the influence of the tides to estimate the power output of a farm of tidal current turbine devices situated in an open channel.

The model employed a number of empirical correction factors and improvements to encapsulate some of the reality behind the true behaviour of tidal current velocities in such a channel.

The model was implemented into a software package for supply/ demand matching. Furthermore, a case study was carried out for the island of Islay on the West coast of Scotland to assess the potential of an embedded generation approach to farms of these devices within Scotland's electricity grid.

\* CHP is not strictly a renewable resource but is useful in complementing renewables as it has significant carbon saving benefits.

## Table of Contents

<b>1</b>	<b><i>Introduction</i></b>	<b>11</b>
1.1	<b>The Importance of Renewable Energy</b>	<b>12</b>
1.2	<b>Potential Pitfalls of Renewable Energy</b>	<b>13</b>
1.3	<b>The Significance of Marine Energy</b>	<b>15</b>
1.4	<b>The Role of Tidal Energy</b>	<b>15</b>
1.5	<b>Scotland's Position</b>	<b>17</b>
1.6	<b>Opportunities for Embedded Generation as Opposed to Transmission Grid-Connected Strategy</b>	<b>18</b>
1.7	<b>Analogy with Large Scale Hydro to Micro-Hydro Power Plants</b>	<b>19</b>
1.8	<b>The Need for a Channel Model</b>	<b>21</b>
1.9	<b>Thesis Objectives &amp; Methodology</b>	<b>22</b>
<b>2</b>	<b><i>A Review of Marine Renewable Generation in Scotland</i></b>	<b>25</b>
2.1	<b>Energy Supply Strategies for Marine Renewables in Scotland</b>	<b>25</b>
2.1.1	A Brief Review of Scotland's Electricity Network	25
2.1.2	Base-load Electricity Supply Strategy for Marine Renewables	28
2.1.3	Grid Connection & Extension Issues	29
2.1.4	Embedded Generation	30
2.1.5	Energy Storage as an Option	32
2.1.6	Use of Complementary Forms of Generation	33
2.2	<b>Supply Demand Matching Techniques</b>	<b>34</b>
2.2.1	Definition of and Main Uses	34
2.2.2	Software Tools for Comparison of Supply & Demand Profiles	34
2.3	<b>Tidal Currents</b>	<b>37</b>
2.3.1	Definition and Application	37
2.3.2	Tidal Current Energy Extraction Devices	37
2.3.3	Advantages of Tidal Current Over Other Forms of Renewables	41
2.3.4	Drawbacks of Tidal Current Power	42
2.3.6	Variability of Tidal Current Velocity	43
2.4	<b>Modelling the Assessment of Tidal Current Behaviour &amp; Energy Extraction</b>	<b>46</b>
2.4.1	CFD Models	46
2.4.2	Admiralty Tidal Diamond Data (ATD)	46
2.4.3	Proudman Oceanographic Laboratory Method (POL)	48
2.4.4	Tide 2D	48
2.4.5	Bryden/ Couch Model (1-D Channel Analysis)	49
2.4.6	Full Harmonic Analysis of a 30 Day Tidal Record	51
2.4.7	Double Cosine Method (Fraenkel)	56
2.4.8	Tidesim	57
2.4.9	Previously Developed Channel Model	57
2.4.10	Comparison & Summary of Models	65
<b>3</b>	<b><i>Development of Enhanced Channel Model Algorithm</i></b>	<b>67</b>

<b>3.1</b>	<b>Modelling of Astronomical Variations</b>	<b>69</b>
<b>3.2</b>	<b>Accounting for Local Non-Astronomical Variations</b>	<b>76</b>
3.2.1	Depth, Width and Roughness of Channel	77
3.2.2	Packing Density of MCT devices in the flow	82
3.2.3	Blockage Effect of Placing MCT's in a Channel	82
3.2.4	Ebb and Flood Differences	83
3.2.5	Directionality of Flow	84
3.2.6	Accelerated and Retarded Flow Rates at Site of Energy Extraction	85
<b>3.3</b>	<b>Turbine Performance Details &amp; Channel Solidity</b>	<b>89</b>
<b>3.4</b>	<b>Pseudocode for Enhanced Channel Model Algorithm</b>	<b>91</b>
<b>3.5</b>	<b>Implementing the Model – An Example</b>	<b>96</b>
<b>3.10</b>	<b>Adaptation of Model to MERIT</b>	<b>105</b>
<b>4</b>	<b><i>Case Study - Islay</i></b>	<b><i>114</i></b>
4.1	Local Geography & Demographic of Islay	115
4.2	Domestic Dwellings	119
4.3	Agricultural	119
4.4	Industrial (Distilleries)	120
4.5	Combining Supply Profiles to Improve Matching Capability	122
4.6	Combining Demand Profiles to Improve Matching Capability	131
4.7	The Use of Storage to Improve Matching Capability	132
4.8	The Use of Demand Side Management (DSM) to Improve Quality of Matching	133
4.9	Auto Search Facility on MERIT for Best Match Scenario	134
<b>5</b>	<b><i>Conclusions</i></b>	<b><i>136</i></b>
5.1	Enhanced Channel Model	136
5.2	Autonomous Versus Network Grid Connected Strategy	137
5.3	Conclusions from Case Study	137
5.4	Replication of Channel Model to Other Locations	138
<b>6</b>	<b><i>Recommendations &amp; Further Work</i></b>	<b><i>140</i></b>
	<b><i>Glossary of Terms</i></b>	<b><i>141</i></b>
	<b><i>References</i></b>	<b><i>142</i></b>

## Index of Figures

Figure 1	Interconnected UK Grid System	Page 26
Figure 2	Scotland's Transmission Network	Page 27
Figure 3	UK Population Concentration	Page 29
Figure 4	Schematic of Voltage Levels from Distributed to Transmission Grid	Page 30
Figure 5	Architecture of Embedded Generation	Page 31
Figure 6	Rotor Concepts for Tidal Current Turbines	Page 39
Figure 7	Seaflow Prototype by MCT Ltd.	Page 40
Figure 8	Twin Rotor Design from MCT Ltd.	Page 41
Figure 9	Spring/ Neap Cycle	Page 45
Figure 10	ATD Data	Page 47
Figure 11	Channel Model, Side View & Top View	Page 58
Figure 12	Input of Harmonic Constants to Enhanced Channel Model	Page 70
Figure 13	M2 Constituent for Aberdeen	Page 70
Figure 14	M2+S2 Constituent for Aberdeen	Page 71
Figure 15	M2+N2+S2 for Aberdeen, showing Perigean Spring Tides	Page 72
Figure 16	7 Major Constituents for Aberdeen (Jan 2001)	Page 72
Figure 17	Comparison of Predicted Data with Measured Data for Aberdeen Jan 2001	Page 73
Figure 18	Linear Regression Analysis of Data for Aberdeen Jan 2001	Page 74
Figure 19	Comparison of Predicted Data with Measured Data for Rona Jan 2001	Page 75
Figure 20	Linear Regression Analysis of Data for Rona Jan 2001	Page 75
Figure 21	Predicted Tidal Heights for 2 Ports Either Side of Channel	Page 76
Figure 22	Schematic for channel dimensions & bathymetry	Page 78

Figure 23	Hydraulic Radius	Page 79
Figure 24	Comparison of 3-d stream-wise flow development with varying levels of energy extraction layer integrated velocity for $\sigma$ -layer 5	Page 87
Figure 25	Channel Model Schematic with Reference Axes	Page 87
Figure 26	IF Condition for Rated and Cut-in Conditions	Page 89
Figure 27	Channel Model Input Module for Turbine Loss Coefficient Or Blockage Factor	Page 90
Figure 28	Flowchart for Pseudocode of Channel Model Algorithm	Page 91
Figure 29	Sample from Admiralty Tidal Stream Atlas NP206	Page 96
Figure 30	Comparison of Spring Tide Data	Page 97
Figure 31	Linear Regression Analysis of Spring Tide Data	Page 98
Figure 32	Comparison of Neap Tide Data	Page 99
Figure 33	Linear Regression Analysis of Neap Tide Data	Page 100
Figure 34	Raw Power Available to a 50 unit MCT farm in Pentland Firth over 1 month	Page 101
Figure 35	Raw Power Available to a 50 unit MCT farm in Pentland Firth over 1 year	Page 101
Figure 36	Comparison of Available Power with Turbine Power Output	Page 102
Figure 37	True Power Output for 1 Month	Page 102
Figure 38	Channel Model Metrics Showing Capacity Factor for 50 MCT Farm	Page 103
Figure 39	Full channel Model User Interface	Page 104
Figure 40	Channel Model Implemented to MERIT as Tidal Interface	Page 106
Figure 41	Tidal System User Interface	Page 106
Figure 42	Tidal Turbine User Interface	Page 107
Figure 43	Matching of MCT Supply Profile Against Islay Total Demand	Page 104

Figure 44	Failure to Capture Slack Tides for 1 Hour Time steps	Page 109
Figure 45	Power output from Channel Model at 10 Minute Resolution	Page 110
Figure 46	Maxima for Spring Tides Rona	Page 110
Figure 47	Maxima for Spring Tides (Aberdeen)	Page 111
Figure 48	Undisturbed Flow Velocity in Pentland Firth for 2001	Page 113
Figure 49	Total Electrical Demand for Islay	Page 114
Figure 50	Map of Islay	Page 115
Figure 51	Islay Grid	Page 116
Figure 52	Map of Sound of Islay	Page 117
Figure 53	True Power Output for a Single 15m Diameter dual rotor MCT for 1 Month Duration	Page 118
Figure 54	Total Electrical Demand from all Domestic Dwellings on Islay	Page 117
Figure 55	Total Agricultural Demand on Islay	Page 120
Figure 56	Islay's Distilleries	Page 120
Figure 57	Total Electrical Demand from all Distilleries on Islay	Page 121
Figure 58	Electrical Demand from Ardbeg Distillery	Page 122
Figure 59	Electrical Demand from Bowmore Distillery	Page 122
Figure 60	Islay Total Electrical Demand against 6xMCT Farm Output	Page 123
Figure 61	Port Askaig Total Electrical Demand against 1xMCT Farm Output	Page 123
Figure 62	Residual from 6 1.3MW Bonus Wind Turbines against Total Demand for Islay (1Year)	Page 127
Figure 63	Combinations of Demand Profiles	Page 131
Figure 64	Best Match from Auto Search Facility	Page 135

### Index of Tables

Table 1	Scotland's Generating Sites	Page 25
Table 2	HW and LW time and heights for Aberdeen in Jan 2001 as given by Admiralty Tide Tables	Page 54
Table 3	Angular Velocities of Each Tidal Constituent	Page 58
Table 4	Summary of Models	Page 65
Table 5	Harmonic Constants for Aberdeen (from Admiralty NP 201-06)	Page 59
Table 6		Page 88
Table 7	Comparison of Channel Model Data and Tidal Stream Atlas Data for Spring Tide Conditions	Page 97
Table 8	Daily Matching Analysis of Supply Option Ensemble	Page 124
Table 9	Monthly Matching Analysis of Supply Option Ensemble	Page 125
Table 10	Yearly Matching Analysis of Supply Option Ensemble	Page 126
Table 11	Minimal Benefit of adding 50,000 x 100W Poly South PV Panels to a combination of supply from 3 MCT's and 3 Wind Turbines	Page 129
Table 12	Scenarios for Wind, MCT Combinations – Yearly Matching	Page 130
Table 13	Results of Matching All Supply and Demand Combinations	Page 132
Table 14	Storage Options for Scenario 3	Page 133
Tables 15-17	DSM Options for Scenario 3	Page 133
Table 19	Results of MERIT Auto Search Facility	Page 134

## 1 Introduction

The need for renewable generation is becoming increasingly important on a global scale as most of the developed World attempts to address the problems of climate change and fossil fuel depletion. Added to this, at least in the context of the UK, is the issue of security of supply. Indeed, the increasing reliance on imported gas and oil from potentially unstable regions of Europe and the Middle East means that more attention is being placed on renewables, which of course are a home-grown resource and introduce much in the way of more secure forms of energy supply.

On a more local scale, the UK and in particular Scotland has been identified as possessing significant resource in tidal energy; with areas such as the Pentland Firth, Yell Sound, the Sound of Islay and Kyle Rhea being identified as particularly abundant in such resources [1]; offering the potential for large scale marine current turbine farms. Unfortunately the remoteness of these locations means that they are some distance from the nearest HV transmission network and so the potential for grid connection is understandably limited. One obvious solution could be to extend the HV transmission lines to reach those remote locations. However this is both costly and disruptive to miles of countryside, leading to vociferous opposition from some stakeholders and organisations and posing the serious question as to who will meet the cost.

A viable alternative is to restrict the output of such tidal farms to the distribution network in an attempt to meet the local electrical demand of communities in close proximity. Many concessions will have to be made, primarily, concerning the variability of the output particularly during slack tides and throughout the year with spring and neap tides [2].

However, a method of using other forms of renewable energy as well as conventional generation could allow these gaps and periods of lower output to

be filled. Demand side management could also provide a solution, albeit less desirable in current society.

### ***1.1 The Importance of Renewable Energy***

There is an emerging market for renewable generation of electricity; almost directly as a result of some governments of the developed World facing up to the threats posed by climate change and dwindling fossil fuel reserves.

The UK Government has signed the Kyoto Protocol. The Government's Climate Change Programme set out its proposals for meeting its target of a 12.5 per cent reduction in greenhouse gas emissions, under the Kyoto Protocol and EC Member States agreements, in the period 2008-2012. [3]

Renewable energy is an integral part of the Government's long-term aim of reducing CO<sub>2</sub> emissions by 60% by 2050. The Government has set a target of 10% of electricity supply from renewable energy by 2010. [3]

In 2003, approximately 2.7 per cent of the total amount of electricity in the UK came from renewable sources [3]

In April 2002, the Government introduced the Renewables Obligation, which requires all licensed electricity suppliers in England and Wales to supply a specified and growing proportion of their electricity from renewable sources, and provides financial incentives for them to do so. In Scotland, the Renewables Obligation (Scotland) performs the equivalent function. Scotland can already boast to produce around 12% of its total electricity generation from renewables. [3]

Having established a moral and indeed practical requirement that renewable energy be developed to provide carbon-free sources of energy, the question arguably now became; which of these technologies would provide the best option for widespread deployment?

## **1.2 Potential Pitfalls of Renewable Energy**

### Over-dependence

From the experience of Denmark and Germany who began building large numbers of on-shore wind turbine farms from the 1970's onwards, a lesson of over-dependence on one type of renewable generation should be heeded. [4]

### Saturation of land Area and Stakeholder Objection

In terms of feasible sites for on-shore wind, there could be a situation in the future in which a "saturation point" will be reached. This point has still not been reached, at least not in terms of physical land capacity.

Of course, installing wind farms out from the UK coastline is a viable alternative and indeed can yield slightly higher output from increased wind speed out to sea. However, the same underlying problems of intermittency still apply with off-shore wind farms.

Whilst there may yet be many sites in Scotland which are physically suited to the development of wind farms, the far wider problem of public opposition continues to be the deciding factor. The proposed Edinbane wind farm on Skye is a prime example of this, where developers AMEC had the proposal agreed by local council only to have the whole program put in jeopardy by the objections of only a small but vocal minority of the local community. [5]

The argument of the opposition group SWAG is broad and in many aspects is flawed from a technical sense. Much of their opposition seems to be based on

aesthetic factors [6] and however much renewable energy developers would like to be given a free reign, a concession must be made that ultimately in a democratic society it is very often public opinion which prevails and not the net benefits if viewed from a wider perspective.

### **Power quality**

However, there is another side to the oppositional body to wind farm projects; that of the quality of power they produce, in terms of the impact on baseload thermal power stations which will have to increase or decrease their output depending on the wind velocity at those wind farms.

This has led a number of opponents of wind power to suggest that if a large proportion of Scotland's electricity generation came from wind farms, then should either very low or very high winds occur simultaneously at the majority of its wind farms, output could fall drastically thus requiring the base load thermal power stations to increase output rapidly. [7]

This intermittency of the wind resource can lead to uncertainty of supply. This uncertainty is not good for efficiency of a thermal power station which may have to act in a back-up capacity; since having to continuously vary power output does not make for ideal operating conditions and can increase CO<sub>2</sub> emissions during operation.

### **Capacity Factor**

Capacity factor is the energy produced during a certain period divided by the energy that would have been produced had the device been running continually and at maximum output for the same period of time.

This parameter will essentially determine much of the economical effectiveness of any generation plant, renewable or non-renewable.

Capacity factors of successful wind farm operations range from 0.20 to 0.35. These can be compared with factors of more than 0.50 for fossil-fuel power plants and over 0.60 for some of the new gas turbines. [8]

In the context of renewable generation, care should be taken to maximise the capacity factor in order to reduce costs. However it can also be argued that lowering the capacity factor is conducive to better base load matching, especially over the lunar cycle [24].

### ***1.3 The Significance of Marine Energy***

There are clear advantages to any form of renewable energy which does not exhibit undesirable features such as intermittency of power output, low capacity factor and dependence on weather conditions and requirement for duplication of generation capacity.

It could be argued that marine power exhibits significantly less of these undesirable constraints and therefore is an extremely viable form of renewable energy [9]. There is also a vast marine energy resource available in UK waters and particularly in Scotland [1].

Additionally, Scotland also possesses the expertise from the offshore and oil industries which could be harnessed, with many transferable skills that could be easily applied to marine renewable energy projects.

### ***1.4 The Role of Tidal Energy***

It is widely considered that of all the marine renewable energy industries, tidal energy is the closest to commercial viability [10].

With the density of water significantly greater than that of air (approx 1000:1), even relatively small current velocities can produce a large power output. Care has to be taken though to be conservative and realistic when estimating the power capacity of any particular site, as many other factors, not least channel blockage and conflicts with fishing and merchant vessels, will greatly reduce the theoretical maximum power capacity to a more realistic and conservative value. The gross and misleading initial estimates of the power capacity for the Pentland Firth are a perfect example of this.

“The potential Scottish resource is approximately 85 TW hr per annum. The Pentland Firth has been described as the Saudi Arabia of tidal current power”[11]

Such outlandish claims like this are unhelpful for the sustained and sensible development of the industry as well as stability for investors.

Academics like Ian Bryden with a proven history in the field, are imposing a degree of realism to the subject area, which is much better for giving realistic projections for investors and allowing a more stable and sustainable approach to the growth of the industry in Scotland and elsewhere. He, amongst others, has helped to curb the outlandish claims made initially regarding tidal resource.

The pre-commercial status of the marine current turbine industry is also a factor when considering its merits against other marine renewable industries.  
[10]

Wind power will continue to be the leader in the renewable energy markets due to its firm and established track record since the late 70's.

## **1.5 Scotland's Position**

Scotland has been identified as possessing a considerable marine energy resource. [12]

The Marine Energy Group (MEG) of the Forum for Renewable Energy Development in Scotland (FREDS) released a report [13] in 2004 which identified that by the year 2020:

- 10% of Scotland's Energy Production can come from Marine Energy
- Installed capacity could exceed 1.3 GW
- Scottish based marine energy companies could be supplying major international export markets
- 7,000 jobs could be created
- Scotland should lead the way in the R&D and certification of marine energy devices

It could be argued that Scotland is in a similar situation now to that of Denmark in the 1970's with their wind power industry.

Scotland is ideally placed to mimic the Danish success story with many of the World's leading academics and experts in wave and tidal energy resident in the UK. Aside from the energy issue there is a considerable potential to export technology worldwide and become a World leader in marine energy technology.

Benefits to the national economy will result from the creation of an export economy and a skilled jobs market.

## ***1.6 Opportunities for Embedded Generation as Opposed to Transmission Grid-Connected Strategy***

With much of Scotland's marine energy resource being located in very remote areas of the country, any proposed farm of marine renewable devices would either be some distance from the nearest HV transmission network or the existing network would not be compatible with a large flux of power to the network.

This greatly limits the potential for large scale deployment of marine renewable devices in such areas.

It could be, however, that the wrong approach is being pursued and instead of attempting to maximise the power output in order to supply to the national grid via the transmission network some engineers and scientists argue that limiting the power output to a level which could be used locally via embedded generation would have a number of benefits;

- There would be no need for the extension and/or upgrade of transmission lines to the area which is both costly and damaging to the countryside
- A much higher capacity factor will result from operating a lower rated power and achieving the rated power more frequently for any given site
- The cost of the project will be kept down by the higher capacity factor and without the considerable costs of transmission line extension/upgrade
- There could be a potential for community part or full ownership of the project

Many concessions will have to be made, primarily, concerning the variability of the output [14]. However, a method of using other forms of renewable energy as well as conventional generation could allow these gaps and periods of lower output to be catered for.

### ***1.7 Analogy with Large Scale Hydro to Micro-Hydro Power Plants***

Given the argument for restricting output to local needs as opposed to maximising output for grid connection, an analogy can be drawn with the experience of micro hydro power plants.

Large scale hydro power plants such as Cruachan power station are crucial elements to the power generation strategy of Scotland's electricity grid, where the operators Scottish Power are able to use the pumped storage facility to increase power to the grid within seconds of a significantly increased demand being made.

There are also smaller scale hydro power facilities such as the two stations on the River Clyde at Lanark Hydro Electric Scheme, which do not attempt to export large amounts of power to the national grid but are able to meet local demands more readily.

The stations, Bonnington (output 11 MW) and Stonebyres (output 6 MW), were developed by the Clyde Valley Electrical Power Company to satisfy a growing demand for electricity after the First World War.

They harness energy from three waterfalls - Bonnington Linn, Corra Linn and Stonebyres Linn, known collectively as the "Falls of Clyde".

Instead of a dam, an ingenious tilting weir regulates the river to maintain, within specified limits, a "head" at the tunnel intake.

### When is hydropower micro?

The definition of micro hydropower varies in different countries and can even include systems with a capacity of a few megawatts. One of the many definitions for micro hydropower is: hydro systems up to a rated capacity of approximately 300 kW. The limit is set to 300 kW because this is about the maximum size for most stand alone hydro systems not connected to the grid, and suitable for "run-of-the-river" installations. [15]

Micro hydro, or small-scale hydro, is one of the most environmentally benign energy conversion options available, because unlike large-scale hydro power, it does not attempt to interfere significantly with river flows. [15]

This demonstrates an intelligent use of resources, where the power output is limited somewhat with the pursuit of a more modest but cost effective power supply strategy and where the energy extraction is not deemed to interfere significantly with the resource.

There are strong parallels here with small scale deployment of MCT units as opposed to large scale farm deployment where the tidal current velocity may be detrimentally affected by excessive energy extraction.

Adding this to the additional constraint of conflicts with marine wildlife, fishing vessels, MOD and coastguard, it could be argued that as with micro hydro, where the power take-off is sensible and unlikely to affect the resource itself and interfere with the environment or other users of the waterway, so small scale deployment of MCT's for embedded generation, should be promoted against the large scale grid-connected strategy.

## **1.8 *The Need for a Channel Model***

After researching the subject matter of tidal current energy extraction devices it became increasingly apparent to the author that there was a pressing need for a simple way to estimate electrical output from a tidal current turbine farm.

Some models do currently exist, each with its respective merits and limitations. However, it was apparent that most of these existing models were complex in nature and did not allow for repeatability at different sites with any real degree of ease.

A previously developed model [10] was identified as a suitable medium to bridge this gap between demand for a much simpler repeatable model and the existing complex models already available.

A conclusion had been reached that the channel model in question [10] was deemed to be physically correct in principal; however it need much in the way of improvement to ensure a higher degree of realism.

In particular, the model only considered spring tide conditions; a concession made by the original developers and justified by highlighting that the analysis was done at “best case scenario”.

Admittedly, for a more rigorous and realistic model, this over simplification would need to be addressed. Indeed a number of variables and other important factors would need to be accounted for in any improvement of the model. This will be dealt with in more detail in section 3.

## **1.9 Thesis Objectives & Methodology**

This thesis discusses the options which exist for marine current energy extraction modelling and what methods could be developed to support this strategy. A case study approach was adopted, in which data on electrical demand for the Scottish island of Islay was compared with predicted supply profiles from MCT farms situated in the immediate region of the island.

A supply/ demand matching analysis was carried out using renewable energy supply & demand software. In order to produce valid data for the electrical supply profiles of the MCT farms, an improved channel model was developed and radically improved to include temporal variations, which takes into account spring/ neap variations, as well as slack tide, difference in energy hot spots depending on ebb and flow conditions, effects of energy extraction and lastly local influences such as channel width and depth and position of the devices in the water column.

The project also highlighted the benefits of tidal energy in terms of the ability to predict with a good degree of accuracy the resource at a certain point at any given time. Tidal energy has huge potential advantages over other renewable forms of generation such a wind, which can be intermittent and unpredictable; therefore requiring duplication of generation capacity in many cases. The use of a tidal current turbine farm would mostly avoid the additional costs associated with duplication of generation due to better predictability of electrical output.

However it should be noted that tidal current turbine farms would not entirely avoid the problems of intermittency. Indeed the amount of energy which can be extracted from any given location at any point time will vary greatly depending on position in the diurnal cycle, with large differences between spring and neap output. The degree of intermittency will however, be significantly less severe than is the case with wind power, and can be

potentially overcome by the clever use of complementary renewable and conventional generation.

Crucially for tidal current energy, however, the intermittent periods can largely be predicted from tidal modelling; thereby allowing other renewable or conventional generation (i.e diesel generators) or use of storage to be initiated in advance of these periods.

This subject of intermittency was dealt with in two distinct and separate sections; section 3.1 and sections 3.2-3.7 respectively.

Firstly, the variation due to spring neap cycle, diurnal cycle and slack tides will be considered; in other words the astronomical phenomena.

Secondly, the local variations due to channel width and depth, bottom roughness, ebb flow differences, effects of energy extraction, position of the devices in the water column and lastly the influence of weather fronts and pressure variations.

Objectives- The objectives of this thesis were to:

- Enhance a previously developed channel-based model to provide a more realistic representation of tidal current velocity
- Identify variations inherent in the daily, monthly and yearly cycles of the astronomical tide producing forces
- Carry out a supply/ demand matching analysis using the supply profiles generated by the channel model against demand profiles for a case study community in close proximity to the proposed tidal current turbine farms.
- Comment on the effectiveness of the model and its usefulness in providing supply profiles for renewable energy planner activities and software such as MERIT

## **Methodology**

The methods used were as follows:

- Extend and improve the model to include more astronomical effects as well as local variations in tidal current velocity; thus producing a more realistic and accurate algorithm
- Implement into Merit to allow supply/ demand matching analysis
- Reach general conclusions on using output locally on the distributed grid as opposed to the HV network grid
- Provide more specific conclusions regarding the site investigated in the case study section

## 2 A Review of Marine Renewable Generation in Scotland

### **2.1 Energy Supply Strategies for Marine Renewables in Scotland**

#### **2.1.1 A Brief Review of Scotland's Electricity Network**

Power generation in Scotland is dominated by 3 major companies; Scottish Power, Scottish and Southern Energy and British Energy.

The main generating sites in Scotland are:

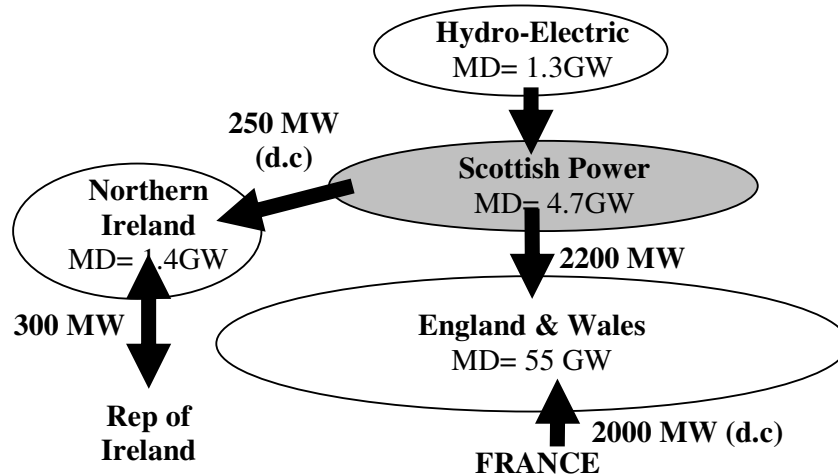
**Table 1 Scotland's Generating Sites**

<b>Station</b>	<b>Company</b>	<b>Capacity</b>	<b>Fuel</b>	<b>Commissioning/ Likely Closure</b>
Cockenzie	Scottish Power	1,200 MW	Coal	1967 / 2010
Longannet	Scottish Power	2,304 MW	Coal	1970 / 2020-25
Hunterston B	British Energy	1,150 MW	Nuclear	1976 / 2011
Torness	British Energy	1,250 MW	Nuclear	1988 / 2011
Peterhead	Scottish and Southern Energy	2,500 MW	Gas	1980 / 2030+
Chapelcross	BNFL	196 MW	Nuclear	1959/ Likely to be renovated for biomass

Since there are relatively few central power sources and many users at considerable distance from those sources, then a grid system for transmission of electricity must be implemented. To reduce losses in the transmission lines, the current is transformed from DC to AC and stepped up to a higher voltage.

The transmission system in the U.K is similar to many others throughout the world. In Scotland the network is connected to the much larger national grid system by 400kV, 275kV and 132kV circuits. This allows interconnectivity to and from and other regions in the U.K and Western Europe. This is illustrated in fig. 1.

**Figure 1 Interconnected UK Grid System (Values for 1999) [16]**



A notable observation from Figure 2 is that currently there are no significant high voltage (HV) “supergrid” transmission lines in the North West of Scotland. This will have implications for any renewable facilities being set up in that region. The reasons for this are fairly simple and can be attributed to the locations of the major power stations in Scotland

Scotland also exports electricity to Northern Ireland via the Moyle Subsea Interconnector which comprises a 275kV AC transmission line and a High Voltage Direct Current (HVDC) line. This allows Scottish power companies access to the retail markets in both Northern Ireland and the Republic of Ireland. It is clear that there is also a 400kV transmission line linking the Scottish network to England and Wales and effectively to France and the rest of the Western European systems. This is a vital piece of infrastructure if excess electricity production from new renewable energy sources in Scotland is to be given access to other markets in the UK and Europe.



### **2.1.2 Base-load Electricity Supply Strategy for Marine Renewables**

Base-load generation is the method of generating power at a level which is as constant as can be achieved. This baseload will supply the majority of a country's overall electrical demand. The powerplants designed for baseload supply are designed to run at a constant output. This allows for high efficiency to be achieved in the turbines of the thermal power stations which act as the backbone of the electrical supply to the UK national grid. Any fluctuations or rapid increases in electrical demands are generally handled by CCGT which have a greater ability to increase or decrease power output within a very short period of time. In Scotland and Wales the use of pumped storage is also an extremely valuable resource whereby essentially "cheaper" electricity generated by thermal power station at night is used to pump water to an elevated height, thereafter enabling an on-demand resource which can be put to the grid within minutes.

Since the majority of Scotland's electrical demand is met by base-load generation, with more readily controllable forms of generation such as CCGT and pumped storage (hydro), it goes without saying that regardless of how much renewable generation is promoted and seen to be environmentally friendly, the country must continue to operate a reliable mix of base-load power stations. In the future this will most likely continue to be provided by thermal power stations, be it coal, gas and oil or newly built nuclear power stations to replace the rapidly ageing ones conceived in the 50's and currently still in operation.

Some scientists and engineers however, have investigated into the possibility of using renewable forms of energy to provide this future base-load of supply.

Wind energy, whether offshore or onshore, is considered by some to be too stochastic and intermittent to merit base-load use [17]

Base-load Electricity supply strategy for tidal current turbines is another option which has been considered. The idea is based on using 3 separate sites whose tidal output is out of phase; the aggregate output being of constant 3-phase supply identical to that produced from the generators of conventional thermal power stations. [17]

### 2.1.3 Grid Connection & Extension Issues

**Figure 3 UK Population Concentration [1]**



Currently in Scotland there is a pronounced concentration of the country's population around the central belt and consequently the further North one travels, the lesser the extent of the HV transmission grid. The major exception is a single HV transmission line to the location of the old Dounreay nuclear power station.

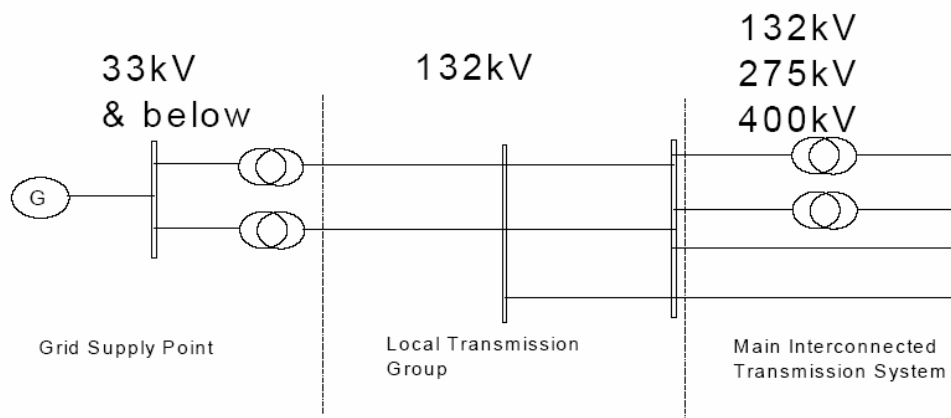
This bodes well for any large scale deployment of MCT's in the Pentland Firth as such a large scale farm could conceivably be connected to this HV line. However it is the region of Scotland's West Coast and the Hebridean islands

which pose the most significant problems for network grid connection of large scale MCT farms since in those regions there is no HV network coverage.

*“The difficulties of Grid connections are probably the single most serious problem facing the successful exploitation of wave and tidal energy in the UK, and one which no single company can solve alone” [17]*

#### 2.1.4 Embedded Generation

Figure 4 Schematic of Voltage Levels from Distributed to Transmission Grid



The predicted growth in renewable energy schemes has implications for the existing electricity network; which would be required to connect a large number of smaller schemes (termed distributed generation), often in remote areas where the capacity to absorb and or transmit electricity is limited.

One potential solution would be to invest significant funds in upgrading the existing infrastructure to bypass transmission bottlenecks. In addition to the impact of distributed generation on the operation of the transmission and distribution network, there is the additional issue of the eventual closure of the existing large generation stations, most of which are coastal. Thus the existing transmission system is designed to accept large injections of electricity at planned geographic positions. The expected increase in development of

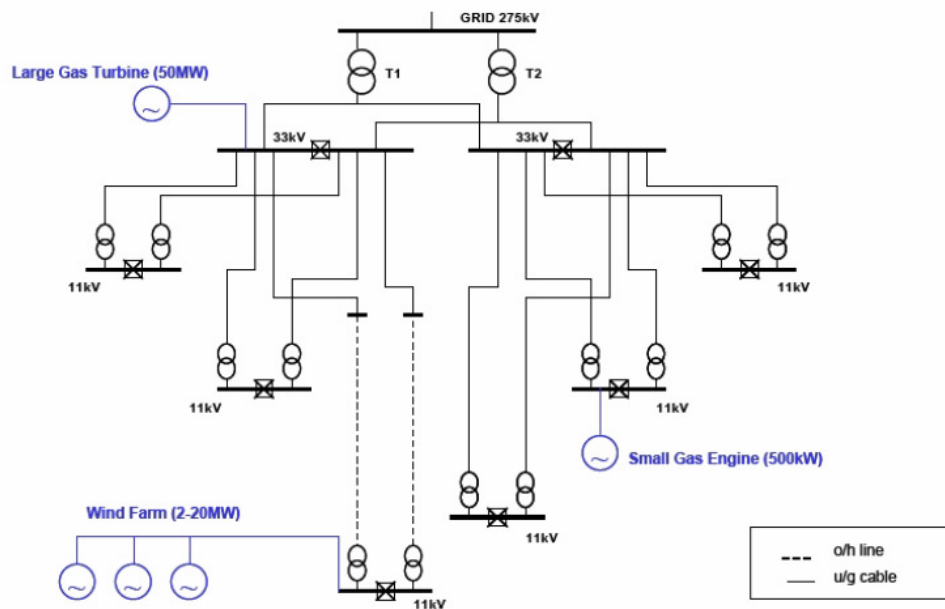
distributed generation means that there will be a need to adapt the electricity grid to cope with the change in the pattern of generation in Scotland.

Embedded generation is the strategy of supplying electrical power to the distribution network (<132kV). Employment of this strategy has particular benefits for community wind farms, large scale CHP and now potentially for MCT farms or farms of wave power devices. [18]

The architecture of some examples of embedded generation is shown in Figure 5.

**Figure 5 Architecture of Embedded Generation [21]**

# Embedded Generation



The main advantages of opting for embedded generation for marine renewable forms of power production are that:

- Power can be delivered to distribution network to meet local demand, thus negating the need for large, expensive and costly transmission

lines and GSP's which are unlikely to be currently in place given the remoteness of most locations of significant marine energy resource.

- No significant current losses will occur from transmitting electrical energy over long distances

The main drawbacks are that

- The marine energy resource available may be far greater than the demand from all the communities within the distribution network. Thus there may be an opportunity for producing energy on a much larger scale which will be missed simply due to logistics and an insufficient electricity network
- Additionally, any MCT farm will most likely be operated at well below the maximum power output for the turbine units comprising the farm, in order to ensure a high capacity factor and hence low costs. This is a sensible approach financially speaking but serves to highlight the inherent waste of much of the available energy from restriction to the "small scale" approach at any particular site.
- This may have additional impacts on the economics and commercial viability of MCT farms, as economies of scale for large batch production as well as the benefits of exporting significant energy amounts to the national grid and ability to earn ROC's\* could potentially be lost through limiting output to the distribution grid.

### **2.1.5 Energy Storage as an Option**

Embedded generation of MCT farms and indeed other renewables can lead to problems in terms of matching supply and demand. Since the amount of power produced is a function of the resource availability over time, there will inevitably be periods where the supply falls short of the demand. Equally, there will be instances where the supply over-shoots the demand. In both cases, the use of storage would act to smooth these residual excesses and deficits.

\*ROC's are renewable obligation certificates, explained in [35]

The most common form of storage is in batteries (usually lead-acid for power applications) used in conjunction with an inverter.

Flywheels are also useful for small-scale applications but high maintenance and risk of failure restrict its suitability.

Pumped storage is another option. But this has limitations due to the fact that once a pumped storage scheme has released its entire store of water it will take some time to refill, and refilling the reservoir is dependent on the price of electricity to justify the economy of the scheme; further limiting the options for frequent and on-demand power output.

The last option is hydrogen storage resulting from the use of excess electrical power to produce hydrogen via electrolysis. This option could offer significant benefits over batteries such as minimal losses over time. However, the hydrogen infrastructure is currently not in place and while this is the case, there applications for hydrogen storage are limited.

### **2.1.6 Use of Complementary Forms of Generation**

Combining supply profiles from a number of different forms of renewable generation can result in an aggregate supply profile which has a better matching performance against a certain demand than each of the supply profiles could achieve individually.

The reason for this is that by combining supply profiles each generated by a different part of the climate dataset (i.e wind velocity/ direction and solar radiation) there is a greater chance of achieving power from one source when the power output is either low or zero from the other source.

The more independent supply options added, the better the quality of the aggregate output will be. This will further be investigated in Section 4.5.

## **2.2 *Supply Demand Matching Techniques***

### **2.2.1 Definition of and Main Uses**

Supply demand matching is the action of comparing the electrical or heating load demands from a specific project with the supply options for electrical or heating output available to that project.

In conventional thermal power stations (with the exception of nuclear) the output can be varied to account for change in demand. CCGT power plants are particular adept at this.

Renewable energy however, does not have the luxury of being able to increase the resource on demand. For this reason supply demand matching is an essential tool for assessing the feasibility of renewable energy projects, whether embedded generation or national grid connection strategies are being pursued.

### **2.2.2 Software Tools for Comparison of Supply & Demand Profiles**

#### RETScreen

Developed by Natural Resources Canada's (NRCan) and CANMET Energy Technology Centre -Varenes (CETC-Varenes) in Canada, this software can be used world-wide to evaluate the energy production, life-cycle costs and greenhouse gas emission reductions for various types of energy efficient and renewable energy technologies (RETs). The software also includes product, cost and weather databases; and a detailed online user manual. [19]

## Homer

Developed by the National Renewable Energy Laboratory at the U.S Department of Energy, this software is a computer model that simplifies the task of evaluating design options for both off-grid and grid-connected power systems for remote, stand-alone, and distributed generation (DG) applications. HOMER models both conventional and renewable energy technologies:

### Power sources:

- solar photovoltaic (PV)
- wind turbine
- run-of-river hydro power
- generator: diesel, gasoline, biogas, alternative and custom fuels, co fired
- electric utility grid
- microturbine
- fuel cell

### Storage:

- battery bank
- hydrogen

### Loads:

- daily profiles with seasonal variation
- deferrable (water pumping, refrigeration)
- thermal (space heating, crop drying)
- efficiency measures

[20]

## MERIT

Merit is a software package designed by ESRU at the Department of Mechanical Engineering, Strathclyde University [21] aimed at providing a mechanism for matching supply and demand for renewable energy applications in Scotland.

Via its user interface it allows the generation of supply and demand profiles and enables matching analysis to be performed.

The program contains a large database of electrical and heating demand profiles for a number of areas in Scotland as well as a considerable amount of climate data for the country also.

This climate data is invaluable in linking with the various supply options to gauge the effects of climate on the output of the renewable supply options.

For example, MERIT contains a number of supply options for real wind turbines, with the performance curves and parameters from the manufacturer being included in the interface for inclusion in the power equation. Combining these parameter with climate real climate data for wind speed and direction makes for a realistic model of power output from the turbine.

A stark observation from both RETScreen and HOMER is the absence of a supply option model for tidal current turbines or indeed any marine energy device.

Given that the MERIT is open source with a GNU licence there is a real possibility of using this program for implementation of a tidal current device profile. Added to this is an association with the developers of the software at the ESRU unit.

## **2.3 Tidal Currents**

### **2.3.1 Definition and Application**

**Tidal Current** is the horizontal movement of the water caused by gravitational interactions between the Sun, Moon, and Earth. The horizontal component of the particulate motion of a tidal wave. It is part of the same general movement of the sea that is manifested in the vertical rise and fall called tide.

Tidal current is the horizontal component of the particulate motion, while tide is manifested by the vertical component. The observed tide and tidal current can be considered the result of the combination of several tidal waves, each of which may vary from nearly pure progressive to nearly pure standing and with differing periods, heights, phase relationships, and direction.

**Tidal Wave** is a shallow water wave caused by the gravitational interactions between the Sun, Moon, and Earth. Essentially, high water is the crest of a tidal wave and low water, the trough. Tidal current is the horizontal component of the particulate motion, while tide is manifested by the vertical component. The observed tide and tidal current can be considered the result of the combination of several tidal waves, each of which may vary from nearly pure progressive to nearly pure standing and with differing periods, heights, phase relationships, and direction. [21]

For the purposes of this report focus shall be on tidal current, as it is this horizontal component which tidal current turbines utilise to extract energy.

### **2.3.2 Tidal Current Energy Extraction Devices**

Initially, the majority of devices proposed to extract tidal energy in general were of the tidal barrage type, in which the aim was to utilise the energy

available from the rise and fall of the water level at a certain point. Viable sites were however limited to those with a large tidal range. Several types of device have been designed to capture tidal stream energy: [23]

**Tidal current turbines** – These work on a similar principle to wind turbines and indeed may look quite similar. Both horizontal- and vertical-axis machines are being investigated, some with ducting/cowling around the rotor. The turbine may be coupled directly to a standard generator via a gearbox, or use an alternative power train design;

**Reciprocating tidal stream devices** – These have hydrofoils which move back and forth in a plane normal to the tidal stream, instead of rotating blades. One design uses hydraulic pistons to feed a hydraulic circuit, which turns a hydraulic motor and generator to produce power; and

**Venturi effect tidal stream devices** – In these, the tidal flow is directed through a duct, which concentrates the flow and produces a pressure difference. This causes a secondary fluid flow through a turbine. Alongside these options, there is a debate about the relative merits of fixing devices to the seabed for stability and deploying floating devices to allow retrieval for maintenance.

Tidal power can also be extracted from **tidal barrage and tidal lagoon** systems. The tidal barrage is a long-established, technically-proven concept which essentially involves a structure with gated sluices and low-head hydro turbines. Bridging two sides of an estuary, the principle of operation is to allow water to flow into the area behind the barrage with the flood tide and out during the ebb tide. As water flows out, the collected head of water turns the turbines to generate power. A tidal barrage has been in operation at La Rance on the northern French coast for more than 40 years, and schemes have previously been proposed in the UK, notably at the River Severn. The tidal lagoon operates in a similar way to the barrage, but uses an impoundment structure rather than a barrage.

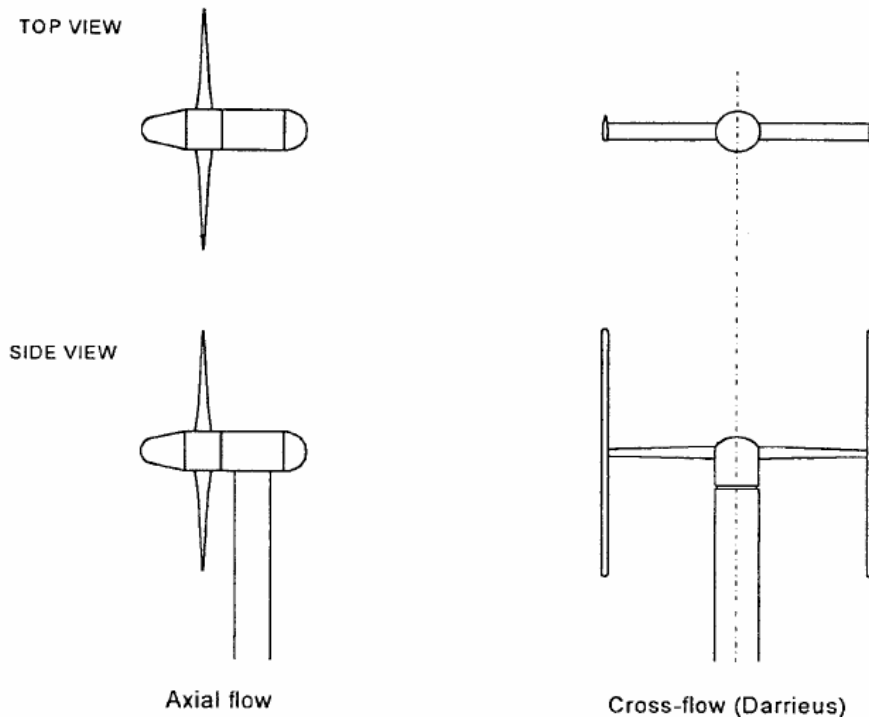
A gradual progression towards tidal current energy and hence turbine-type devices has begun to unfold, as the potential for such technology starts to be fully appreciated. The technological and mechanical similarities with wind, whilst not to be overstated, are certainly evident in the fact that both types of device convert the kinetic energy of a fluid (i.e sea water or air) into mechanical energy using a turbine rotor, which in turn will be used to drive a generator. The similar power equations reflect this, as can be seen below:

The power,  $P$ , available from a tidal current of free-stream velocity  $V$  is,

$$P = \frac{1}{2} \rho A V^3$$
, where  $\rho$  is the density of water  $\text{kg/m}^3$  and  $A$  is the cross sectional area ( $\text{m}^2$ ) of the rotor used to intercept the flow.

The consequence of this cube law relationship is a high degree of sensitivity towards the free-stream velocity  $V$ , whereupon even a small change in  $V$  can have a comparatively large change in  $P$ .

**Figure 6 Rotor Concepts for Tidal Current Turbines**



Many different designs for tidal current turbines have been suggested and researched. Some of these have been developed to prototype stage for testing and some have been built to full scale for pre-commercial testing.

Common features of all marine current energy devices include a rotor, a drive-train and a generator.

Currently the most advanced design, and most likely to become the standard design for the industry, is that of the Seaflow prototype by MCT Ltd.

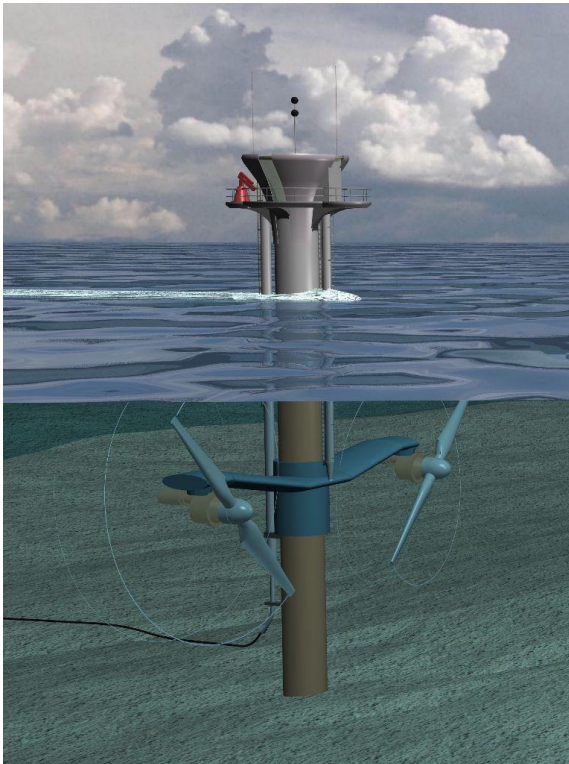
This is a horizontal axis axial flow type device similar to a conventional HAWT (horizontal axis wind turbine) and is shown below in figure 7

**Figure 7      Seaflow Prototype by MCT Ltd. (image courtesy of MCT Ltd.)**



This is the type of device upon which the channel model will be based. The turbine could conceivably have either a single rotor as shown in figure 7 or a twin rotor configuration as is shown in figure 8. The rated power of the former is approximately 500kW and the latter a full 1 MW.

**Figure 8 Twin Rotor Design from MCT Ltd. (image courtesy of MCT Ltd.)**



### **2.3.3 Advantages of Tidal Current Over Other Forms of Renewables**

Tidal current has the major advantage of being largely predictable for any given time. This cannot be said to the same extent for wind power, where a drop in wind can occur without warning, leading to a drop in output and uncertainty of supply. Thus large scale wind farms connected to the grid commonly require additional backup via duplication of generation capacity when connected to the national grid. This is a costly and arguably un-environmentally friendly option, since most duplication will come from coal, nuclear or CCGT plants.

Given the predictability of the tidal resource, it could be argued that as a form of renewable energy tidal power may be the most attractive. What should not

be overlooked in any way is the inherent variability of the tidal resource both from astronomical and meteorological influences.

The key advantage however is that the main variability of the tidal current resource is caused by wholly predictable astronomical effects and even the meteorological effects such as storm surges and pressure drops are in some way predictable through measurement further out to sea before they reach the coastline.

Another distinct advantage for a device of this type is the close alliance with wind turbine technology. The configuration of a rotor rotating by a moving fluid and connected to a drive train, a gearbox and a generator are all common features of the two technologies.

Thus, existing expertise in the field of wind turbines can be considered at least partially transferable to this sector of renewable energy. Such a compatibility will undoubtedly have benefits for projects costs and learning curves for the MCT industry as many of the latest studies have identified [14]. The harsh marine environment is a concept not unknown to the oil and gas sector in Scotland's North East Coast where experience of risk assessment of operation in the marine environment could be useful to the MCT industry.

#### **2.3.4 Drawbacks of Tidal Current Power**

Primarily, the major drawback of tidal current energy is the inherent variability of the resource. This means that the output from an MCT farm at a single site is, on its own, not suitable for a base load supply strategy.

Some attempts have been made to address this issue, with efforts being made to assess the possibilities of providing a 3-phase power supply from using power take-off from 3 sites, where the output of each site is 120 degrees out of phases with the next. Clever use of pumped storage can further smooth the aggregate power curve [24]. However, this solution is far

from ideal and involves high costs and complicated power electronics not to mention a requirement for HV transmission lines to each of the sites.

In other words, if such a strategy was proposed today, it could not possibly be achieved with the poor power infrastructure at many of the most suitable sites. This adds weight to the argument for embedded generation to supply or supplement the electrical demand of local communities in the close proximity to the site of tidal resource.

### **2.3.6 Variability of Tidal Current Velocity**

The Earth's tides are caused by the gravitational attraction of the moon and the sun acting upon the oceans of the rotating earth. The relative motions of these bodies cause the surface of the oceans to be raised and lowered periodically, according to a number of interacting cycles. These include:

- a half day cycle, due to the rotation of the earth within the gravitational field of the moon
- a 14 day cycle, resulting from the gravitational field of the moon combining with that of the sun to give alternating spring (maximum) and neap (minimum) tides
- a half year cycle, due to the inclination of the moon's orbit to that of the earth, giving rise to maxima in the spring tides in March and September
- other cycles, such as those over 19 years and 1 600 years, arising from further complex gravitational interactions.

The amplitude range of a spring tide is commonly about twice that of a neap tide, whereas the longer period cycles impose smaller perturbations. In the open ocean, the maximum amplitude of the tides is about one metre. Tidal amplitudes are increased substantially towards the coast, particularly in estuaries. This is mainly caused by shelving of the sea bed and funnelling of the water by estuaries. In some cases the tidal range can be further amplified by reflection of the tidal wave by the coastline or resonance. This is a special effect that occurs in long, trumpet-shaped estuaries, when the length of the

estuary is close to one quarter of the tidal wave length. These effects combine to give a mean spring tidal range of over 11 m in the Severn Estuary (UK) [25]. As a result of these various factors, the tidal range can vary substantially between different points on a coastline. The amount of energy obtainable from a tidal energy scheme therefore varies with location and time. Output changes as the tide ebbs and floods each day; it can also vary by a factor of about four over a spring-neap cycle. Tidal energy is, however, highly predictable in both amount and timing.

### Diurnal/ semidiurnal Cycle

There are numerous components to the tide. The basic tide is the cyclic rise and fall of the water surface as the result of the tide-generating forces. The simplest way of classifying tides is by the dominant period of the observed tide. This is based on the ratio ( $F$ ) of the sum of the amplitudes of the two main diurnal components ( $K1$  and  $O1$ ) to the sum of the amplitudes of the main semi-diurnal components ( $M2$  and  $S2$ ). There are three types of tides-diurnal, semidiurnal, and mixed-which are a result of tide-generating forces and location on the earth.

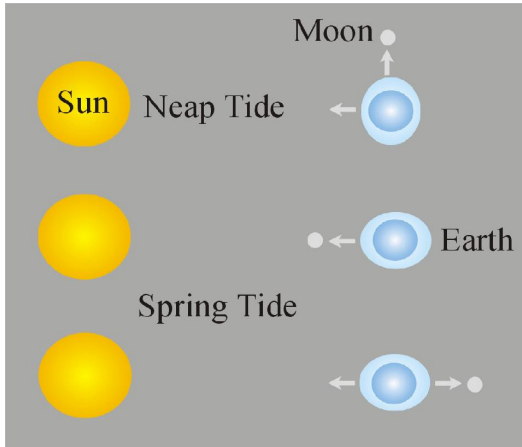
**Diurnal:  $F > 3$ .** A diurnal tide is one high and one low water level in a lunar day (24.84 hours).

**Semidiurnal:  $F < 0.25$**  Semidiurnal tides produce a tidal cycle (high and low water) in one-half the lunar day (12.42 hours) or two nearly equal tidal cycles in one lunar day.

**Mixed:  $0.25 < F < 3$**  Mixed tides are a combination of diurnal and semidiurnal characteristics. There is a marked inequality in the heights of the succeeding tides, especially low waters, and there is also an inequality in time. There are usually two high and two low waters each day.

### **Spring & Neap Tides**

**Figure 9 Spring/ Neap Cycle [25]**



Spring and Neap Tides: Due to the unequal rotational rhythms of the members of the Sun-Moon-Earth system, their forces are periodically in and out of phase. Every 14.3 days (twice a month) the Earth, Moon, and Sun are aligned in phase. At this time the gravitational forces reinforce each other to form higher than average tides called "spring tides". When spring tides occur the Sun and Moon are said in conjunction (at new Moon) or at opposition (at full Moon). Also twice a month the Moon and Sun are at right angles to the Earth and the forces are subtracted from each other to form lower than normal tides called "neap tides" and the Moon is said to be in quadrature.

Not all spring tides are the same size. Springs nearest the equinoxes (21 March and 21 September - when day and night are of equal length all over the world) are slightly bigger.

## ***2.4 Modelling the Assessment of Tidal Current Behaviour & Energy Extraction***

There are two distinct areas in which the above section title can be split; namely between the areas of tidal current behaviour and energy extraction. Most of the models or methods highlighted here only deal with one of those areas. Ultimately, the ideal model would involve both areas.

### **2.4.1 CFD Models**

With the advent of computational fluid dynamics (CFD), there have been many techniques developed using this technology in the context of tidal energy. A report released recently by Supergen [27] gave an appraisal of the best of these packages to date. The main problem with the use of such packages is their complexity. They require significant man-hours as well as access to parallel computing in many cases where the code and problem geometry are too complex for a single pc workstation to process.

For the purposes of this thesis, and with the intention of carrying out an investigation into the merits of embedded generation for tidal power, it was decided that to use such a program would be impractical in terms of time and money, as well as overly complex for the objectives of the thesis. For this reason, a simpler model based on hydrodynamics was opted for.

### **2.4.2 Admiralty Tidal Diamond Data (ATD)**

To obtain tidal diamond data for a specific site, a measurement buoy is anchored for at least 12 hours at the site of interest. Every hour a measurement is taken from a current meter and the tidal current velocity is recorded just below the surface. This method, however, requires execution during a meteorologically calm period, to negate the effects of residual flows. These measurements are then factored based on the mean spring and neap tidal range from a chosen reference port. Below is an example of a Tidal Stream Atlas produced using ATD method

**Figure 10 ATD Data**

Location: 50° 7.2'N 5°49.5'W			
Reference Port: Devonport			
Hours	Direction	Speed (knots)	Speed (knots)
		(springs)	(neaps)
HW - 6	332°	0.4	0.2
HW - 5	002°	1.5	0.7
HW - 4	009°	2.4	1.2
HW - 3	010°	2.5	1.2
HW - 2	009°	1.6	0.8
HW - 1	031°	1.1	0.5
HW	123°	0.6	0.3
HW + 1	168°	1.7	0.8
HW + 2	181°	2.5	1.2
HW + 3	194°	2.5	1.3
HW + 4	210°	2.1	1.0
HW + 5	223°	1.1	0.6
HW + 6	295°	0.4	0.2

It is claimed [27] that the results from this method are equivalent to using the harmonic constituents M2 and S2 (the gravitational effects of the moon and sun). However, the main disadvantage of tidal diamonds is that the observation period on which they are based is very short (typically <25 days); hence not allowing for capture of anything but the most basic of tidal constituents. Additionally, confidence in results is limited by the fact that the results are generated from interpolation between sparse tidal stream data.

A further drawback to ATD tidal current data is that data is provided for only major ports or areas of significant maritime activity. For this reason many sites considered suitable for the deployment of MCT farms may indeed be missed entirely by this fairly sparse data set.

### **2.4.3 Proudman Oceanographic Laboratory Method (POL)**

The Proudman Oceanographic Laboratory's numerically modelled hydrodynamic data sets [28] are based on performing harmonic analysis on at least 30 days of tidal height data in addition to considering up to a further 50 local constituents from the POL 12km continental shelf model.

The model uses up to 26 tidal harmonic constants to provide tidal elevation together with current speed and direction at six different depths (sigma levels) deduced from the depth-averaged currents using a set of vertical current profiles. The six sigma levels for the currents are at the depths 0% (surface), 25%, 50% (mid-depth), 75%, 90% (near-bottom) and 100% (bottom).

The details of the model are given in more depth in ref [29].

This method increases the accuracy of tidal current data produced for a specific site, by considering the additional astronomical and local influences which were never addressed by the ATD method.

The ATD or POL methods are mostly intended for maritime and coastguard use. Hence, neither method addressed in any way the effects of energy extraction on tidal currents. This would limit their use in the context of assessing specific sites for suitability for MCT farms.

Also, since these programs are commercial, it is only possible to use them at considerable financial cost to the user.

### **2.4.4 Tide 2D**

Tide 2D is a harmonic frequency domain program [40] that solves the non-linear, shallow water equations for sea level and depth averaged velocity using a finite element discretisation in space and harmonic expansion in time.

Continuity

$$\frac{\partial \eta}{\partial t} + \frac{\partial q}{\partial x} = 0$$

Momentum

$$\frac{\partial q}{\partial t} + \frac{\partial M_x}{\partial x} = -gH \frac{\partial \delta}{\partial x} - \frac{Kq|q|}{H^2}$$

Where

The problem with Tide 2D is primarily its complexity and labour intensiveness. In addition it also requires the availability of a complex and detailed finite element model of the area of interest. For the purposes of this thesis, where the objective is to develop a more simple model to provide only a resource estimate, it would be unrealistic to use Tide 2D.

Ideally, a more accessible model would involve a much simpler hydrodynamic engine to provide the tidal water heights for our tidal energy extraction module.

#### **2.4.5 Bryden/ Couch Model (1-D Channel Analysis)**

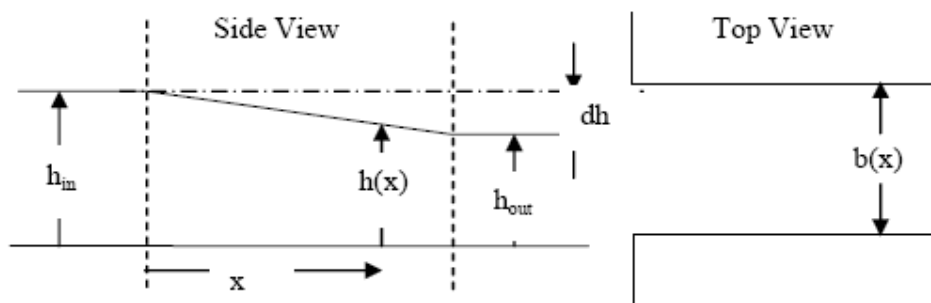
In a paper written by Bryden and Couch, entitled “The Impact of Tidal Energy Extraction” [37], the authors address the issue of what impact would arise both upstream and downstream from tidal current energy extraction of significant size.

Whilst this model is not a mechanism for generating detailed tidal current velocity data, it does address the more pressing issues of both the upstream and downstream effects of extracting energy from an open channel. Only the relevant details of Bryden’s approach and the salient conclusions will be

referred to here. However, the author refers to the reader to the full paper [37] for more in depth coverage of the model's approach.

The model considers the retarding force on a slug of water which would result from energy extraction and factors this up to the scale of an entire channel. It then used the TD\_2d code (ref) and expands this to 3d by using transformation to the vertical axis ( $\sigma$ ), in other words a layered approach.

### Schematic of layered (sigma) approach [10]



Some of the most interesting conclusions from this paper, and in particular from the 2d-sigma co-ordinate approach, were:

- A reduction in stream-wise flow velocity occurs in the mid-layer region of the vertical profile where the turbine will be placed, both upstream and downstream of the extraction site, as would be expected (and in-line with experience from wind turbines)
- The largest of these velocity deficits occurs in the immediate vicinity of the extraction site and the downstream wake (this is line with the conclusions of ref 10.)
- In the surface and bottom layers, the region upstream of the extraction site experiences a reduction in velocity
- In the same surface and bottom layers, the region this time downstream of the extraction site experiences a velocity **increase** of anything up to 20%, even though energy has been extracted from the

system. This would be consistent with the idea that the inlet water is experiencing a diverting force as it is directed around the turbine.

- At the extraction site itself, flow velocity near the sea bed increases
- Increased surface flow velocity coupled with a reduction in flow velocity in the interior creates high shear in the horizontal flow between  $\sigma = 0.65$  and  $\sigma = 0.75$ , where  $\sigma$  is the ratio of vertical position in the channel to channel depth. This will have implications on the issue of dispersal of biological species and indeed waste.

Although this paper provided substantial insight into losses due to energy extraction, it did not lend itself too well to direct implementation into a simple model for a case study approach. However, if some of the findings of this paper could be adopted in a simpler way via a channel model approach, then this would act to provide a higher degree of realism to the model, in which energy extraction effects could be carefully considered and factored into the algorithm.

#### **2.4.6 Full Harmonic Analysis of a 30 Day Tidal Record**

In any hydrodynamic model for tidal current flow in a channel there is a requirement for accurate water height data. For any subsequent resource evaluation and site capacity estimation there must be a large amount of data available (usually of at least 1 year).

One option is to use harmonic analysis of a 30-day tidal record to determine the phase and amplitude of the most influential tidal constituents.

Once these harmonic constants had been determined for each site of interest, a very accurate prediction of the tide at any time (t) could be made by adding the sum of the water height contributions from each constituent to the mean water level ( $z_0$ ). This approach is shown in greater depth below:

There are many different steps involved in obtaining the final numbers that go into a tide table. Before a tidal prediction can be made for a port, a long sequence of tidal observations for that port is needed (called a *time series*). This time series will include all the astronomical effects and local coastline/depth effects (which make up the tide) as well as the weather induced effects called the surge.

There are certain frequencies that are known to occur in the tide. Some of these have already been listed in Section 2.3.6.

- 12 hour (12:00:00.0) repeated pattern (cycle) due to the gravity of the sun.
- 12:25:14.164 cycle due to the gravity of the moon.
- 24:00 and 24:50:28.328 cycles caused by the differences in the two tidal bulges.
- 27.2122 day cycle caused by change in lunar declination (Moons angle to the Earth).
- 27.5546 day cycle caused by a regular change in the Earth-Moon distance.
- 29.5306 day cycle caused by the phases of the moon.

Each of these cycles is called a tidal *harmonic constituent* and the *frequencies* of each of these are known very accurately. Therefore it is easy to find them in a sequence of observations using a method called *tidal analysis*. Once each constituent is identified, its size (*amplitude*) and time of 'arrival' (*phase*) is stored. These two values (known as a harmonic constant) are unique for every location.

The amplitude and phase for each constituent combined with the fixed speed of that constituent allows us to predict its contribution to the overall tide forward or backward in time almost indefinitely. Adding up the effects of all the constituents at a given location enables prediction of the overall tide at any time in the future or past.

Most tide tables just list the time and height when the water is at a maximum and minimum level in each tidal cycle. This leads to approximately 2 high waters and 2 low waters every 24 hours and 50 minutes.

Even a simple harmonic method using only the first 7 harmonic constants could predict all of the following tide variations identified in Section 2.3.6 [28].

### **Implementing the Harmonic Method**

It was possible to predict the variation in water height from astronomical influences at a particular location to a good degree of quality via the use of harmonic analysis of a tidal record of at least 30 days.

Taking the example of the Pentland Firth, the two ports considered in the channel model to be representative of independent reservoirs of water either side of the channel were Aberdeen and Rona.

#### Harmonic Analysis of a 30-day HW and LW Tidal Record at Aberdeen

The source of the 30-day tidal record was Admiralty Tide Tables NP 201-06 2001 and The Macmillan Reeds Nautical Almanac 2001. [29]

Firstly the HW and LW times and heights were input into a spreadsheet format.

**Table 2 HW and LW time and heights for Aberdeen in Jan 2001 as given by Admiralty Tide Tables**

Date		Time	Time Diff (mins)	Predicted Height (m)
01/01/2001	HW1	5:25:00 AM	0	3.6
01/01/2001	LW1	10:59:00 AM	334	1.7
01/01/2001	HW2	5:23:00 PM	384	3.8
01/01/2001	LW2	11:39:00 PM	376	1.4
02/01/2001	HW1	6:16:00 AM	397	3.5
02/01/2001	LW1	11:50:00 AM	334	1.8
02/01/2001	HW2	6:15:00 PM	385	3.7
03/01/2001	LW2	12:34:00 AM	369	1.5
03/01/2001	HW1	7:13:00 AM	399	3.5
03/01/2001	LW1	12:54:00 PM	341	1.9
03/01/2001	HW2	7:14:00 PM	366	3.6
04/01/2001	LW2	1:37:00 AM	383	1.6
04/01/2001	HW1	8:16:00 AM	399	3.5

This allowed the predicted HW and LW data from the Admiralty Tide Tables to be tabulated and plotted in a graph alongside the predicted tide height resulting from the harmonic method. In this way, the accuracy of the predicted values from the harmonic method was easily gauged.

The next step was to input the harmonic constituents given by these nautical publications. The form which the harmonic constituents took was a cosine function with amplitude  $A$ , angular velocity  $\omega$  and a phase angle  $\phi$ :

$$f(t) = A \cos(\omega t + \phi)$$

Since the angular velocity (in degrees per solar hour) for each constituent was known from astronomical knowledge of the motion of the earth sun and moon, then all that was left to calculate was the amplitude and phase angle; known collectively as the harmonic constants for each site. This was unique to each site.

The different constituents are sums and differences of small integral multiples of 5 basic astronomical speeds, which are shown below:

$T$  the rotation of the Earth on its axis, with respect to the Sun, 15 degrees/hour  
 $h$  the rotation of the Earth about the sun, .04106864 degrees/hour  
 $s$  the rotation of the Moon about the Earth, .54901653 degrees/hour  
 $p$  the precession of the Moon's perigee, .00464183 degrees/hour  
 $N$  the precession of the plane of the Moon's orbit, -.00220641 degrees/hour.

These were then used to determine the angular velocities of each constituent:

**Table 3 Angular Velocities of Each Tidal Constituent**

Symbol	Angular Velocity, $\omega$	Amplitude	Phase
M2	$2T-2s+2h=28.984$ degrees/ solar hour	not known	not known
N2	$2T-3s+2h+p = 28.439$ degrees/ solar hour	"	"
S2	$2T = 30.000$ degrees/ solar hour	"	"
K1	$T+h = 15.041$ degrees/ solar hour	"	"
O1	$T-2s+h = 13.943$ degrees/ solar hour	"	"
M4	$2xM2=57.968$ degrees/ solar hour	"	"
M6	$3xM2=86.952$ degrees/ solar hour	"	"

To calculate the amplitude and phase or (harmonic constants) of each constituent a method called harmonic analysis was employed.

This involved taking writing each constituent in the form;

$$A(t) = A_0 + A_1 \cos(vt) + B_1 \sin(vt) + A_2 \cos(wt) + B_2 \sin(wt)$$

Taking the long term average of the terms has been shown to give  $\frac{1}{2}$  the values of each coefficient (ref ), according to the trigonometric properties;

$$A = \text{twice the long-term average of } R(t)\cos(vt)$$

$$B = \text{twice the long-term average of } R(t)\sin(vt).$$

Ideally, if this harmonic analysis has already been carried out then it is much easier to simply add the harmonic constant to the equations for predicted tide as shown below:

H(t)= mean sea level + contribution from sum of harmonic constituents

$$H(t) = H_0 + A_{M2} \cos(\omega_{M2}t + \phi_{M2}) + A_{N2} \cos(\omega_{N2}t + \phi_{N2}) + A_{S2} \cos(\omega_{S2}t + \phi_{S2}) \\ + A_{K1} \cos(\omega_{K1}t + \phi_{K1}) + A_{O1} \cos(\omega_{O1}t + \phi_{O1}) + A_{M4} \cos(\omega_{M4}t + \phi_{M4}) + A_{M6} \cos(\omega_{M6}t + \phi_{M6})$$

The harmonic constants have already been calculated via harmonic analysis for many standard ports. In the US this information is readily available to any third party. However, in the UK the information has been deemed property of the Crown Estate and as such is restricted to authorised publications, usually available for a small fee.

One such publication was the Admiralty Tide Tables NP 201-06 [29]. This provided the basic harmonic constants for a number of standard ports sufficient for the purposes of the enhanced channel model (see Section 3).

#### **2.4.7 Double Cosine Method (Fraenkel)**

Calculate the max spring tide velocity and the min neap tide velocity and use a previously derived [page 2 of ref 31] equation to approximate the intermediate points.

$$V = \left[ K_0 + K_1 \cos\left(\frac{2\pi t}{T_1}\right) \right] \cos\left(\frac{2\pi t}{T_0}\right), \text{ where } K_0 + K_1 \text{ are constants determined}$$

from the mean spring peak and the ratio between the mean spring peak and the mean neap peak current velocities,  $T_1$  is the spring neap period (353h) and  $T_0$  is the diurnal period (12.4 h).

This method, which accounts for both spring/neap and semi-diurnal cycle variations, meant that data could be extrapolated for a period of as much as a year.

Hence, this method lends itself well to supplying accurate supply profiles for supply/ demand matching analyses, where monthly and yearly demand profiles are being considered.

This then gave the ideal theoretical current velocity in the channel, without having corrected for  $K_L$ , the frictional losses due to local channel geometric effects. The problem with this approach was that it grossly simplifies the actual variations via the use of a crude cosine function and also cannot account for shallow water effects or other harmonics of the astronomical constituents.

#### **2.4.8 Tidesim**

Tidesim is proprietary to Robert Gordon University, Aberdeen. Very little information is available on this software although it appears to be a powerful hydrodynamic model requiring the input of complex grid information on sea bed bathymetry and channel dimensions and has appeared in many papers written by the University [37].

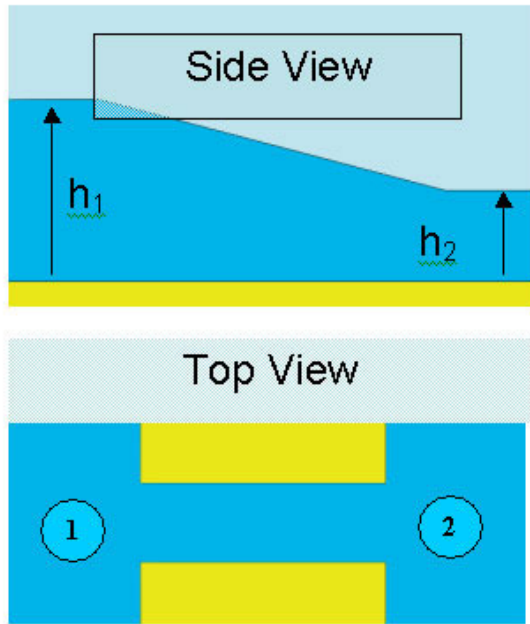
#### **2.4.9 Previously Developed Channel Model**

This is a simple hydrodynamic head loss model [10].

It can be observed that tidal currents tend to develop in channels between land masses. Each channel is of course unique in terms of its width and depth variations, roughness etc. The basic premise of this channel model method was therefore to take a real channel and idealise it into a simple mathematical model. The basic assumptions were as follows;

- Flow in the channel originates from the out – of – phase rise and fall in two tidal reservoirs at the end of the channel.
- The reservoirs were considered to be large and therefore their rise and fall independent of any flow in the channel.
- The effects of seabed topology on the flow velocities were neglected

Figure 11 Channel Model, Side View & Top View



Step 1:

Water level data from two reservoirs on either end of the channel were obtained such that when the tidal height at the first reservoir is at a height  $h_1$  the second height  $h_2$  is out of phase by an angle  $\Phi$  or at a different height. These heights were therefore expressed by a sine approximation given by the equations

$$h_1 = h_1 \sin \omega_1 t$$

$$h_2 = h_2 \sin (\omega_2 t + \Phi)$$

Where  $\omega$  is the angular velocity of the approximation sine waveform or in terms of the period of the tide at each site  $\omega_n = 2\pi/T_n$ , where  $T_n$  is the tidal period at site  $n$  and  $\phi$  is the phase angle between the two water heights.

Step 2:

The ideal (theoretical) depth averaged flow velocity in the channel ( $V_{th}$ ) was therefore estimated as

$$V_{th} = \sqrt{2g(h_1 - h_2)}$$

Step 3:

This theoretical velocity was then compared with actual measured marine current velocity ( $V_{act}$ ) of the channel to estimate an effective loss coefficient for the channel ( $K_L$ ):

$$V_{act} = \sqrt{\frac{2g(h_1 - h_2)}{1 + K_L}}$$

Step 4:

The effect of channel blockage was then investigated by installing marine current turbines (MCT's) or indeed any form of blockage in the channel with a turbine coefficient  $K_T$ . With  $K_T$  known (representative of the number of turbines) and  $K_L$  already found from step 3 above, the new channel velocity was estimated from

$$V_{new} = \sqrt{\frac{2g(h_1 - h_2)}{1 + K_L + K_T}}$$

As  $K_T$  increases (meaning more turbines), the depth-averaged channel velocity decreases.

The extractable power from the channel is directly proportional to  $K_T$  and channel velocity and therefore it was expected that power would reach a maximum at some point.

Step 5 : Optimum Value of  $K_T$

A trial and error method was used to find the  $K_T$  value corresponding to maximum power. However for economical reasons, the optimum value of  $K_T$  was not the value corresponding to maximum power but rather the value beyond which there is no significant increase in extractable power to justify the additional cost of turbines to be installed. This optimum  $K_T$  value was

found by finding the slopes at various points on the Power against  $K_T$  curve. The optimum point was where the decrease in slope as compared to the slope at the beginning minimizes the power drop off.

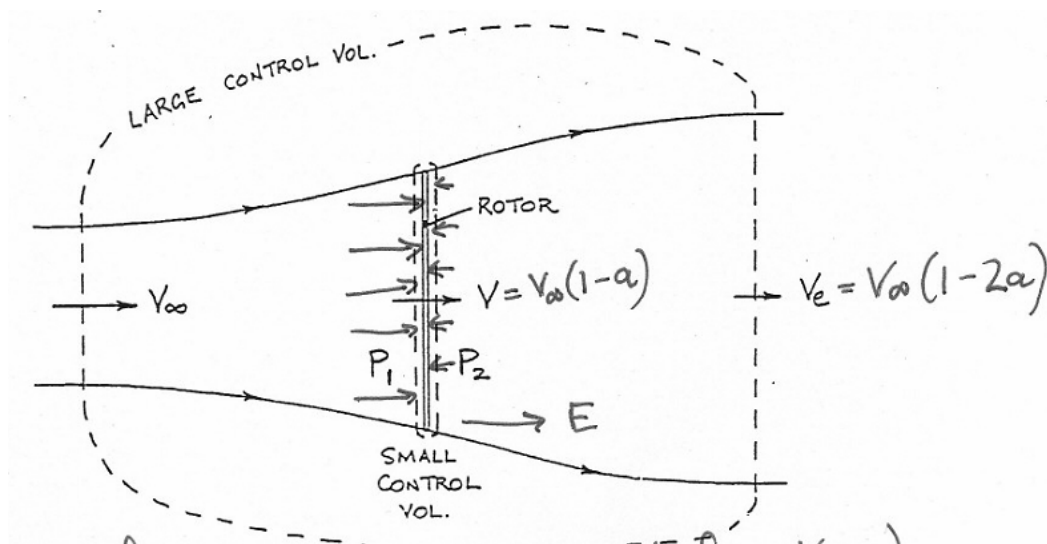
#### Step 6: Calculating a representative number of Turbines

An investigation was carried out into what the optimum  $K_T$  value represented in terms of number of turbines. This was investigated by expressing solidity in terms of the turbine swept area.

$$\text{Solidity, } \sigma = \frac{\sum \text{MCT Rotor Areas}}{\text{Area of Channel}} = \frac{A_{MCT}}{A_{channel}}$$

This was further explained utilising one-dimensional Betz Theory for a MCT which is very similar in approach to that of a wind turbine.

Consider the flow through a disc representing the plane of rotation of a MCT or wind turbine rotor. The streamlines form the boundaries of decelerating flow, which contains the turbine disc, as shown in the diagram below



$a$  is the axial induction factor and is a measure of how much the wind or tidal current has decelerated from the free-stream velocity  $V_\infty$ .

It is assumed that there is only one component of velocity; an axial component with values  $V_\infty$  at entry,  $V$  at the plane of the rotor and  $V_e$  at the exit.  $P_1$  and  $P_2$  are the pressures immediately upstream and downstream of the rotor, respectively. Large and small control volumes are drawn as shown in the diagram.

For the large control volume the energy equation is

$$\frac{P_\infty}{\rho} + \frac{V_\infty^2}{2} = \frac{P_e}{\rho} + \frac{V_e^2}{2} + \frac{w}{kg} \quad \text{and} \quad P_\infty = P_e = \text{atmospheric pressure}$$

$$\therefore \text{work extracted at the rotor, } \frac{w}{kg} = \frac{V_\infty^2 - V_e^2}{2}$$

$$\text{So across the rotor disk, } \frac{P_1}{\rho} + \frac{V^2}{2} = \frac{P_2}{\rho} + \frac{V^2}{2} + \frac{w}{kg}$$

$$\therefore \frac{w}{kg} = \frac{P_1 - P_2}{\rho} = \frac{V_\infty^2 - V_e^2}{2}$$

For the large control volume the momentum equation is:

$$\dot{m}[V_e - V_\infty] = E = \text{external force}$$

And for the small control volume, the momentum equation is:

$$0 = A(P_1 - P_2) + E$$

The external force exerted on the control volume is a retarding force, which reduces the momentum of the fluid as it flows through the system. This force comes from the rotor and its supporting structure. The rotor of course experiences an equal and opposite force due to the wind, in the direction of flow.

$$\text{So } m[V_{\infty} - V_e] = A(P_1 - P_2)$$

$$\text{or } \rho AV[V_{\infty} - V_e] = \frac{1}{2} \rho A (V_{\infty}^2 - V_e^2) \text{ - from equation (1)}$$

$$= \frac{1}{2} \rho A (V_{\infty}^2 - V_e^2) (V_{\infty} - V_e)$$

$$\text{where } V = \frac{V_{\infty} + V_e}{2}$$

$$\text{The power from the rotor, } P = m \frac{V_{\infty} + V_e}{2}$$

$$= \rho AV \frac{V_{\infty} + V_e}{2}$$

$$= \frac{\rho A}{4} (V_{\infty} + V_e) (V_{\infty}^2 - V_e^2)$$

$V$  could also be written as  $V = V_{\infty}(1 - a)$ . It follows that the exit velocity  $V = V_{\infty}(1 - 2a)$ . Substituting it is possible to write:

$$P = \frac{\rho A}{4} (V_{\infty} + V_{\infty} - 2aV_{\infty})(V_{\infty} + V_{\infty} - 2aV_{\infty})(V_{\infty} - V_{\infty} + 2aV_{\infty})$$

$$= \frac{\rho AV_{\infty}^3}{4} (2 - 2a)(2 - 2a)2a$$

$$= 2\rho AV_{\infty}^3 (1 - a)^2 a$$

$$= 2\rho AV_{\infty}^3 [a - 2a^2 + a^3]$$

$$\text{For maximum power } \frac{dP}{da} = 0, \text{ i.e. } 1 - 4a + 3a^2 = 0$$

$$\text{Then } (1 - 3a)(1 - a) = 0$$

$$\text{So } a = 1 \text{ or } a = \frac{1}{3}$$

$a = 1$  gives minimum power

So the maximum power which may be extracted occurs when the axial induction factor  $a = \frac{1}{3}$

$$\text{i.e. } P_{\max} = 2\rho AV_{\infty}^3 \left(1 - \frac{1}{3}\right)^2 \cdot \frac{1}{3} = \frac{8}{27} \rho AV_{\infty}^3$$

The power coefficient  $C_p$  is defined as  $\frac{P}{\frac{1}{2} \rho AV^3}$  and so has a maximum value of

$$C_{P_{\max}} = \frac{P_{\max}}{\frac{1}{2} \rho AV^3} = \frac{16}{27} = 0.593$$

This is the Betz limit and is regarded as the absolute upper limit for wind turbine performance.

Using a similar method for a MCT, the momentum equation can be used to show that the external force exerted on the control volume acts to retard the flow and reduce the momentum of the fluid (water in this case) within that system.

$$\begin{aligned} \text{External force, } E &= \dot{m}[V_\infty - V_e] \\ &= \rho A V_\infty (1-a)[V_\infty - V_\infty(1-2a)] \\ &= \rho A V_\infty^2 (1-a)(2a) \\ &= \frac{4}{9} \rho A V_\infty^2 \quad \text{if } a = \frac{1}{3} \text{ for max power extraction} \end{aligned}$$

So assuming that the external retarding force E can be expressed in terms of a coefficient of drag,  $C_D$ ,

$$C_D = \frac{E}{\frac{1}{2} \rho A V_\infty^2} = \frac{\frac{4}{9} \rho A V_\infty^2}{\frac{1}{2} \rho A V_\infty^2} = \frac{4}{9} \times \frac{2}{1} = \frac{8}{9} \quad \text{for maximum power extraction (} a = 1/3 \text{)}$$

Applying this result for the coefficient of drag associated with maximum power extraction, it is possible to investigate the optimum number of MCT's in a channel by considering solidity of the turbines in that channel.

The solidity is considered to be the collective swept area of the MCT's as a fraction of the total cross-sectional area of the channel.

Using momentum equation to determine the change in pressure  $\Delta P$  and assuming  $V_\infty = V_e$  it can be shown that the rate of change of momentum of the water in the channel is given by

$$\begin{aligned} \frac{d}{dt}(mV) &= 0 = A_{channel} \cdot \Delta P - E \\ \therefore \Delta P &= \frac{E}{A_{channel}} = \frac{\frac{4}{9} \rho A_{MCT} V_\infty^2}{A_{channel}} = \frac{4}{9} \rho \sigma V_\infty^2 \\ \therefore \rho g \Delta H &= \frac{4}{9} \rho \sigma V_\infty^2 = K_T \rho \frac{V_e^2}{2} \\ \text{Since } V_\infty &= V_e \quad \text{so } K_T = \frac{8}{9} \sigma = C_D \cdot \sigma \end{aligned}$$

From this it is clear that we can specify  $K_T$  in terms of the solidity of the channel  $\sigma$ .

Using this method suggested that for maximum power extraction, the drag coefficient defined in the equation for the drag force:

$$F_D = C_D \frac{1}{2} \rho A_{MCT} V_e^2 \quad \text{should be } C_D=8/9$$

Number of turbines = solidity \* Area of Channel/MCT rotor area

$$\text{Or } n = \sigma \times \frac{A_{\text{channel}}}{A_{MCT}}$$

This outcome allowed the consideration of a “plane” of MCT’s installed in a channel with a certain  $\sigma$  value, causing a certain change in hydraulic pressure  $\Delta P$  and giving rise to a change in head  $\Delta H$ .

An attempt was made to use a basic 2d CFD model in FLUENT to validate the value of  $K_T$  [10]. However, the results proved inconclusive.

By varying the value of  $K_T$  the effect of increasing the number of turbines in a channel could be gauged by observing the loss of power which resulted from the reduction of the current velocity in the channel.

Having selected the number of MCT’s,  $n$ , and thus having specified the value of  $K_T$ , the power generated and energy produced over a period of 1 month was estimated by the following method.

The power produced at any time was estimated from the power equation, with a trapezoidal method was used to estimate the energy

## 2.4.10 Comparison & Summary of Models

**Table 4 Summary of Models**

	Advantages	Disadvantages
ATD	Reasonably easy to perform a quick analysis.	Limited confidence due to crude interpolation between sparse tidal stream data, observation period on which they are based is very short (typically <25 days); hence not allowing for capture of anything but the most basic of tidal constituents.
POL	Samples data for longer period and so takes into account more astronomical effects Accounts for many local effects using the complex 12km continental shelf model	Time consuming and complicated software, does not account for local effects, weather, bottom roughness, channel width etc. Also does not account for blockage effects in channels. Software is also expensive and requires information from the POL 12km shelf model which is again proprietary to Proudman Laboratories and as such is inaccessible to

		the author. Lastly, the resolution of the tidal data provided is not readily available in form suitable to allow use in supply/ demand matching analysis.
Bryden/ Couch	Accounts for energy extraction	Does not generate velocity data
Tidesim	Comprehensive	Not available outside Robert Gordon University
Previously Developed Channel Model	Much simpler spreadsheet based approach. Accessible and easily modified.	Requires measured data for tidal current velocities in order to calculate a value for losses due to the channel itself. This limits the use of the model to only sites for which such data is available. Doesn't account for spring/ neap variations in its current format.

The main disadvantage to all of these existing models was the need for large data sets, whether measured or calculated, and a complicated, time-consuming procedure. Potentially a much less time-consuming yet accurate method was that of the previously developed channel model [10]. However, it clearly needed much improvement beyond its current state.

### 3 Development of Enhanced Channel Model

#### Algorithm

After consideration it became obvious that the limitations to the previously developed channel model were as follows:

- Original model was only calculated for spring tide conditions. This was hugely unrealistic if the overall energy capacity of a site was to be estimated accurately.
- It failed to capture spring neap variation and slack tides
- Local effects such as ebb flow differences and channel geometry were neglected

From careful study of all of the existing models or techniques, it was evident that a number of factors existing in a real channel would ultimately affect the validity and realism of the output for a simple channel model. These were:

- 1) The accounting for astronomical variation in the tidal current velocities in a channel out with simply addressing ebb/ flood tides
- 2) Feedback or blockage effects on current velocity/ elevation
- 3) Global variations due to channel depth and width
- 4) Local variations due to position in water column and position along channel
- 5) Directionality of flow and velocity hotspots
- 6) Degree of solidity pertaining to the packing density of the MCT devices.

Some of these factors had already been addressed in the previously developed model [10], whilst clearly others had not. This seriously limited the power of the model in its original state.

However, it was entirely possible to enhance the model to include these factors and thus produce a package which was comprehensive in its coverage of the governing factors, yet accessible and easy to use without requiring excessive man-hours or significant processing power.

Such a model could then be used as a tool for assessing the suitability of sites already earmarked for potential development of large MCT farms. The supply profile data generated by the model could then be used in supply/ demand matching analyses of real case study communities via renewable energy supply/ demand matching software.

The focus of the improvement of the previously developed channel model described in section 2.4.5 was placed on:

- Carrying out a harmonic analysis of tidal records to generate accurate water level data for two ports either side of the channel of interest or else relying on the harmonic constants already provided by nautical publications
- Accurately predicting the theoretical tidal current velocity in that channel for a 1 year period based on astronomical constituents including spring/ neap variations
- Calculating for channel losses without having to rely on availability of measured tidal current velocity data, thus extending the use of the model to include any site for which there is water height data available
- Accounting for blockage effects and losses due to placement of MCT devices in said channel

### 3.1 Modelling of Astronomical Variations

To correct for spring neap variation would have required a large amount of data input especially if supply profile data was required for a large period of the magnitude of a year or more. Two options studied were:

**Option 1** – The double cosine method described in section 2.4.7 grossly simplifies the actual variations via the use of a crude cosine function and also cannot account for shallow water effects or other harmonics of the astronomical constituents.

**Option 2** – The Full Harmonic Analysis described in Section 2.4.6 simply calculates tidal water heights for the year based on measured data of a 30 day period, taking tidal range from the appropriate (nearest) standard reference port and employing a harmonic method to determine the influences of each harmonic constituent.

Option 2 was chosen as the superior method and, where provided by nautical publications such as [29], the harmonic constants would be taken as known *a priori*. This enabled the production of a simple harmonic model which would only need the input of values for the first 7 basic harmonic constants. However, the water heights generated by taking these 7 basic harmonic constants alone may need to be validated against the more accurate water height data as calculated though full harmonic analysis in the same publication. Section 3.1.2 demonstrates this.

#### 3.1.1 Implementing the Simple Harmonic Model

**Table 4 Harmonic Constants for Aberdeen (from Admiralty NP 201-06)**

No.	PLACE	ML Z <sub>0</sub> m	HARMONIC CONSTANTS				Zone UT(GMT)				S.W. CORRECTIONS			
			M <sub>2</sub> g°	S <sub>2</sub> g°	H <sub>2</sub> H.m	H <sub>2</sub> H.m	K <sub>1</sub> g°	O <sub>1</sub> g°	H <sub>1</sub> H.m	H <sub>1</sub> H.m	1/4 diurnal f <sub>4</sub>	F <sub>4</sub>	1/6 diurnal f <sub>6</sub>	F <sub>6</sub>
244	ABERDEEN .....	2.54	025	1.30	063	0.44	205	0.11	050	0.13	137	0.017	043	0.002

**Figure 12 Input of Harmonic Constants to Enhanced Channel Model**

WATER LEVEL DATA				Aberdeen 2001						
Date/Time	Month	Seasonal Change (m)	Time (hours)	Main Astronomical Constituents					Shallow water corrections	
				M2	S2	N2	K1	O1	1/4 diurnal (M4)	1/6 diurnal (M6)
00:00:00	January	0.1	0	1.177881	-0.222143	-0.299098	0.051803	-0.129999	0.000995113	0.001418713
01:00:00	January	0.1	1	0.763804	-0.382285	-0.274067	0.024847	-0.126079	-0.013859267	0.001483141
02:00:00	January	0.1	2	0.158402	-0.439993	-0.182877	-0.00381	-0.114726	-0.015696835	-0.001260992

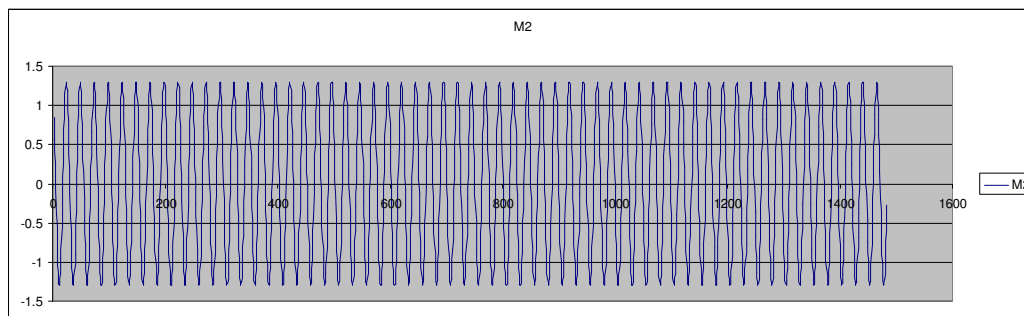
Substituting the values for the harmonic constants at Aberdeen in the equation for water height prediction yielded:

$$H(t) = H_0 + A_{M2} \cos(\omega_{M2}t + \phi_{M2}) + A_{N2} \cos(\omega_{N2}t + \phi_{N2}) + A_{S2} \cos(\omega_{S2}t + \phi_{S2}) + A_{K1} \cos(\omega_{K1}t + \phi_{K1}) + A_{O1} \cos(\omega_{O1}t + \phi_{O1}) + A_{M4} \cos(\omega_{M4}t + \phi_{M4}) + A_{M6} \cos(\omega_{M6}t + \phi_{M6})$$

$$H(t) = 1.3 * \cos((0.505866 * t) + 0.8625) + 0.44 * \cos((0.5236 * t) + 2.1) + 0.3 * \cos((0.4964 * t) + 10) + 0.11 * \cos((0.2625 * t) + 13.63) + 0.13 * \cos((0.2434 * t) + 3.586) + 0.017 * \cos((1.011732 * t) + 2.3634) + 0.002 * \cos((1.5176 * t) + 0.4945)$$

NB: the angular velocities above were given in rad/ solar hour and the phase of each was given in hours.

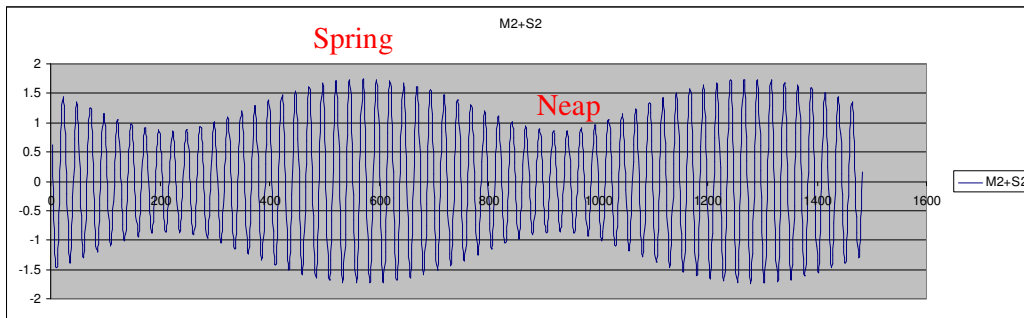
**Figure 13 M2 Constituent for Aberdeen**



The M2 constituent had by far the largest coefficient. This term alone would give the tide if the sun could be neglected, and if the moon orbited in a perfect circle in the plane of the earth's equator. For Aberdeen, starting at midnight on Jan 1, 2001, this term was:

$$M2=1.3 \text{ COS}(0.505866t+0.8625)$$

**Figure 14 M2+S2 Constituent for Aberdeen**

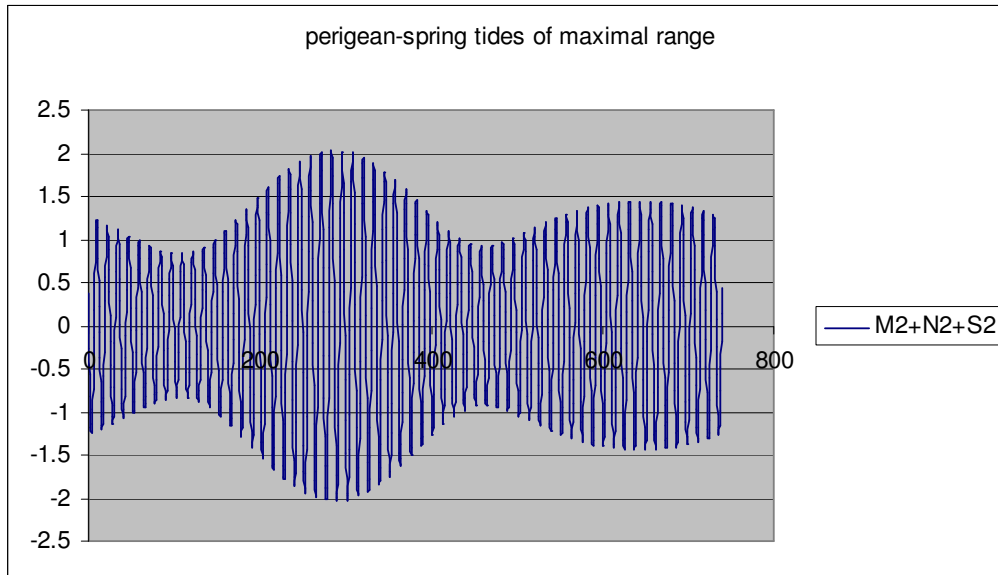


The constituent S2 would give the solar tide if the sun was always in the earth's equatorial plane and the earth's orbit was a perfect circle. The plot of M2 + S2 shows the combined tidal effect of this ideal sun and the ideal moon of the previous figure.

#### Evaluation of Each Tidal Constituent

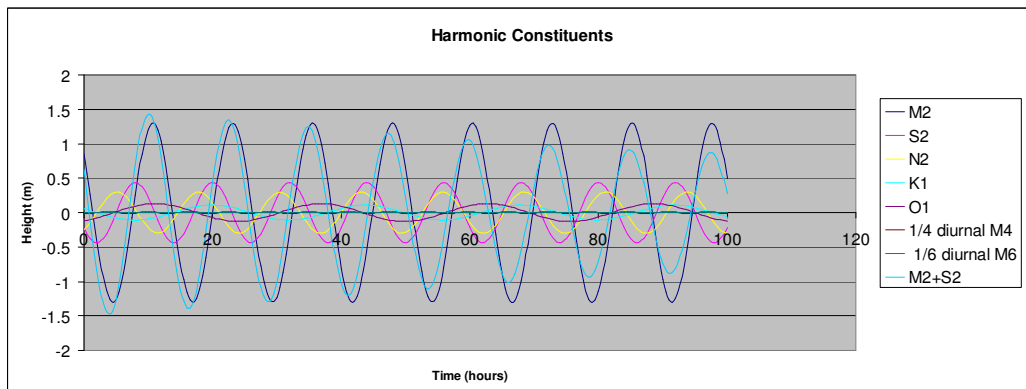
Spring tides occur when  $M_2$  and  $S_2$  are in phase so that both waves peak at the same time causing tides of greater range. Neap tides occur when  $M_2$  and  $S_2$  are out of phase and tend to cancel one another, reducing tidal range. But if the interest lies in tides of maximum range, consider what happens when  $M_2$ ,  $S_2$ , and  $N_2$  all peak at about the same time. This results in the so-called *perigean-spring tides* of maximal range that occur several times a year.

**Figure 15** M2+N2+S2 for Aberdeen, showing Perigean Spring Tides



This format of the harmonic method is repeated for each of the 7 major constituents until a sufficient spectrum of waveforms is obtained in order to predict the tidal variation in water height at that port.

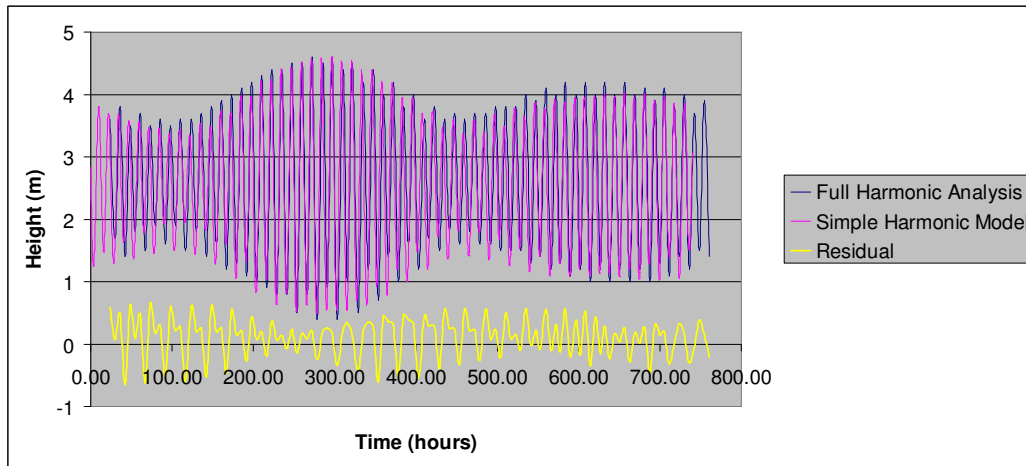
**Figure 16** 7 Major Constituents for Aberdeen (Jan 2001)



### 3.1.2 Validating the Simple Harmonic Model

When the amplitudes and phases of each constituent were added together the resultant waveform was then compared with predicted data for the same port resulting from full harmonic analysis using more than the first 7 basic tidal constituents

**Figure 17 Comparison of Predicted Data from Simple Harmonic Model with that of Fully Harmonic Analysis for Aberdeen Jan 2001**



The yellow line shows the residual or the difference between the values generated from the simple model and the fully comprehensive harmonic analysis for the same time period and port.

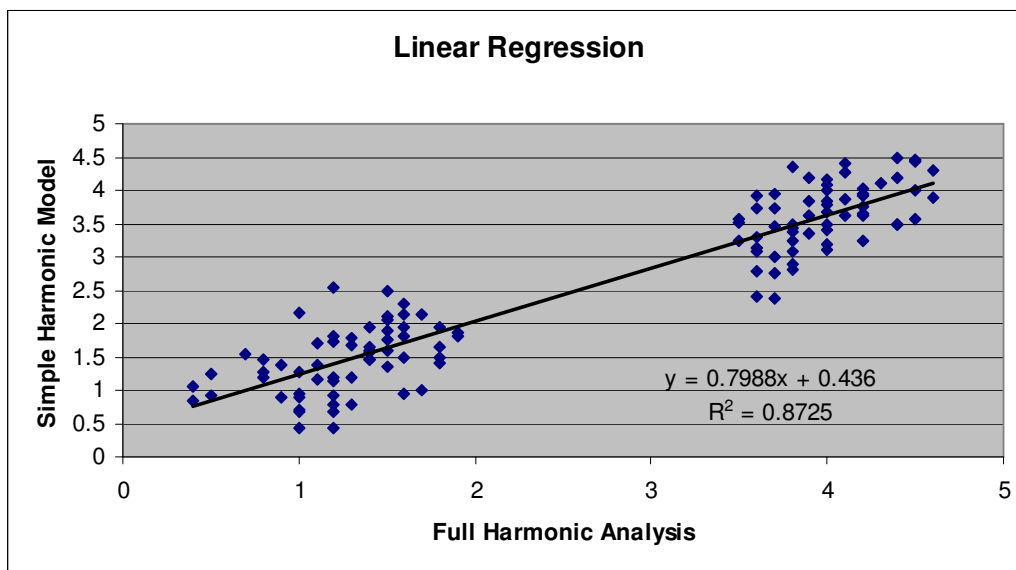
A strong correlation between the two datasets was evident. Whilst the majority of the tidal spectrum can be recreated using the 7 main tidal constituents chosen here, there will inevitably be a number of harmonics which are not accounted for. This was clearly shown in the residual. However, for the purpose of providing reasonably accurate data to the channel model, this level of accuracy was deemed to be sufficient. The average of the residual values for Aberdeen over this one month time period was 0.09m. So on average the predicted data from the simple harmonic model was slightly under-predicting compared to the actual measured data. This could be due to other resonant frequencies from shallow water effects which the simple 7 constituent approach cannot adequately model.

It should be noted that the variation of the tidal height over time was very well modelled by the simple harmonic model and that any slight under-prediction of the amplitude of the water height was significantly less important than failure to model the phase and overall variation over time. Indeed, it is the temporal variation which will have the greatest implications when performing a

supply/demand matching analysis. Thus the predicted data for tidal variation of water height at the 2 selected ports was sufficiently accurate to allow this simple harmonic model to be used in the enhanced channel model.

A simple linear regression analysis was also performed to ascertain what degree of accuracy the predicted data from the simple harmonic model had with that of the full harmonic analysis.

**Figure 18 Linear Regression Analysis of Data for Aberdeen Jan 2001**



Equation: simple harmonic model value =  $0.7988x$ (full harmonic analysis value) + 0.436

Correlation Coefficient = 0.8725

This showed a good fit in terms of the correlation between measured data and the predicted data from the harmonic method.

This entire process was repeated for the Secondary Port of Rona. For the purposes of the channel model, this was the other port located at the other side of the idealised channel of the Pentland Firth and representing the other independent reservoir of water.

**Figure 19 Comparison of Predicted Data from Simple Harmonic Model with that of Fully Harmonic Analysis for Rona Jan 2001**

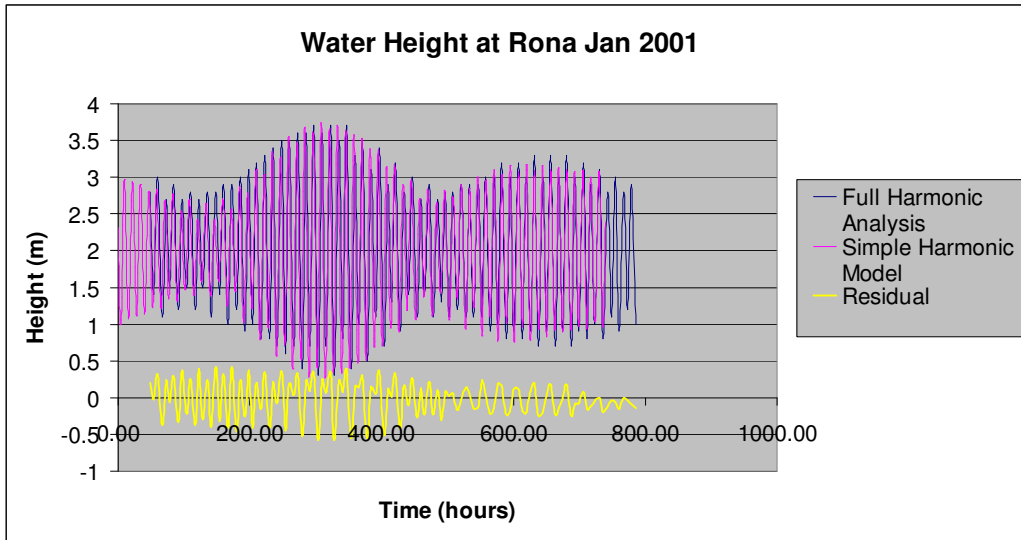
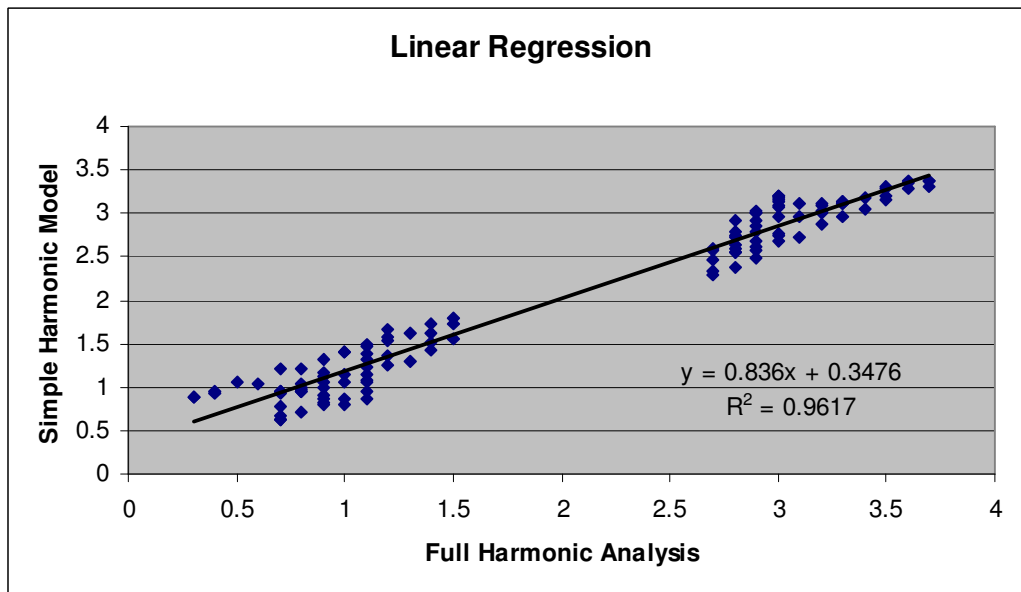


**Figure 20 Linear Regression Analysis of Data for Rona Jan 2001**

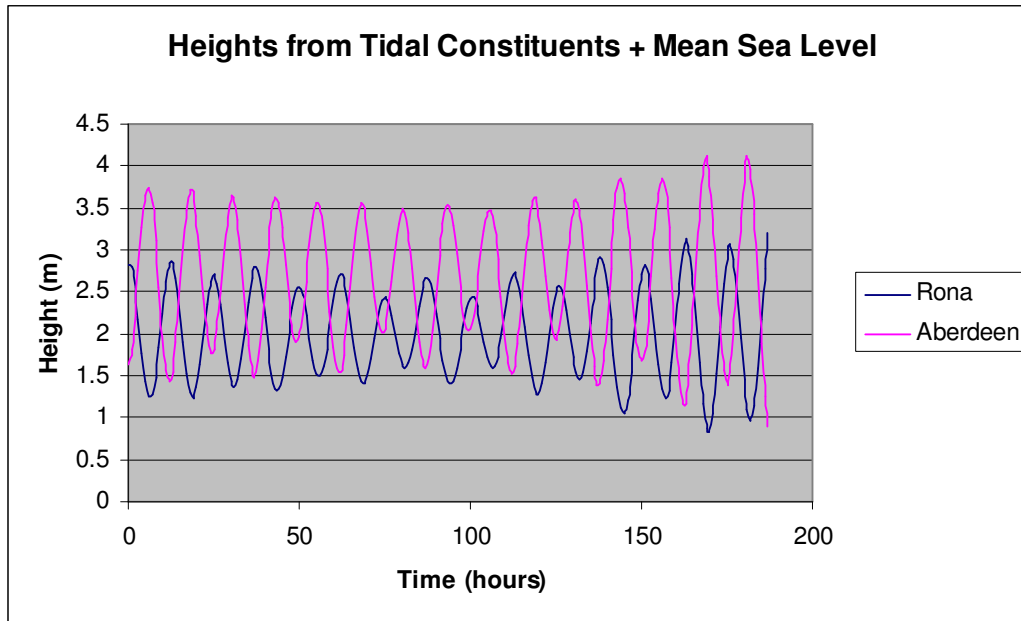


Equation: simple harmonic model value = 0.836x(full harmonic analysis value) + 0.3476

Correlation Coefficient = 0.9617

Now that the tide height variation had been established for each of the 2 ports either side of the idealised channel, the next step was to calculate the theoretical flow velocity which would result from the pressure gradient caused by the head difference existing between the two separate water heights.

**Figure 21 Predicted Tidal Heights for 2 Ports Either Side of Channel**



This was performed using the simple relationship:

$$V_{th} = \sqrt{2g(h_1 - h_2)} \text{ from Section 2.4.9.}$$

This provided a theoretical value for the undisturbed velocity in the channel.

### **3.2 Accounting for Local Non-Astronomical Variations**

In addition to influences from the moon and sun, the velocity experienced by an MCT device placed in that channel is also heavily influenced by a combination of other factors including:

- Depth, width and roughness of channel
- Blockage effect of channel
- Position of energy extraction devices in the flow
- Ebb/flow differences and energy hotspots

- Disparities between inlet and outlet flow rates in channels
- Directionality of the flow
- Storm surges or weather fronts
- Accelerated and retarded flow rates at site of energy extraction depending on y and z position, as identified by I Bryden of RGU [37]

Once the undisturbed flow velocity for the tidal current in the channel had been determined it was then possible to correct and improve these theoretical values to account for local variation in the flow. This was dependent on the bathymetry of the site in question as well as width and depth of the channel etc.

### **3.2.1 Depth, Width and Roughness of Channel**

Whereas the previously developed model used a channel loss correction factor  $K_L$  to bring the theoretical current velocity in the channel down to a value close to the measured values for current velocity at that site, the enhanced channel model will calculate a reduction factor based on the bathymetry of the channel. This will, of course, negate the need for measured data at the site of interest.

Using Manning's equation for flow rate in the channel [35, 41]:

$V = (1/n)R^{2/3}S^{1/2}$  where:

- V is the cross-sectional average velocity (m/s)
- N is the Manning coefficient of roughness
- R is the hydraulic radius (m)
- S is the slope of the channel bed (m/m)

n can range from:

Bed Material	n value
Concrete	0.012-0.018
Firm Soil	0.025-0.032
Coarse Sand	0.026-0.035
Gravel	0.028-0.035
Cobble	0.030-0.050
Boulder	0.040-0.070

[41]

Taking a simple channel of uniform cross-section and with the following dimensions and bathymetry, a value for the mean flow rate is calculated as follows:

**Figure 22 Schematic for channel dimensions & bathymetry**

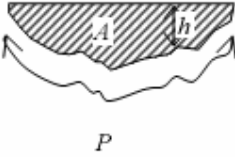


$n = 0.035$  (course sand), length = 10,000m, inlet height=53.5m, outlet height=51.5m, width = 1000m and the hydraulic radius is given by  $R = A/P$  where  $A$  = cross-sectional area of the flow and  $P$  is the wetted perimeter.

**Figure 23 Hydraulic Radius**

**Box 2: Hydraulic Radius**

The hydraulic radius ( $R_h$ ) is sort of like an “equivalent radius” that represents a combined effect of cross-sectional area ( $A$ ) of bottom/bank shape (wetted perimeter,  $P$ ):  $R_h = A/P$ . For wide, shallow streams (depth  $< 0.05$  width), the hydraulic radius is essentially the average depth,  $R_h \approx h$ .



[41]

For the channel above, the hydraulic radius is  $R = \frac{wh}{w + 2h}$

This gives hydraulic radius at inlet and outlet of

$$R_{\text{inlet}} = 48.3\text{m}$$

$$R_{\text{outlet}} = 46.7\text{m}$$

The average hydraulic radius,  $R_{\text{average}} = 47.5\text{m}$

Here, the slope is considered to be ratio of the head difference to the length of

$$\text{the idealised channel or } \frac{h_1 - h_2}{l} = \frac{53.5 - 51.5}{10,000} = 2e^{-4} \text{ m/m}$$

$$V = (1/n)R^{2/3}S^{1/2}$$

$$= \frac{1}{0.035}(47.5)^{2/3}(0.0002)^{1/2}$$

$$= 5.3 \text{ m/s}$$

Since the Bernoulli's theoretical current velocity does not account for the channel dimensions and bathymetry but the Manning's flow rate does; this can be used to approximate the frictional effects of the channel by equating the former with the latter to calculate a value for  $K_L$ .

Now comparing the mean velocity from Manning's equation to the theoretical value from the form of Bernoulli's equation allows us to arrive at a more accurate value for a frictional loss coefficient in the channel  $K_L$  compared to

the value calculated in the previously developed channel model. This new improved equation for find the value of  $K_L$  for use in the enhanced channel model is far more flexible in that it allows the channel dimensions and bathymetry to be changed and will account for those changes in the value of  $K_L$ . i.e

$$\text{Bernoulli's: } V = \sqrt{\frac{2g(h_1 - h_2)}{K_L}} \quad (\text{from previously developed model})$$

$$\text{Mannings: } V = (1/n)R^{2/3}S^{1/2} \quad (\text{accounting for channel dimensions and bathymetry})$$

Calculate  $K_L$ : (new improved equation for channel frictional loss)

$$\begin{aligned} \sqrt{\frac{2g(h_1 - h_2)}{K_L}} &= (1/n)R^{2/3}S^{1/2} \\ K_L &= \frac{(2g(h_1 - h_2))^2}{((1/n)R^{2/3}S^{1/2})^2} \\ &= \frac{4g^2(h_1 - h_2)^2}{\left(\frac{R^{4/3}S}{n^2}\right)} \end{aligned}$$

---

And using the channel above as an example:

$$\text{Bernoulli's: } V = \sqrt{\frac{2g(h_1 - h_2)}{K_L}} = \sqrt{\frac{2g(53.5 - 51.5)}{K_L}} = 6.3 \text{ m/s}$$

$$\text{Mannings: } V = 5.3 \text{ m/s}$$

$$\begin{aligned} \text{Calculate } K_L: \quad K_L &= \frac{6.3^2}{5.3^2} \\ &= 1.4 \end{aligned}$$

---

This value of  $K_L$  will be applied to the theoretical velocity in the channel at each timestep.

Now that the theoretical current velocity has been corrected for the channel bathymetry, the mean channel velocity can be corrected for channel depth to

give a velocity profile against which the vertical position of the MCT's in the channel may be assessed.

### **Velocity Profile with Depth**

The current will vary in velocity as a function of the depth of the flow. The velocity at a height above the seabed,  $Z$ , approximately follows a seventh power law as a function of depth in the lower half of the flow, thus:

$$V_z = \left( \frac{Z}{0.32h} \right)^{1/7} V_{mean}, \text{ for } 0 < Z < 0.5H$$

and in the upper half

$$V_z = 1.07V_{mean}, \text{ for } 0.5H < Z < H$$

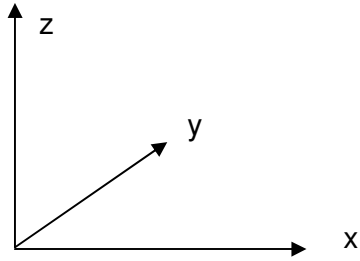
[31]

It can be shown from this approximation that 75% of the energy is to be found in the upper half of the flow. [31]

In practice, for areas of high flow velocities, there will be more complex interactions involving turbulence in the flow, which means this approach was not ideal. However, it was an improvement on the previously developed channel model which simply applied a fudge factor of  $\frac{1}{2}$  to get the effective channel area experiencing the calculated mean current velocity for the channel.

The importance of vertical position in the water column is crucial to the velocity available to each MCT. This is reflected by MCT Ltd who clearly place their rotor axis in the upper half of the flow.

The inclusion of a variable for vertical position in the water column, namely  $z$ , allows the user to experiment with the effect of this parameter on the power output of the MCT devices.



### 3.2.2 Packing Density of MCT devices in the flow

Devices were spaced at twice the rotor diameter laterally and 10x the rotor diameter longitudinally according to the findings of the report [14] which gave packing densities for the following number of units:

- For water depth 20-25m, 5m rotor diameter used, giving 1800 units/km<sup>2</sup>
- For water depth 25-40m, 10m rotor diameter used, giving 82 units/km<sup>2</sup>
- For water depth .40, 20m rotor diameter used, giving 38 units/km<sup>2</sup>

The packing density together with the number of turbines place in that channel would ultimately affect the solidity of the channel and the value of  $K_T$ .

### 3.2.3 Blockage Effect of Placing MCT's in a Channel

Now that a good model had been established to generate the undisturbed flow velocity in the channel, the next step was to correct this for blockage effects due to placing MCT's in the channel.

The effect of blockage was investigated by installing a number of MCT's,  $n$ , in the channel with a turbine coefficient  $K_T$ . With  $K_T$  known (representative of the number of turbines, swept area and channel cross-sectional area) and with the frictional losses in the channel already calculated in Section 3.2.1, the new channel velocity could be estimated from:

$$V_{\text{new}} = \sqrt{\frac{2g(h_1 - h_2)}{1 + K_L + K_T}}$$

As already shown in Section 2.4.9, with increasing  $K_T$  (meaning more turbines placed in the channel), the overall result is decreasing current velocity in that channel. However, it was difficult to determine the relationship between a number of turbines arranged with a certain packing density in a channel and the equivalent solidity for the cross-sectional area dealt with in the above equation.

### 3.2.4 Ebb and Flood Differences

A difference between ebb and flood rates is very common in most channels.

However, the idealised theoretical velocity resulting from the head loss equation in the channel model could not appreciate this phenomenon.

Therefore an ebb or flood correction factor was introduced to ensure this was fully modelled.

ebb/ flood speed differences, convention is to express flood usually as 100% (or 1) and express ebb as a fraction of that :									
e.g ebb flow coefficient t = 1.0, ebb flow coefficient t = 0.8									
if flow direction = +ve, then $V_{\text{flood}} = \text{flood coefficient } t \times Vz$ or									
if flow direction = -ve, then $V_{\text{ebb}} = \text{ebb coefficient } t \times Vz$									

Allowing for these parameters in the channel model algorithm added a further degree of realism, in which local flow phenomena such as ebb/flood differences could be carefully considered and modelled accordingly. Data on the flow angles and rates for a number of sites on Scotland's coasts is readily available [30].

Figures 23 and 25 show the impact of applying an ebb factor of 0.7 and 0.6 for Pentland Firth spring and neap tides respectively.

### 3.2.5 Directionality of Flow

In addition to the magnitude of the flow in ebb and flood varying greatly, there may also be a variation in the angles of the mean flow direction in ebb and flood. In fact, it is unlikely that any channel would experience a 180 degree difference in flow angles for ebb and flood. This of course will affect the component of the mean velocity to which any MCT unit is subjected, assuming the MCT is considered to be directionally fixed and cannot yaw into the incoming flow direction like a large scale wind turbine. This is illustrated below:

Consider that flow may be at an angle to the direction in which MCT is facing. This may also change with flood or ebb conditions Flow Angles in ebb and flood direction (expressed as deviation from purely axial flow)			
e.g.	flood angle (degrees) $\theta+$ =	5	
	ebb angle (degrees) $\theta-$ =	8	
so	$V_A = V_U \cos(\theta+)$	$V_U$ = Undisturbed Velocity $V_A$ = Axial component of Velocity $\theta+, \theta-$ = Angles of deviation (flood, ebb respectively)	
	$V_A = V_U \cos(\theta-)$		
<p style="text-align: center;"><b>FLOOD</b></p>			
This gives the actual flow velocity available to turbine rotors which can then be input into the power equation initially without any limitations such as cut-in speed and rated speed in order to provide the raw power available to the MCT's			

### **3.2.6 Accelerated and Retarded Flow Rates at Site of Energy Extraction**

There have significant studies carried out on wake development downstream of wind turbines, many of which can be applied to the broadly analogous area of marine current turbines. However, the impact of these studies is limited to commenting on the optimum placement of devices relative to one another in an open channel. They cannot address the impact of energy extraction on flow velocities in that channel.

Wind turbines operate in atmospheric flows, where the upper boundary is at a significantly large distance from the volume in which energy extraction takes place. Conversely tidal currents are constrained within a relatively small volume between the seabed and surface and may be further constrained in a channel by means of the land masses on either side. It has been shown in a recent study (37) that the upstream and downstream effects of installing a 'farm' of tidal turbines are potentially more significant than for a wind farm.

From this previous study there were **two** main conclusions regarding the effects of energy extraction. Firstly, even when a significant amount of the potential energy passing through a cross-section is removed, the downstream head loss and mean velocity reduction are relatively small. Secondly, it was determined that more marked reductions in the stream wise flow velocity occurred more locally both upstream and downstream of the site of tidal energy extraction and at the mid layer region of the vertical velocity profile where the rotors of the MCT's were placed.

In more detail it was shown in this previous study that:

- Even when 50% of the potential energy passing through a cross-section is extracted, the downstream head loss is only of the order of 2%, with the velocity reduced by a similar amount throughout the domain.
- The largest velocity deficit in comparison with the unexploited site occurs in the immediate vicinity and downstream wake of the extraction site (7.5% of the undisturbed flow velocity)
- In the surface and bottom layers where no extraction is taking place, upstream of the energy extraction site the velocity is reduced
- However downstream of the extraction site, the velocity is increased (20% at  $\sigma = 0.05$  (bottom), and 1.5% at  $\sigma = 0.95$  (top)), even although energy has been extracted from the system.

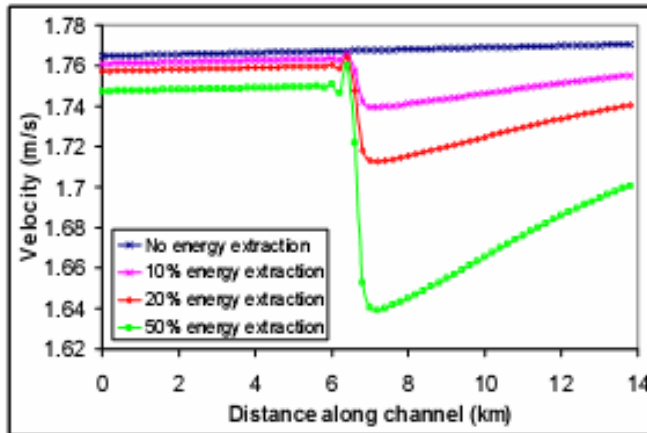
It should be noted that all of these conclusions were drawn by assuming steady state conditions. In reality there would be dynamic feedback effects but this approach provided a reasonable approximation for the enhanced channel model to make use of.

The most important concern for the purposes of the enhanced channel model in this thesis is the velocity reduction in the immediate vicinity and downstream wake of the site of energy extraction as it is this reduction which will affect the output of the turbines. The fact that the flow resumes almost the same velocity profile as it had upstream of the energy extraction site is largely irrelevant unless multiple separate farms are being planned in the same channel.

The experiment in (37) was conducted using a layer integrated approach with 10 layers and each layer adopting the term  $\sigma$ . Energy was extracted from layers 3,4,5,6 and 7 which is in keeping with a turbine blade diameter of around 15 metres, giving 6 metres clearance at the sea-bed to prevent fouling and avoid boundary layer flows, and 9 metres clearance at the surface

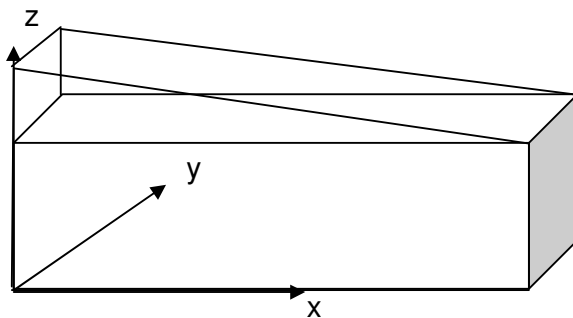
to allow for low tidal amplitudes, storm surge, wave action. Therefore  $\sigma$  layer 5 could be used to investigate the exact vertical position of energy extraction. This is shown in figure 24.

**Fig 24 Comparison of 3-d stream-wise flow development with varying levels of energy extraction layer integrated velocity for  $\sigma$ -layer 5**



To incorporate these phenomena into the enhanced channel model the following approach was developed. The channel was given reference axes x,y and z to represent position in the channel as well as channel length, width and depth respectively.

**Fig 25 Channel Model Schematic with Reference Axes**



A variable  $\sigma$  was adopted (as in (37)) to represent the vertical position as a ratio of the channel depth. Dividing the vertical flow profile into 10  $\sigma$  layers it was possible to impose a velocity reduction in layers 3 to 7, in keeping with

the approach used in (37). This would provide a % reduction in velocity which would be applied to the vertical velocity profile at those layers to give a final value for available velocity to the MCT devices. The extent of the reduction in velocity was gleaned from the results shown in fig 24 and is given by Table 6.

**Table 6      % Reduction of Velocity for Layers 3-7 (of 10) at Varying Levels of Energy Extraction**

<b>Energy Extraction as a Percentage of Total Energy Passing Through CSA</b>	<b>Velocity Deficit as an Approximate Percentage of Undisturbed Flow Velocity</b>
0%	0%
10%	2%
20%	3%
50%	8%

### **3.2.7 Storm Surges or Weather Fronts**

Having considered the complexity of accounting for pressure variations or wind velocity in channel model, it was decided that to include a storm surge component was out with the scope of this thesis. However, it could conceivably be addressed in any further work.

### 3.3 Turbine Performance Details & Channel Solidity

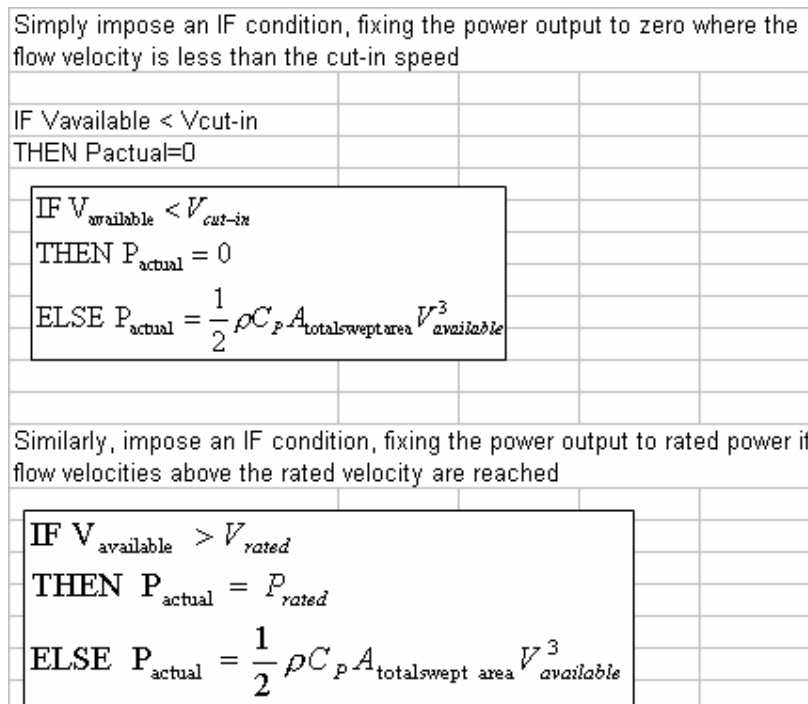
#### Power Coefficient

Although MCT's like wind turbines have rotors whose power coefficient (or  $C_P$ ) varies with tip speed ratio, the operating range of a MCT rotor is far narrower than that of a wind turbine. Hence the cut-in speed would have a  $C_P$  fairly close to the rated speed. For simplicity a constant value of 0.4 was adopted. Future work could look at implementing a power curve for the MCT device.

#### Imposition of Cut-in Velocity and Rated Velocity on Power Equation

A simple IF condition was implemented to impose the rated and cut-on velocities of the MCT. These values are specific to the model and manufacturer of the turbine and can be input to the model.

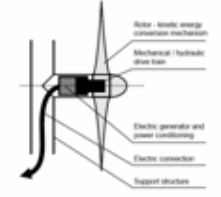
**Figure 29 IF Condition for Rated and Cut-in Conditions**



The actual power output from an MCT was further reduced by efficiency losses from the gearbox and generator and indeed the power coefficient of the turbine rotor (usually around 0.4)

**Figure 27 Turbine Details Input Module**

<b>TURBINE DETAILS</b>		
Manufacturer		MCT Ltd.
Model		Twin Rotor 1MW Rated
Vrated (m/s)		2.35
cutin speed (m/s)		0.75
Prated (kW)		1061.3914
Cut-in Power (kW)		38.63708
Power coefficient (Cp)		0.45
Gearbox/transmission efficiency	$\eta_{gear}$	0.94
Generator efficiency	$\eta_{gen}$	0.95

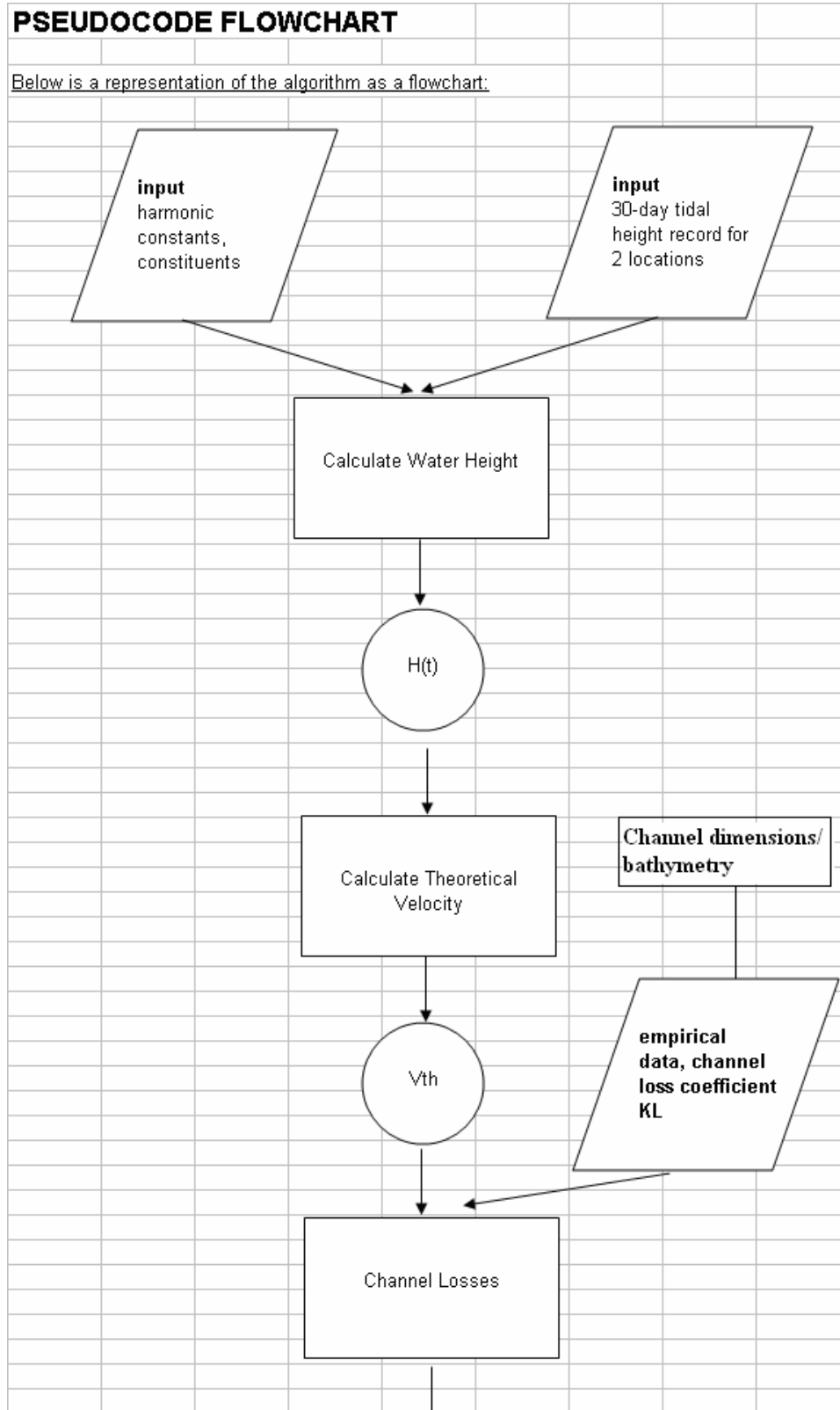
### Final Power Output from Channel Model

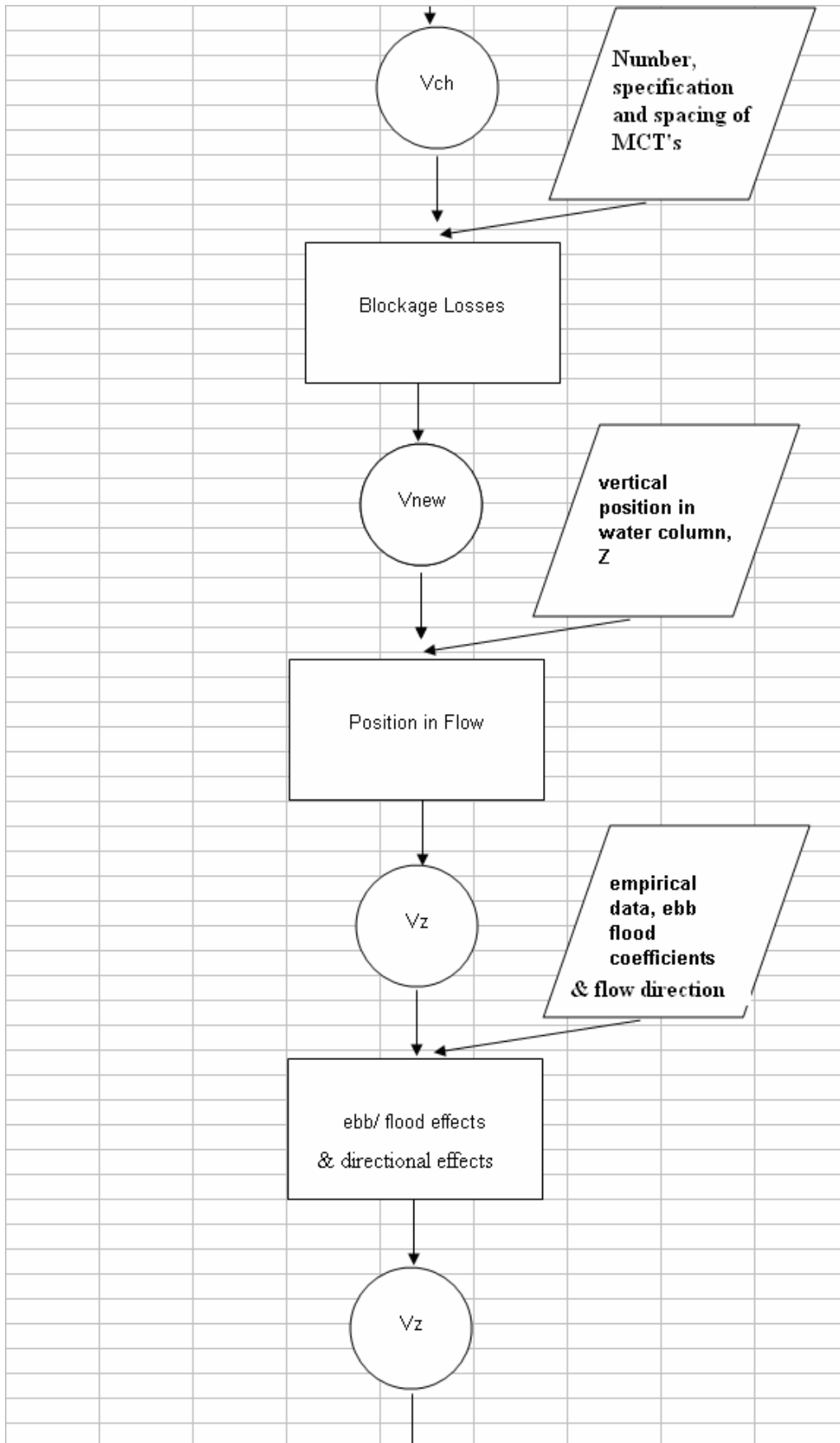
The values for power output from n number of MCT's in the channel formed the final output from the channel model. As such the values of power account for

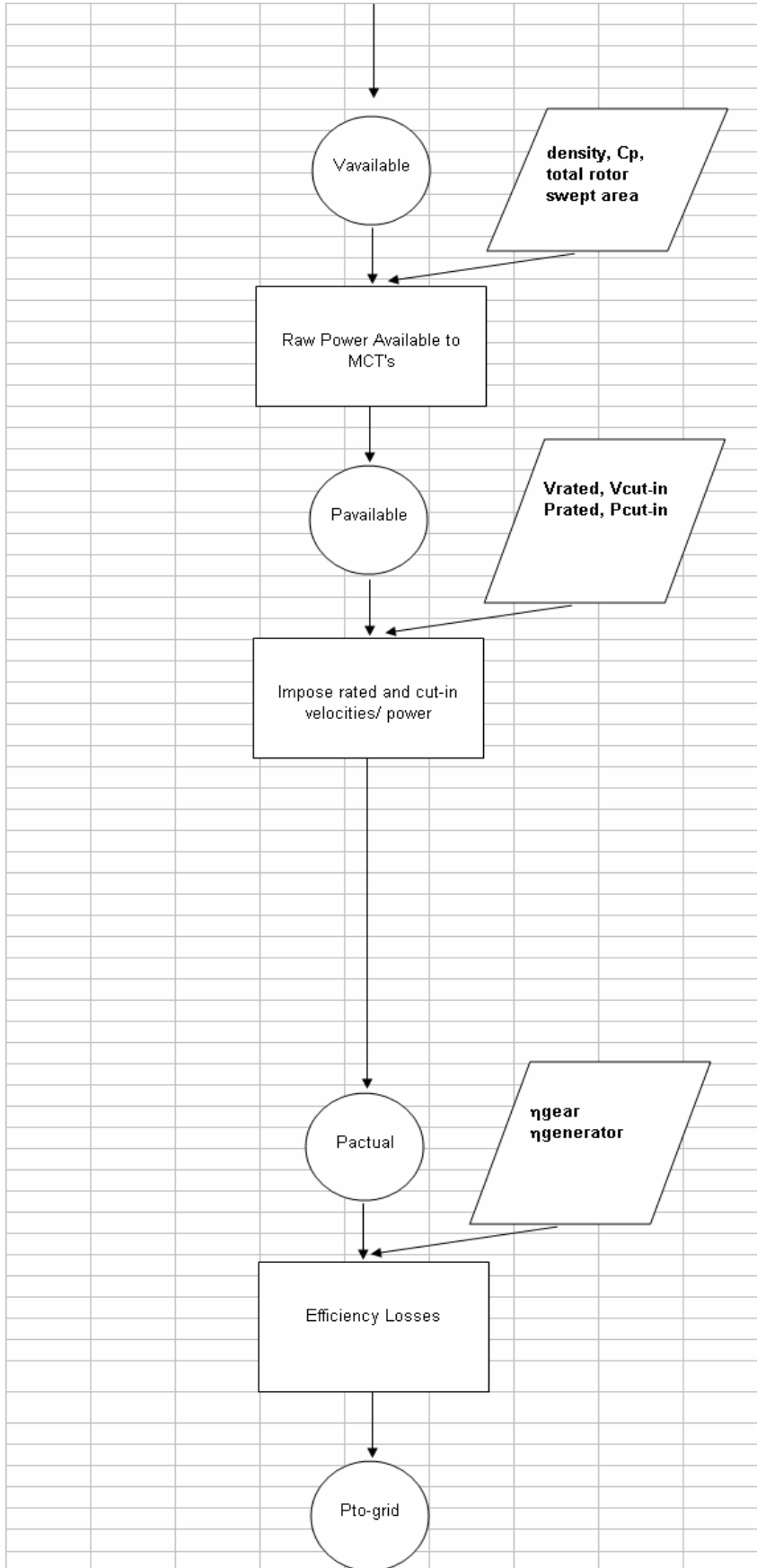
- Velocity available in channel
- Losses to due channel friction
- Losses due to blockage effects of MCT's
- Vertical position in water column
- Ebb/flood differences (magnitude and angle)
- Cut-in Velocity of MCT device
- Rated Velocity of MCT device
- Power coefficient of MCT device
- Solidity of MCT farm with respect to c.s.a of channel
- Efficiency of generator and gearbox

### 3.4 Pseudocode for Enhanced Channel Model Algorithm

Figure 28 Flowchart for Pseudocode







**Discrete Breakdown of Algorithm**

Height at time  $t$  is given by the mean tide height plus the sum of the main astronomical constituents :

$$H(t) = H_0 + M2 + N2 + S2 + K1 + O1 + M4 + M6$$

$$H(t) = H_0 + A_1 \cos(t + \phi_1) + A_2 \cos(t + \phi_2) + A_3 \cos(t + \phi_3) + A_4 \cos(t + \phi_4) + A_5 \cos(t + \phi_5) + A_6 \cos(t + \phi_6) + A_7 \cos(t + \phi_7)$$

Calculate theoretical velocity in channel from head loss potential flow :

$$V_{th} = \sqrt{2g(h2 - h1)}$$

Use a combination of Bernoulli's and Manning's equations for flow rate in the channel to get a value for  $K_L$ :

$$\begin{aligned} \sqrt{\frac{2g(h_1 - h_2)}{K_L}} &= (1/n)R^{2/3}S^{1/2} \\ K_L &= \frac{(2g(h_1 - h_2))^2}{((1/n)R^{2/3}S^{1/2})^2} \\ &= \frac{4g^2(h_1 - h_2)^2}{\left(\frac{R^{4/3}S}{n^2}\right)} \end{aligned}$$

Actual velocity in channel is given by :

$$V_a = \sqrt{\frac{2g(h2 - h1)}{K_L}}$$

$$K_T = C_D \sigma \quad \text{where} \quad n = \sigma \times \frac{A_{channel}}{A_{MCT}} \quad \text{and } n = \text{no. of MCT's in channel}$$

New velocity accounting for losses due to blockage effect from placing MCT's in channel :

$$V_{new} = \sqrt{\frac{2g(h2 - h1)}{K_L + K_T}}$$

Velocity variation with depth in water column is given by :

$$V_z = \left(\frac{z}{0.32H}\right)^{1/7} V_{max} \quad \text{for } 0 < z < 0.5H$$

and in the upper half

$$V_z = 1.07 V_{max} \quad \text{for } 0.5 < z < H$$

ebb/ flood speed differences, convention is to express flood usually as 100% (or 1) and express ebb as a fraction of that :

e.g ebb flow coefficient  $t = 1.0$ , ebb flow coefficient  $t = 0.8$

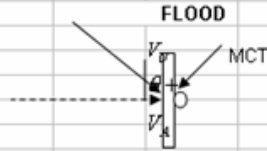
if flow direction = +ve, then  $V_{flood} = \text{flood coefficient } t \times V_z$  or

if flow direction = -ve, then  $V_{ebb} = \text{ebb coefficient } t \times V_z$

Consider that flow may be at an angle to the direction in which MCT is facing. This may also change with flood or ebb conditions  
Flow Angles in ebb and flood direction (expressed as deviation from purely axial flow)

e.g. flood angle  $\theta_+ = 5$   
ebb angle  $\theta_- = 8$

so  $V_A = V_U \cos(\theta_+)$   $V_U =$  Undisturbed Velocity  
 $V_A = V_U \cos(\theta_-)$   $V_A =$  Axial component of Velocity  
 $\theta_+, \theta_- =$  Angles of deviation (flood, ebb respectively)



This gives the actual flow velocity available to turbine rotors which can then be input into the power equation initially without any limitations such as cut-in speed and rated speed in order to provide the raw power

$$P_{available} = \frac{1}{2} C_p \rho A_{totalsweptarea} V_{available}^3$$

Simply impose an IF condition, fixing the power output to zero where the flow velocity is less than the cut-in

IF  $V_{available} < V_{cut-in}$   
THEN  $P_{actual} = 0$

IF  $V_{available} < V_{cut-in}$   
THEN  $P_{actual} = 0$   
ELSE  $P_{actual} = \frac{1}{2} \rho C_p A_{totalsweptarea} V_{available}^3$

Similarly, impose an IF condition, fixing the power output to rated power if flow velocities above the rated

IF  $V_{available} > V_{rated}$   
THEN  $P_{actual} = P_{rated}$   
ELSE  $P_{actual} = \frac{1}{2} \rho C_p A_{totalsweptarea} V_{available}^3$

However, the actual power will then be subjected to losses from the inefficiencies of the gearbox and generator, thus:

Gearbox/transmission efficiency  $\eta_{gear}$

Generator efficiency  $\eta_{gen}$

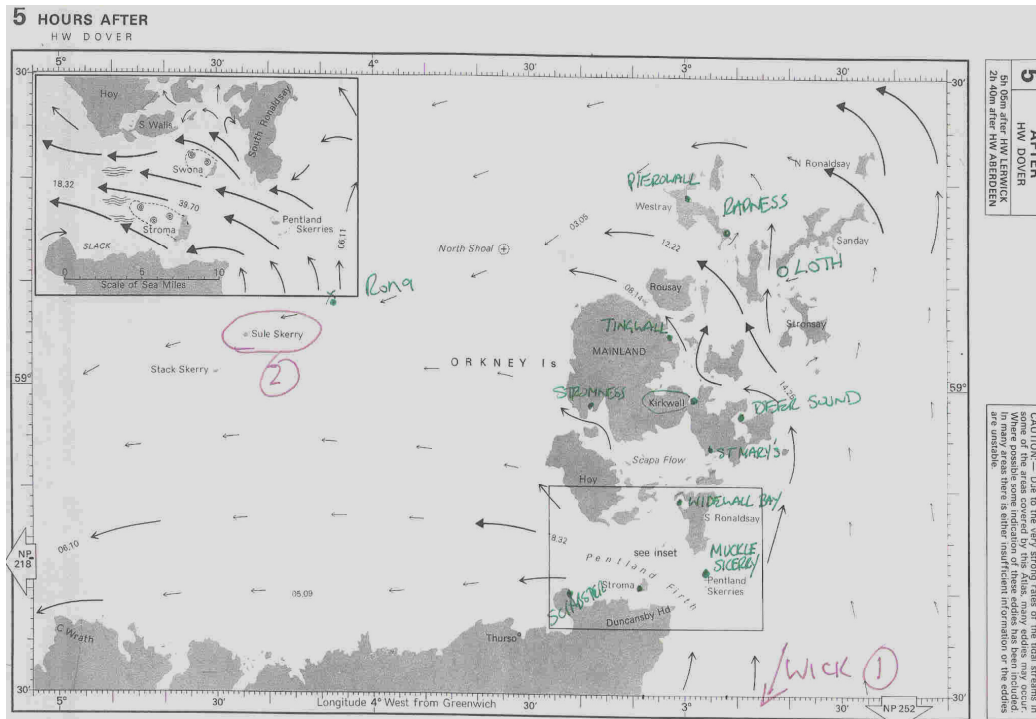
$$P_{to-grid} = \eta_{gear} \eta_{generator} P_{actual}$$

### 3.5 Implementing the Model – An Example

#### 3.5.1 Validation of Predicted Velocity from Channel Model

It was necessary to validate the predicted velocity in the channel to ensure that the channel model was performing to a good degree of accuracy. This was a crucial step and was carried out for both spring and neap conditions. The values for the undisturbed channel velocity  $V_{ch}$  were being checked here against measured values. The Admiralty Tidal Stream Atlas NP209 for Orkney and Shetland Islands provided recorded data for rates of tidal stream, recorded at +/- 6 hours of HW at Dover. This acted as a reference for the times at which the measured data could be compared with the channel model data.

Figure 29 Sample from Admiralty Tidal Stream Atlas [29]

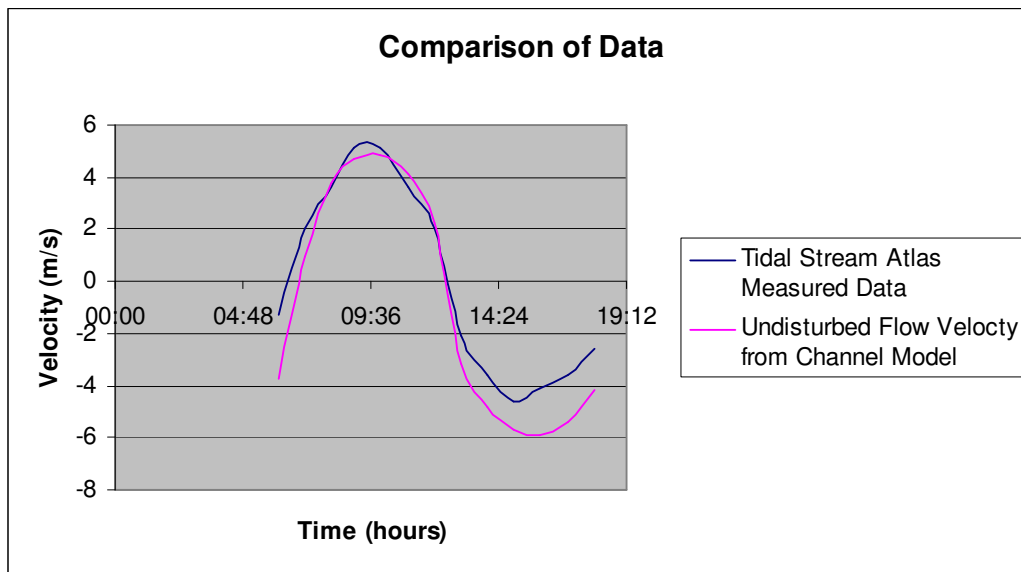


For mean spring measurements from tidal stream atlas, a decision was made to use a date in Jan 2001 which was at spring tide conditions, so data from Jan 11th was used as the predicted data.

**Table 7 Comparison of Channel Model Data and Tidal Stream Atlas Data for Spring Tide Conditions**

Hours After Dover		Actual time	Swona Mean Spring			Undisturbed flow from channel model	Velocity from Channel Model with Ebb Correction factor of 0.7
			Knots	km/h	m/s		
		GMT					
-6	4 hr 5 min after HW Aberdeen	06:09	-2.5	-4.6	-1.3	-3.3	-2.5
-5	5 hr 5 min after HW Aberdeen	07:09	4	7.4	2.1	2.0	2.0
-4	6 hr 5 min after HW Aberdeen	08:09	7	13.0	3.6	4.1	4.1
-3	5 hr 20 min before HW Aberdeen	08:59	10	18.5	5.1	4.8	4.8
-2	4 hr 20 min before HW Aberdeen	09:59	10	18.5	5.1	4.8	4.8
-1	3 hr 20 min before HW Aberdeen	10:59	7	13.0	3.6	4.0	4.0
0	2 hr 20 min before HW Aberdeen	11:59	4	7.4	2.1	1.7	1.7
1	1 hr 20 min before HW Aberdeen	12:59	-4	-7.4	-2.1	-3.5	-2.6
2	20 min before HW Aberdeen	13:59	-7	-13.0	-3.6	-5.0	-3.8
3	40 min after HW Aberdeen	14:59	-9	-16.7	-4.6	-5.8	-4.3
4	1 hr 40 min after HW Aberdeen	15:59	-8	-14.8	-4.1	-5.8	-4.4
5	2 hr 40 min after HW Aberdeen	16:59	-7	-13.0	-3.6	-5.2	-3.9
6	3 hr 40 min after HW Aberdeen	17:59	-5	-9.3	-2.6	-3.9	-2.9

**Figure 30 Comparison of Spring Tide Data**



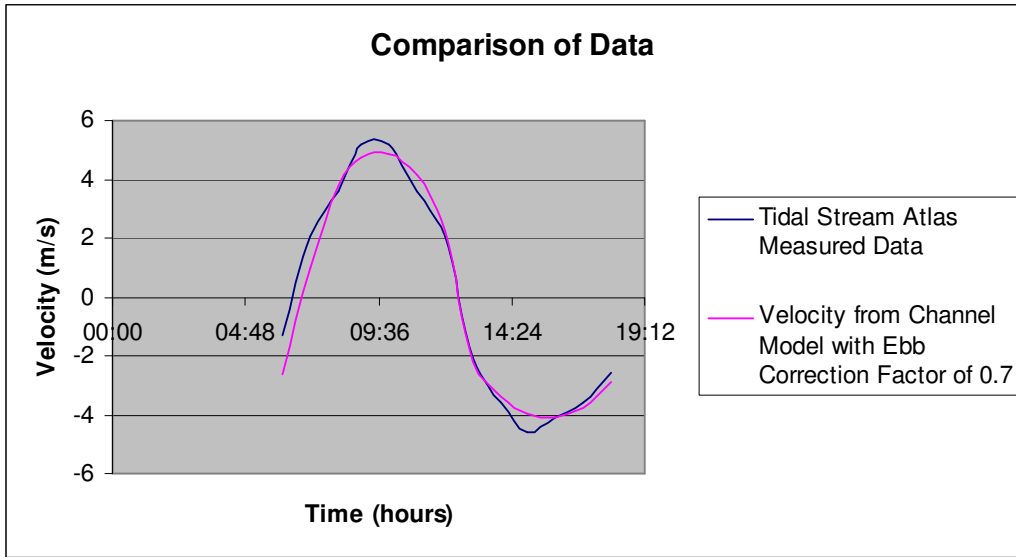
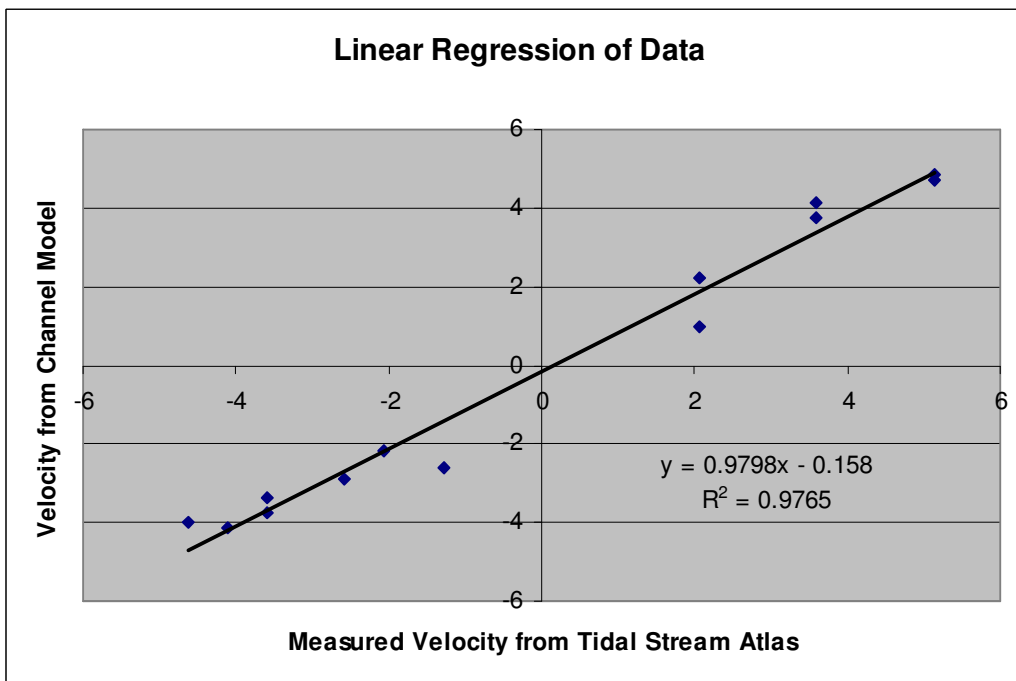


Figure 31 Linear Regression Analysis of Spring Tide Data



Correlation coefficient = 0.9765. This showed a good correlation between the measured data from the Admiralty Tidal Stream Atlas for the mean spring rates and the predicted values from the channel model for the 11<sup>th</sup> January 2001 (spring tide condition).

Similarly, for neap tide conditions this was repeated for 04<sup>th</sup> Jan 2001 and the following results were obtained, again with a close fit.

**Figure 32 Comparison of Neap Tide Data**

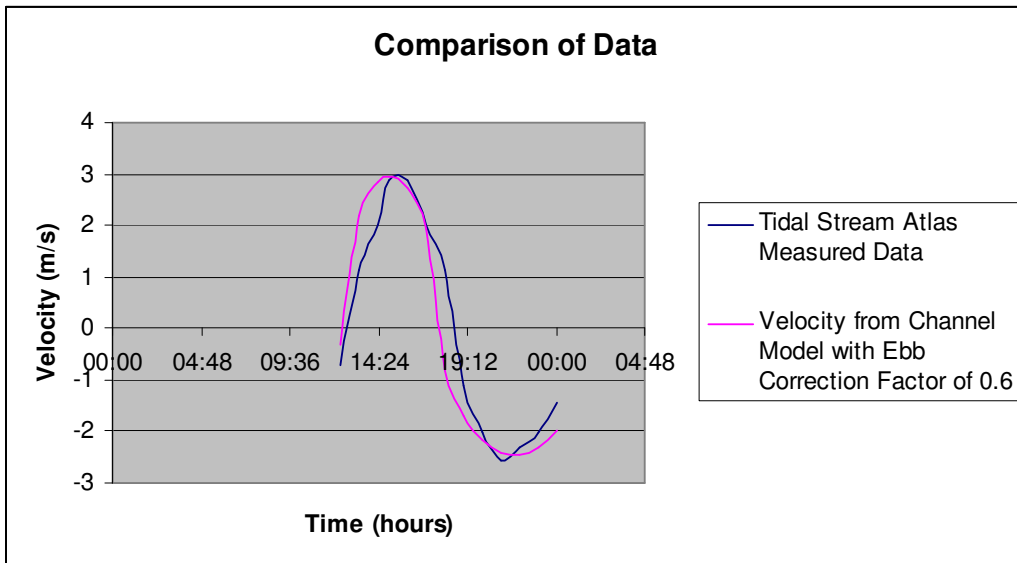
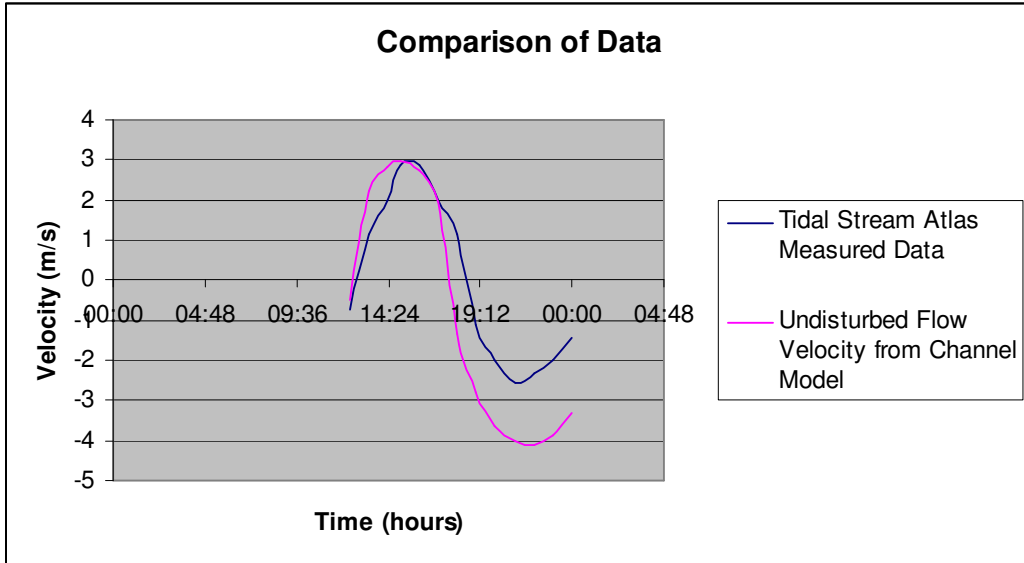
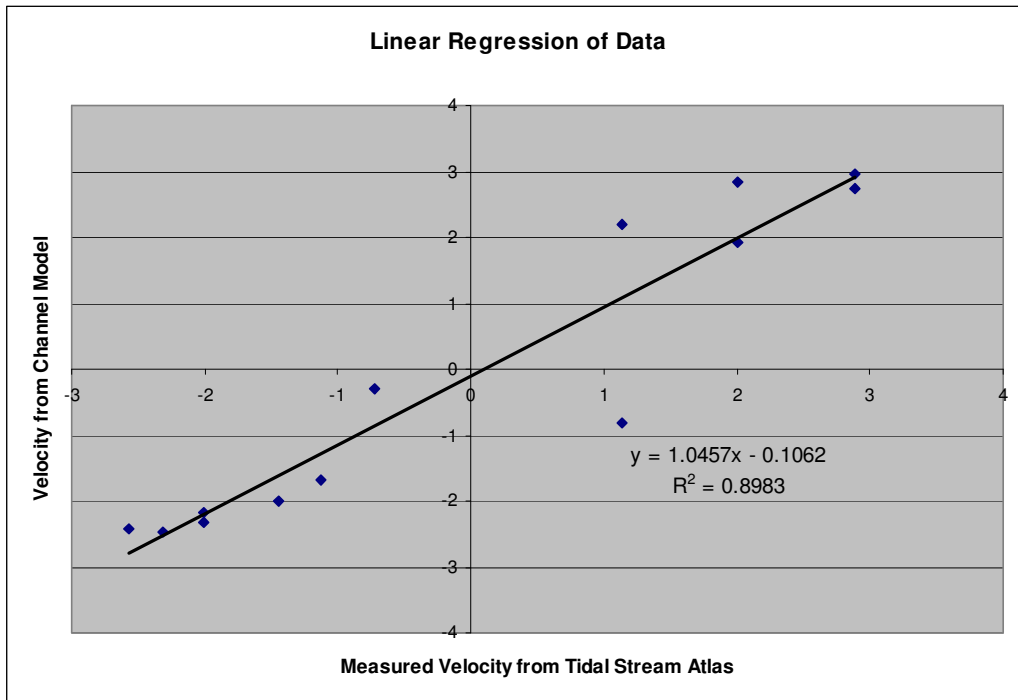


**Figure 33 Linear Regression Analysis of Neap Tide Data**

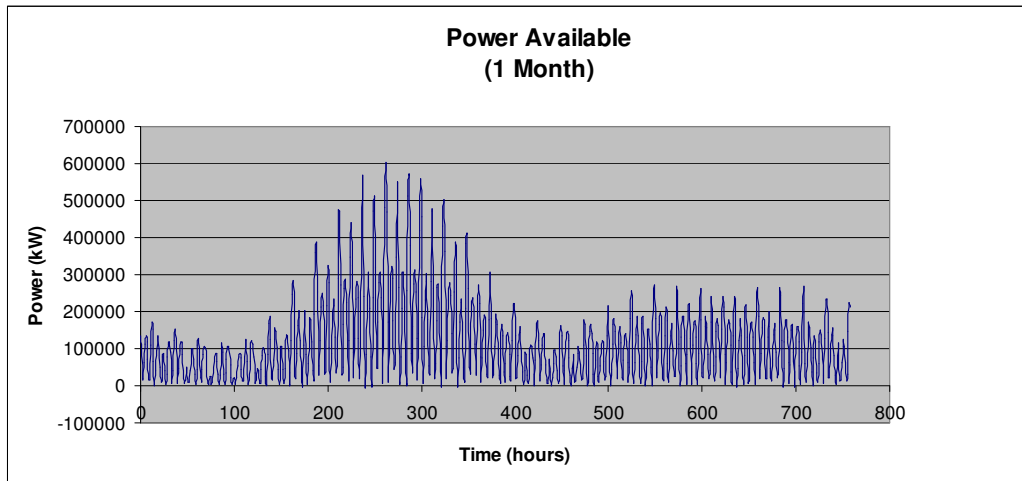


Correlation coefficient = 0.8983

### **Implementation of Enhanced Channel Model**

The power available to a 50-unit farm of MCT's in the Pentland Firth is shown in figure 34. This is the power available to the MCT's from the tidal current flow before corrections are made for gearbox and generator efficiencies and cut-in and rated velocities.

**Figure 34 Power Available to a 50 unit MCT Farm in Pentland Firth over 1 month**



The spring/neap variation can clearly be seen in the power output here and from figure 32 the variation throughout the year (including spring perigee) can be observed.

**Figure 35 Power Available to a 50 unit MCT farm in Pentland Firth over 1 year**

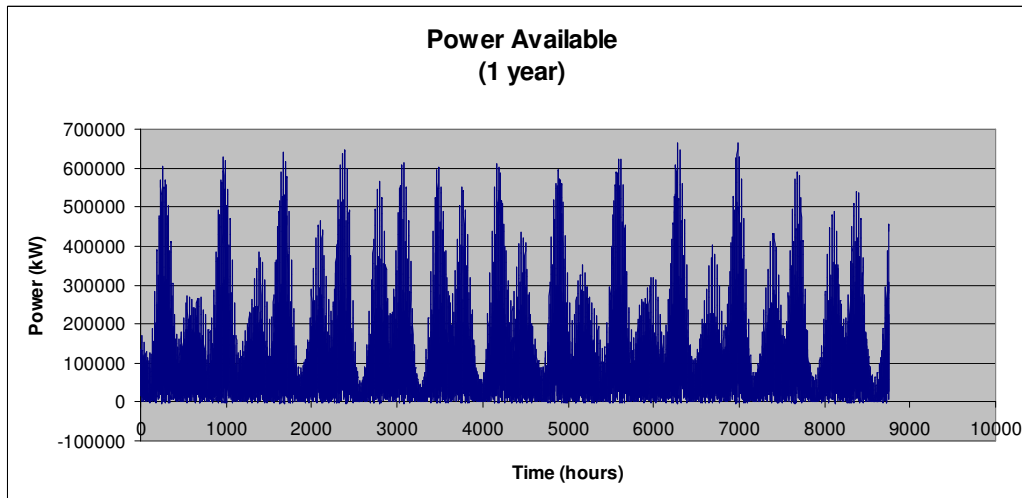
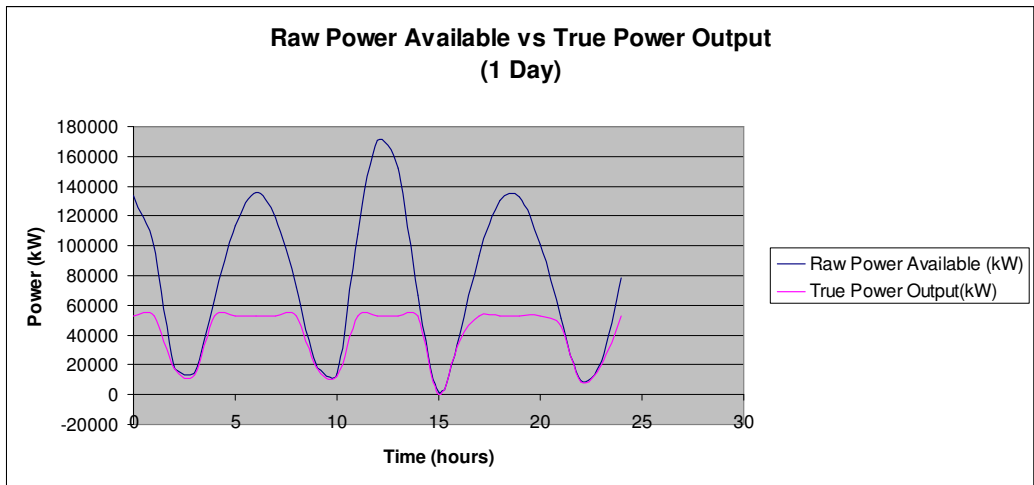


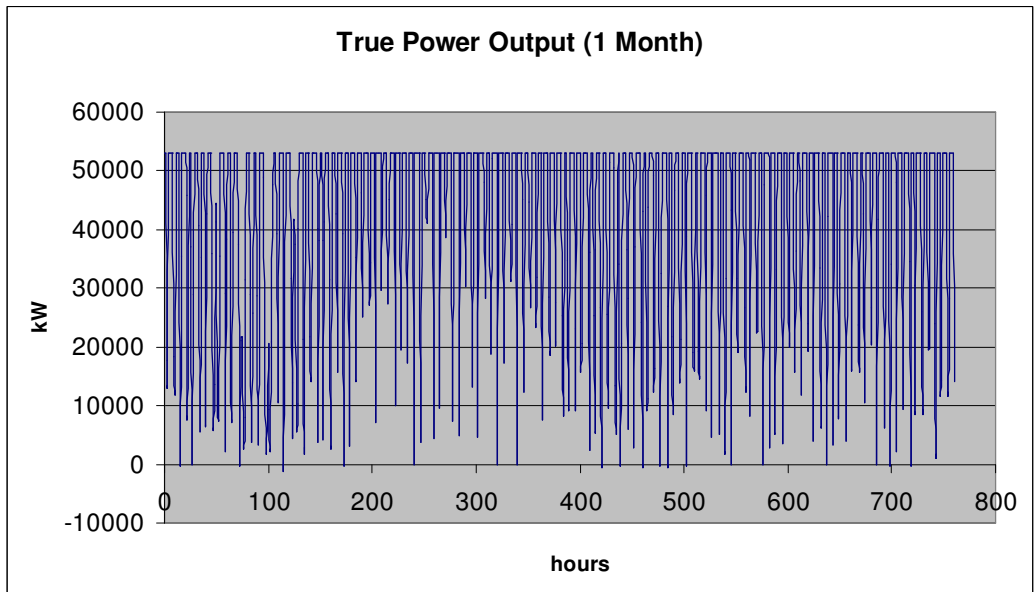
Figure 35 shows how “peaky” the output of a large scale MCT farm can be over the period of 1 year. This was to be expected since even a small change in tidal current velocity can have a drastic change in power due to the cubic relationship between the two.

The power profile once corrected for cut-in and rated conditions looked a little different, given that velocities below the cut-in will produce zero power and velocities in excess of the rated velocity will produce only the rated power and no more. This is reflected in figure 36 below:

**Figure 36 Comparison of Available Power with Turbine Power Output**



**Figure 37 True Power Output for 1 Month**



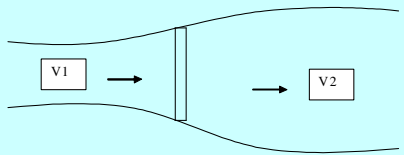
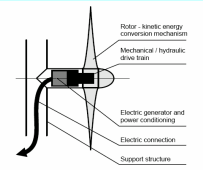
The channel model can also calculate the capacity factor for the MCT farm. This is shown below for the 50 unit MCT farm, where the capacity factor is

0.79. Reducing the rated power of the MCT's will increase this value as the rated power will be achieved more of the time.

**Figure 38 Channel Model Metrics Showing Capacity Factor for 50 Unit Farm of 1MW Rated MCT's**

<b>METRICS</b>	
Site Power Capacity (MW)	12951.658
Rated Power Capacity (MW)	53.069569
Ratio of site capacity to rated capacity (guage of how much available power is being used)	0.0040975
Capacity Factor = Average power/ rated power	
Average Power over year (MW)	41.933673
Capacity Factor	0.7901642

**Figure 39 Full Channel Model User Interface**

<b>CHANNEL MODEL INPUTS AND VARIABLES</b>	
Mean KL Value	1.781 (excludes values above 5)
Max Tidal Current Velocity at 0.000456 KT	5.28
Rated Site Velocity	3.50
Ideal Channel KT value	0.63
No. of MCT's	1
Rotor Diameter (m)	15.9
No. of rotors per MCT device (i.e twin or single)	2
Rotor Area per MCT	397.11302
Total Swept Area of MCT's	397.11302
Channel Depth (m)	60
Channel Width (m)	12900
Channel Cross-sectional Area (m <sup>2</sup> )	774000
Effective Channel Cross-sectional Area (m <sup>2</sup> )	387000
Solidity, $\sigma$ = MCT Swept Area/c.s.a of channel	0.0005131
	
Loss Coefficient due to blockage, $K_t = 8/9\sigma$	0.0004561
Density of Sea water	1025
<b><u>TURBINE DETAILS</u></b>	
Manufacturer	MCT Ltd.
Model	Twin Rotor 1MW Rated
Vrated (m/s)	2.35
cutin speed (m/s)	0.75
Prated (kW)	1061.3914
Cut-in Power (kW)	38.63708
Power coefficient (Cp)	0.45
Gearbox/transmission efficiency	— gear 0.94
Generator efficiency	— gen 0.95
	
<b><u>METRICS</u></b>	
Site Power Capacity (MW)	13108.057
Rated Power Capacity (MW)	1.0613914
Ratio of site capacity to rated capacity (guage of how much available power is being used)	8.097E-05
Capacity Factor = Average power/ rated power	
Average Power over year (kW)	840.50505
Capacity Factor	0.7918898

### **3.10 Adaptation of Model to MERIT**

In order to adapt the channel model for use with the supply demand matching software MERIT, there were two options available.

- Option 1**     Configure Entrack to import output data from the model which then would feed the data into MERIT for supply demand matching analysis
  
- Option 2**     Construct an interface for a TIDAL resource supply option in MERIT allowing the output velocity from the channel model to be added to the My SQL database for MERIT to map to

Given time constraints, the option used was option 2; simply because this was the first option to be made readily available by the kind work of Jae-Min Kim and Jun Hong of ESRU, University of Strathclyde.

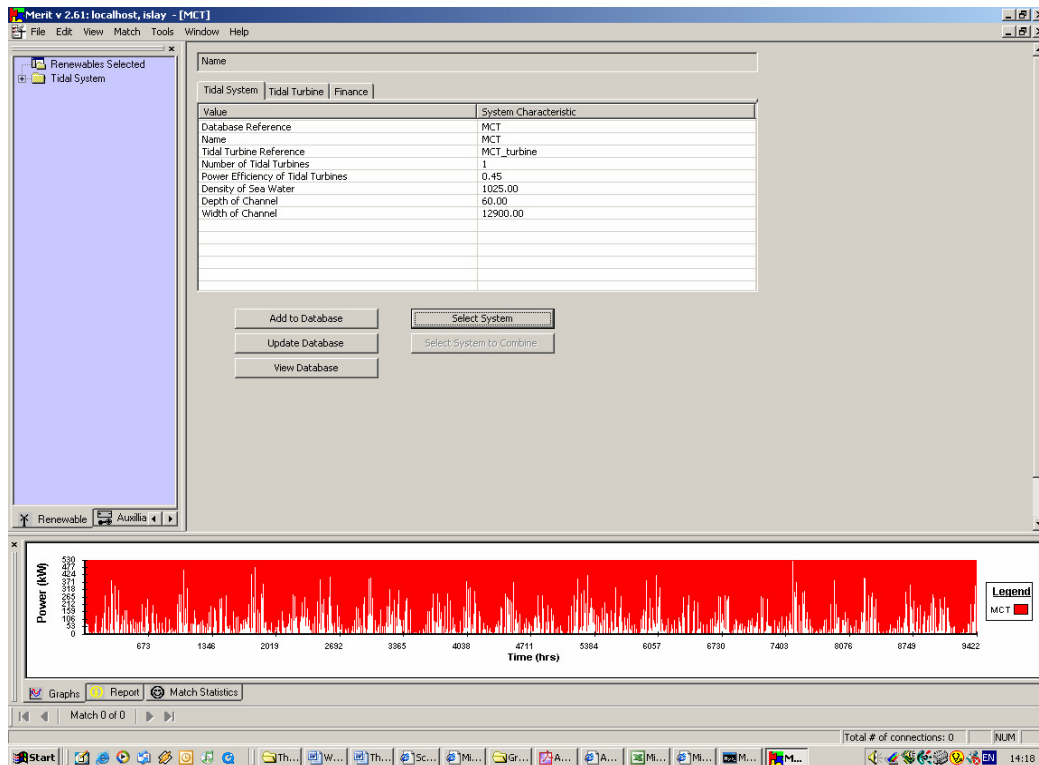
The “Tidal” interface created in MERIT had the main power equation built in to the program and prompted the user to input a number of parameters for the turbine system.

The equation integrated into the interface was:

$$Power = \eta_{gearbox} \eta_{generator} C_p (swept\_area\_per\_turbine) x (no\_of\_turbines) \frac{1}{2} \rho V_{available}^3$$

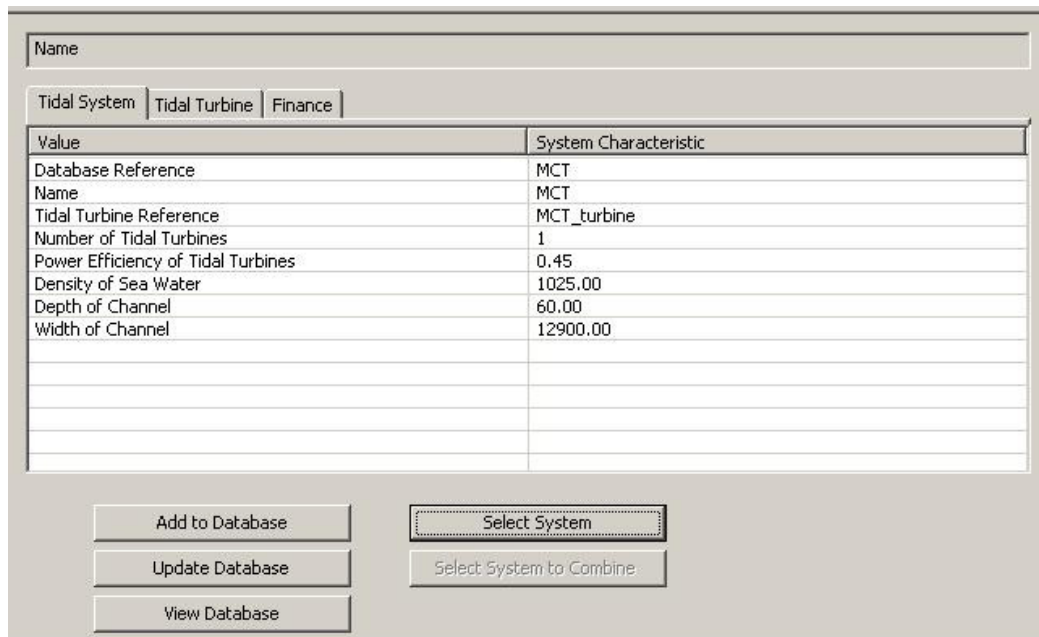
The interface also contained “IF, THEN, ELSE” loops for rated and cut-in conditions, already discussed in section 3.9.

Figure 40 Channel Model Implemented to MERIT as Tidal Interface

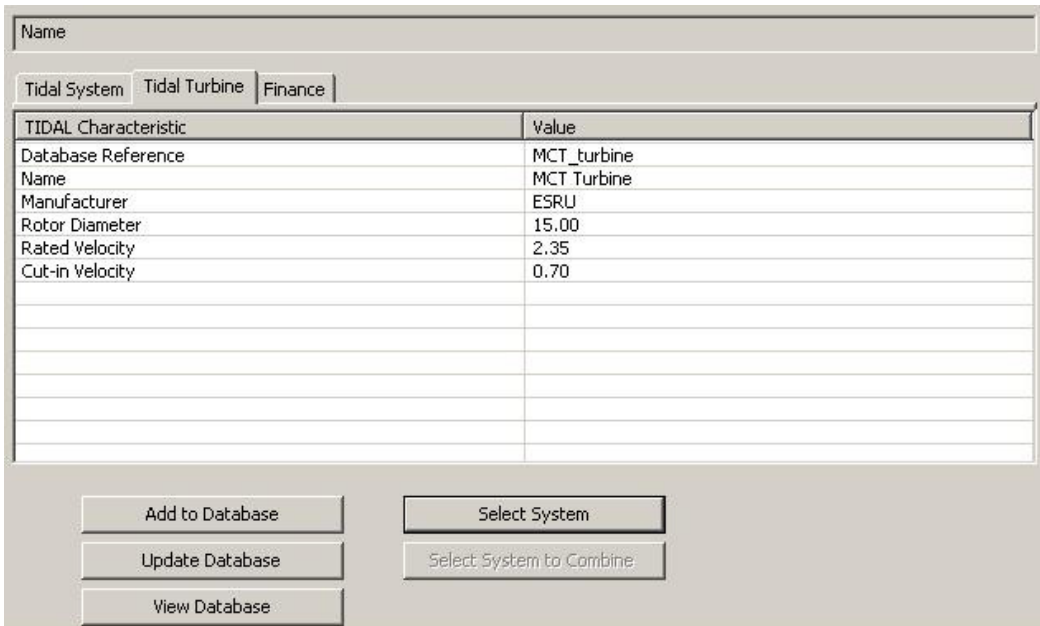


The user was prompted to enter values for  $C_p$ , cut-in and rated velocities, channel dimensions, rotor diameter and number of turbines as shown in figures 41 and 42.

Figure 31 Tidal System User Interface

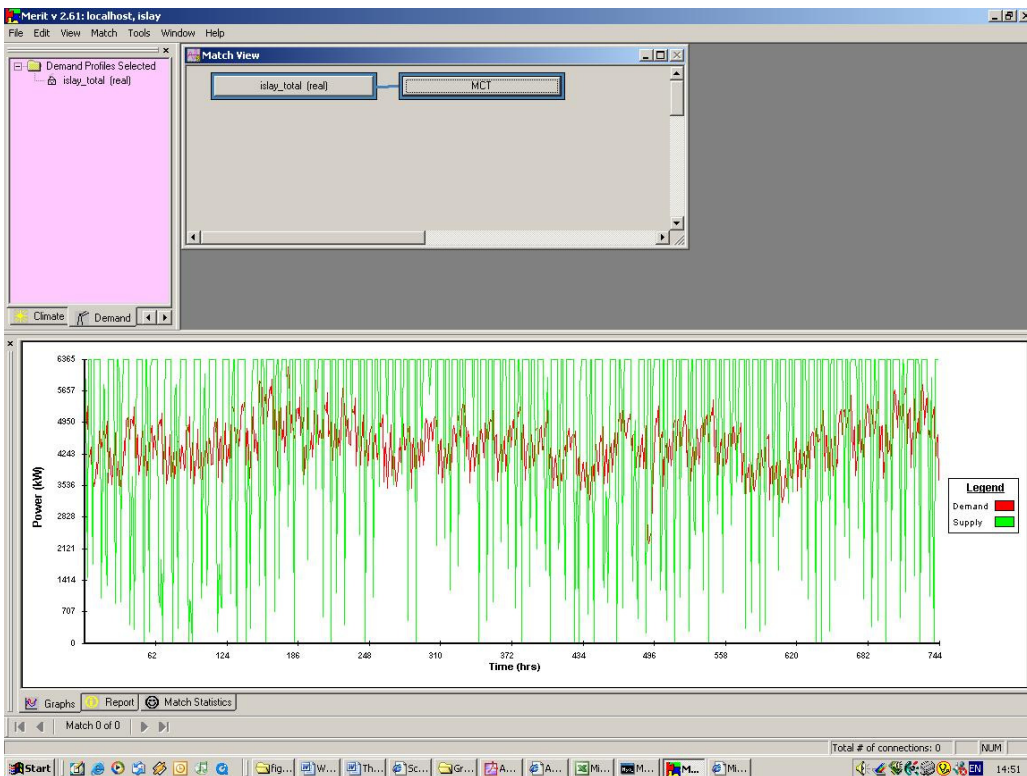


**Figure 42 Tidal Turbine User Interface**



Having input these parameters, the user could then select this system to provide the supply profile for matching against a specific demand profile.

**Figure 43 Matching of MCT Supply Profile Against Islay Total Demand**



Using the match statistics tab, the following information was obtained on the quality of matching the totally electrical output of Islay with 6 MCT's:

Demands:islay\_total (real)

Supplies:MCT

Number of DSM demands: 0

Total Demand: 3.35 MWh

Total Supply: 3.88 MWh

Good Match 7/10

Percentage Match: 77.98

Inequality Coefficient: 0.22

Correlation Coefficient: 0.01

Residual Area:-525105.33

Shared Area:2865458.76

More of this type of supply demand matching will be performed in the case study in section 4.

### **Validation of Adapted Model in Merit**

#### Perigee/ Equinox

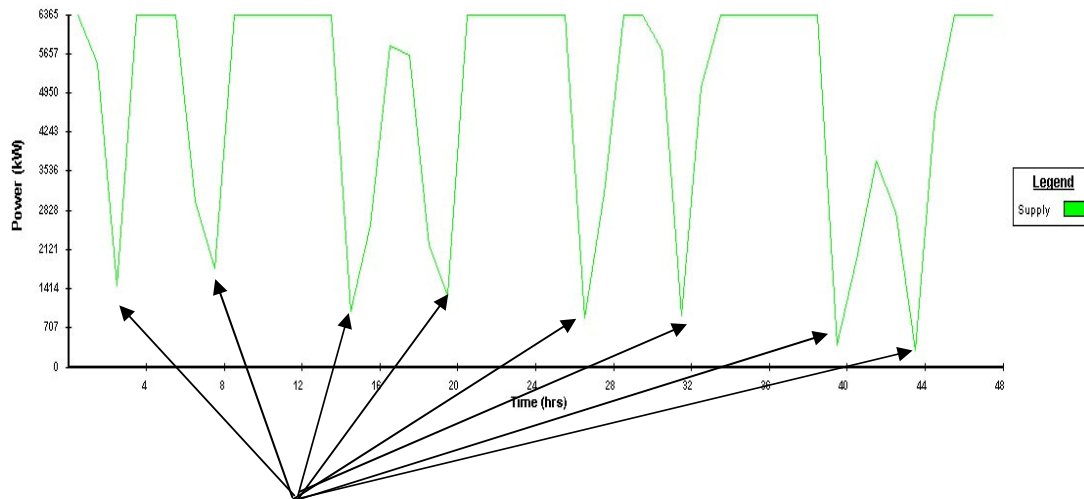
There is a half year cycle, due to the inclination of the moon's orbit to that of the earth, that is known to give rise to maxima in the spring tides in March and September.

From the predicted water height output from the channel model there is a clear variation in the spring tide magnitudes throughout the year. This is the result of the combination of  $N_2+M_2+S_2$  as discussed earlier in section 3.1

## Slack Tides

Unfortunately the channel model when executed at a resolution of 1 hour time steps for compatibility with the resolution of the climate database in MERIT, fails to completely model the very short periods of zero tidal current velocity which occur at slack tides (i.e at HW and LW at the location of the MCT farm). This is shown in figure 44.

**Figure 44 Failure to Capture Slack Tides for 1 Hour Time steps**

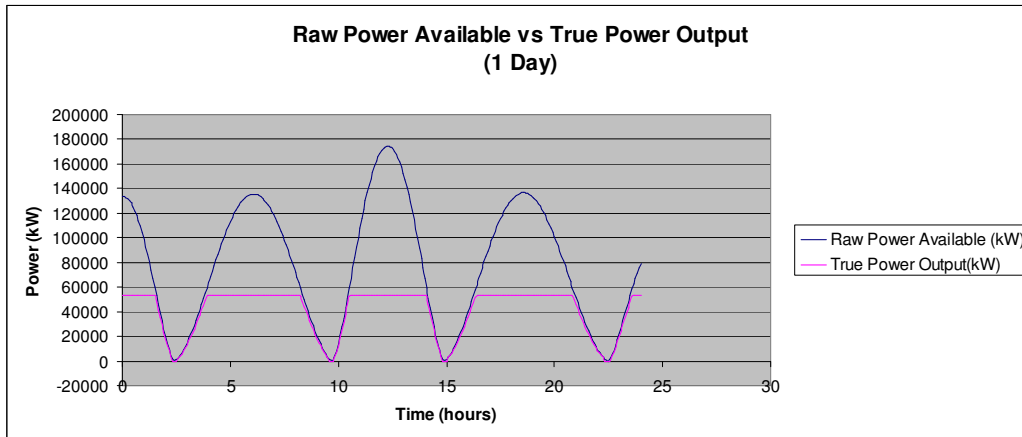


**These should all be zero for slack tides**

To extend to resolution of the channel model to 5 minute time steps for an entire year would require too much processor power and cannot therefore be carried out on a single PC workstation. Despite the channel model taking the form of a simple spreadsheet the number of calculations in each row of the model is large and so a single PC workstation will crash should a 5 minute time step be attempted for the period of an entire year.

However, a 10 minute time step can be carried out for the period of 1 month. This proved to be a sufficient time step in order to capture these short periods of slack tide. This is shown in figure 44 where the power output reaches zero approximately every 6 hours (at slack tide times).

**Figure 45 Power output from Channel Model at 10 Minute Resolution**

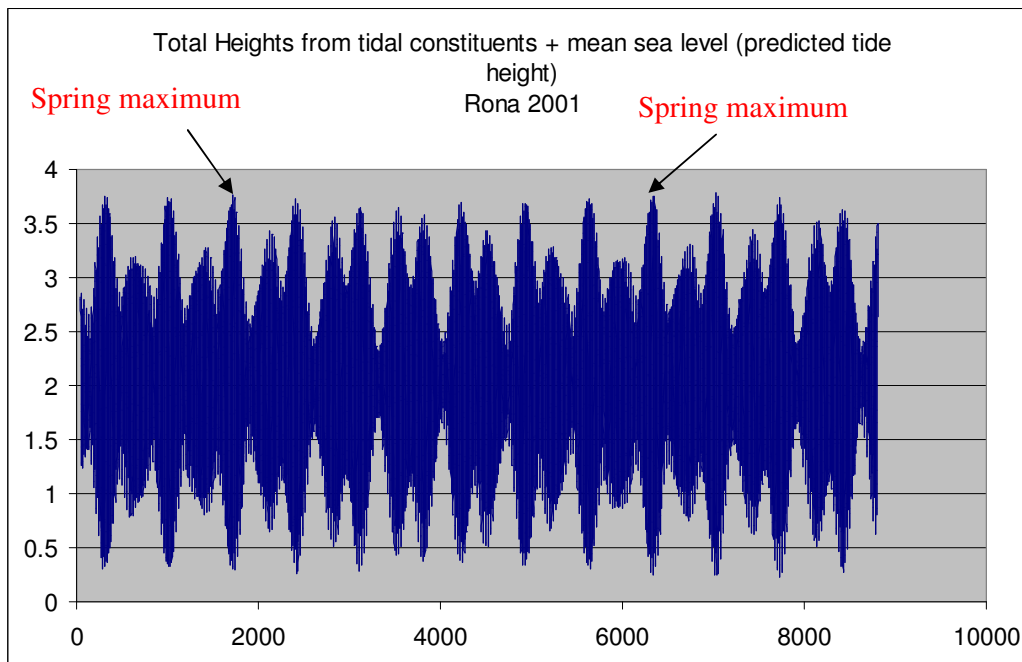


For matching analysis over small time periods such as a day or less, this higher resolution 10 minute time step would need to be executed and the input to the database for MERIT.

At the time writing, MERIT had only been setup up to accept an hourly variation in tidal current velocity and so this new improved capture of slack tides could not be transferred to for the matching analysis.

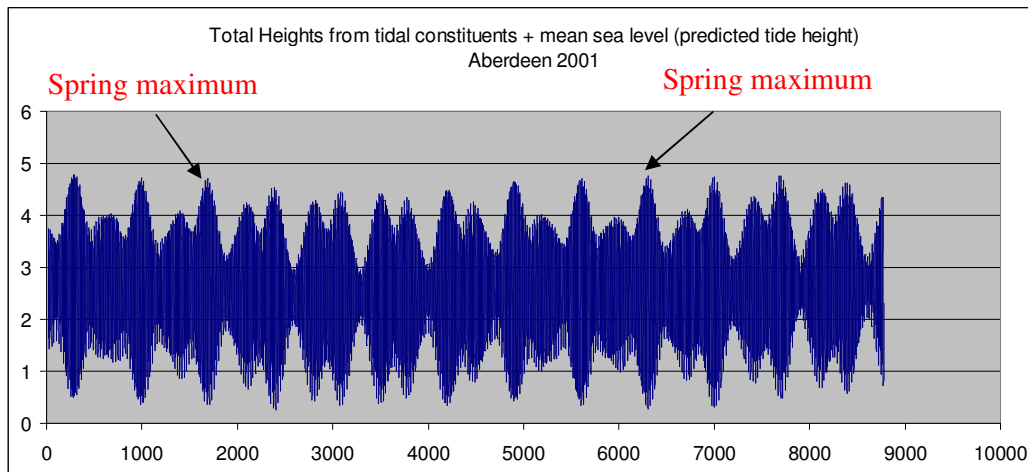
However, this could be completed fairly easily in further work with the developers of MERIT.

**Figure 46 Maxima for Spring Tides (Rona)**



Month	Date	Time (hours)	Rona Water Height (m)
January	12th	23:00	3.73
February	11th	11:00	3.72
March	11 <sup>th</sup>	10:00	3.76
April	9 <sup>th</sup>	10:00	3.73
May	10 <sup>th</sup>	11:00	3.59
June	24th	11:00	3.69
July	24 <sup>th</sup>	11:00	3.66
August	31 <sup>st</sup>	23:00	3.72
September	20 <sup>th</sup>	23:00	3.751
October	19 <sup>th</sup>	23:00	3.749
November	17 <sup>th</sup>	23:00	3.68
December	16 <sup>th</sup>	22:00	3.62

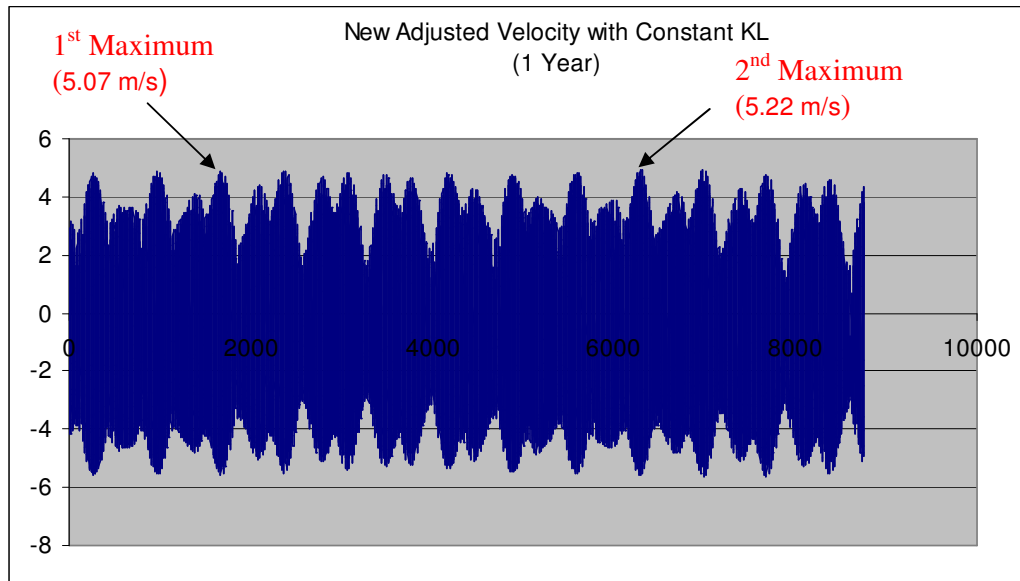
**Figure 47 Maxima for Spring Tides (Aberdeen)**



Month	Date	Time (hours)	Aberdeen Water Height (m)
January	12 <sup>th</sup>	16:00	4.68
February	11 <sup>th</sup>	17:00	4.66
March	11 <sup>th</sup>	16:00	4.71
April	10 <sup>th</sup>	16:00	4.49
May	8 <sup>th</sup>	15:00	4.45
June	25 <sup>th</sup>	17:00	4.48
July	24 <sup>th</sup>	05:00	4.63
August	23 <sup>rd</sup>	05:00	4.66
September	20 <sup>th</sup>	04:00	4.76
October	18 <sup>th</sup>	03:00	4.72
November	17 <sup>th</sup>	04:00	4.76
December	17 <sup>th</sup>	04:00	4.59

When analysed more closely, the values show that indeed a maximum of spring tides occurs twice yearly and are in the months of March and September as predicted. This shows a strong correlation between the model output and reality in terms of the tide heights generated at the two ports either side of the channel. Therefore the resultant tidal current velocity in the channel resultant from the pressure differential between the two out of phase heights should follow the same pattern. Figure 48 demonstrates this to be correct.

**Figure 48 Undisturbed Flow Velocity in Pentland Firth for 2001**



The first maximum velocity of magnitude 5.07 m/s occurs at 09:00 on 10<sup>th</sup> March and second maximum velocity of 5.22 m/s occurs at 23:00 on 20<sup>th</sup> September. This is roughly in line with the maxima for tide heights.

It should be noted here that the negative values (i.e the ebb flow velocity) have been ignored in figure 48, since these velocities have yet to be corrected for ebb factor (see Section 3.4).

## 4 Case Study - Islay

The main advantage for using Islay as a case study lay primarily in the availability of data on electrical demand for the entire island [21].

Secondly, the remote location of the island lent itself well to an assessment into the use of embedded generation where MCT farms were concerned.

Whereas the islands of Lewis, Skye and Uist further North have connection to a 132kV transmission line, this is not the case for the comparatively smaller island of Islay.

Shown in fig 49 is the total electrical demand for the island over one year.

**Figure 49 Total Electrical Demand for Islay [21]**

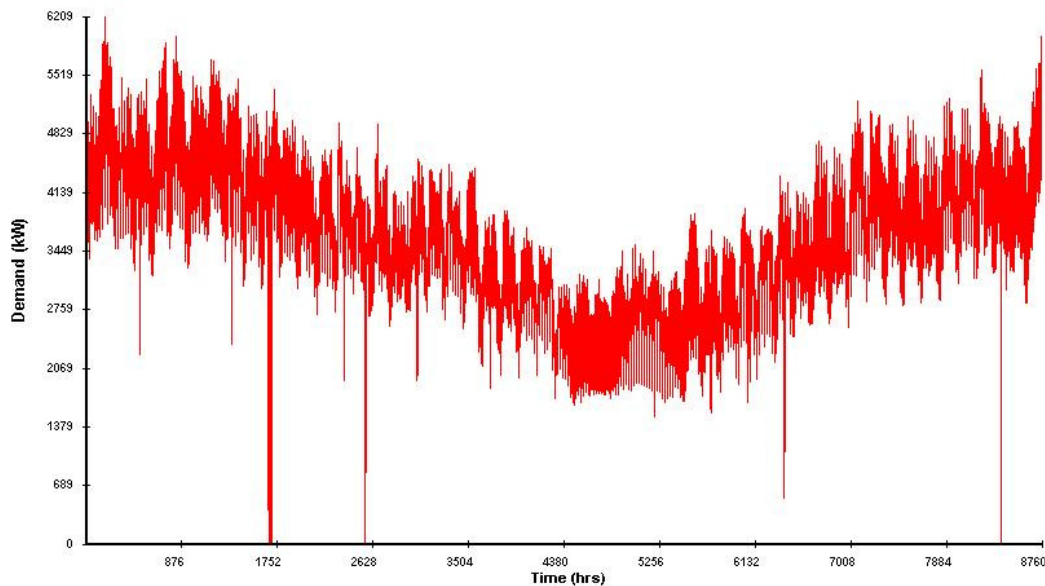


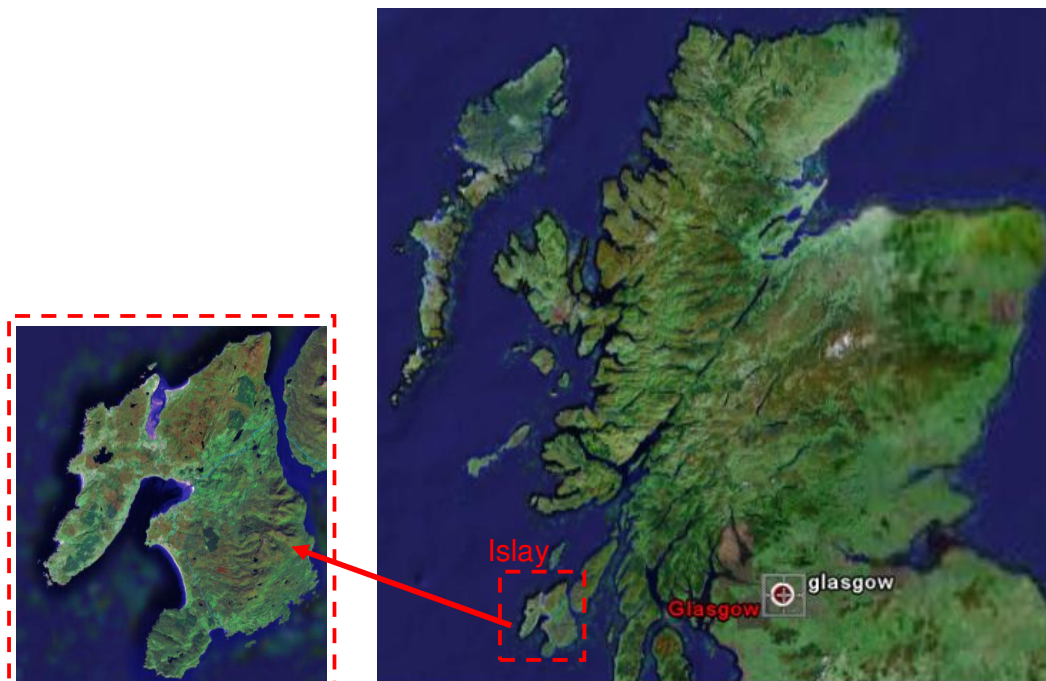
Figure 50 shows that the peak electrical demand for the entire island varies from just over 6 MW in the winter to around 3.5 MW in the summer months.

However, the data was not limited to total demand. The data had in fact been broken down and separated into discrete profiles for various types of consumer and different parts of the island. These decomposed individual

profiles were used in the case study as they offered many possible scenarios for combinations of different demand profiles in order to achieve the best match against the supply profile of an MCT farm.

#### 4.1 Local Geography & Demographic of Islay

Figure 50 Map of Islay



Islay is roughly 25 miles North to South and around 19 miles east to west, though almost split in the middle by two sea lochs - Loch Indaal from the south and Loch Gruinart from the north. It is a low-lying fertile island comprising a number of small villages of which Bowmore and Port Ellen are the largest. The island's population is around 4,000 [32]

This population is spread out among a number of small settlements. The island boasts a thriving whisky industry with 8 malt whisky distilleries [33].

Figure 51 Islay Grid



The normal supply of power to Islay is from the mainland via the Island of Jura. The grid on Islay is generally weak, particularly at the "end of the line" at Portnahaven. This means the Grid must be stiffened before significant additional generation can be connected to the system [34]. The Sound of Isla or "Caol Isla" as it is known locally would offer the ability to host a number of MCT devices in what is essentially an open channel, thus allowing the enhanced channel model to be implemented. Unfortunately the channel also acts as a ferry route but it is envisaged that installing only a small number of MCT's in the channel would avoid conflicts.

Figure 52 Map of Sound of Islay



The channel dimensions were approximated as such:

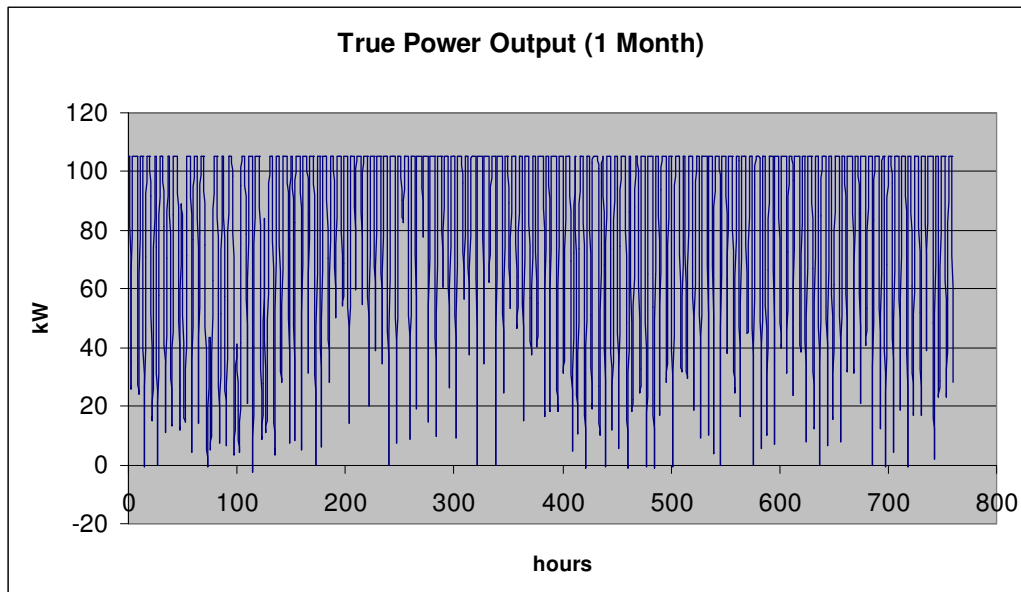
Length=20,000m, average width=3000m, average depth=15m, Manning's roughness coefficient=0.03

Given the shallow dimensions to the channel a 5m diameter rotor was chosen which gave a maximum packing density of around 100/km<sup>2</sup>, although with the constraints of other users for this waterway the packing density would be very low. This size of rotor would mean each MCT with two rotors per device would be rated at just over 100kW.

The resultant frictional losses due to blockage were therefore negligible given the low solidity. But the shallow nature of the channel would be well reflected in the velocity profile calculated in the enhanced channel model.

The output for one 15m diameter dual rotor MCT in the channel for the month of January 2001 looked like this:

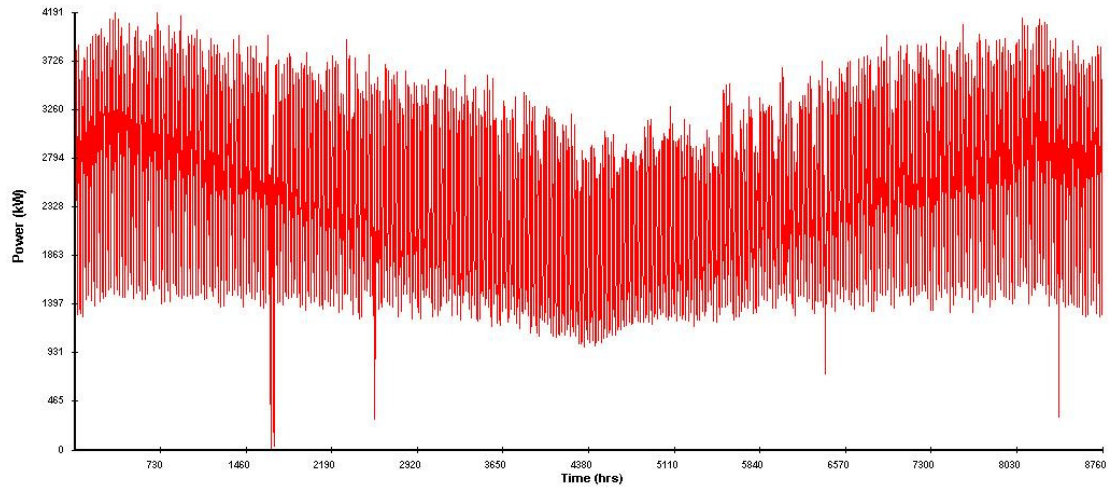
**Figure 53 True Power Output for a Single 15m diameter dual rotor MCT for 1 Month Duration**



The two ports used to represent the two independent reservoirs of water either side of the channel were Girvin well to the South and Scalasaig just to the North of the channel. These two ports provided water height data whose HW and LW times coincided, giving rise to the static head difference needed for the channel model. The enhanced channel model was then executed for these parameters and accordingly the power supply profile for a period of one year was generated in order to be matched against the demand profiles for the various users on the island. It should be noted that only electricity is considered for this study. Further work could include heating demands.

## 4.2 Domestic Dwellings

**Figure 54 Total Electrical Demand from all Domestic Dwellings on Islay**

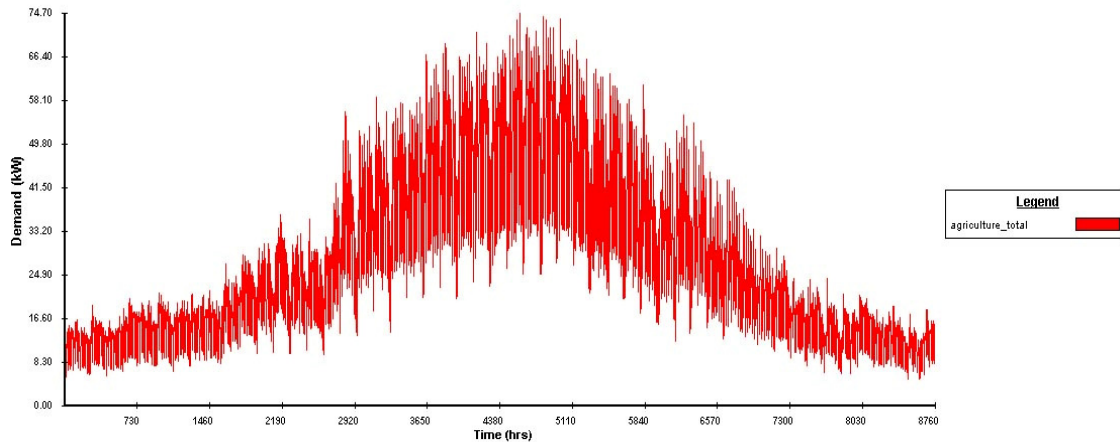


The peak electrical demand is around 4MW of power occurring in the winter whereas the summer minimum demand is around 2.7MW.

## 4.3 Agricultural

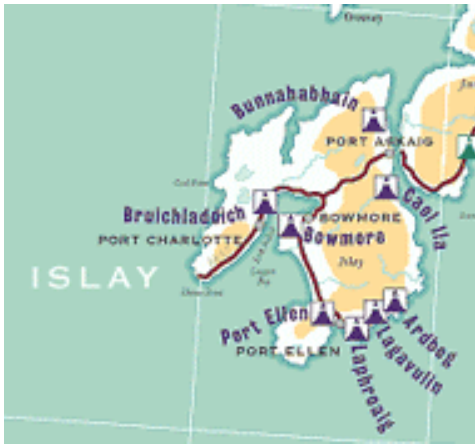
The island's agricultural demand is relatively small and will comprise electrical demand from a small number of farms on the island. Clearly the peak demand occurs in the summer months where harvesting of crops takes place and other farming activities dependent on the season. This "summer peak" could prove useful when combined with some of the more conventional "winter peak" demand profile such as domestic and commercial users.

**Figure 55 Total Agricultural Demand on Islay**



#### **4.4 Industrial (Distilleries)**

**Figure 56 Islay's Distilleries**

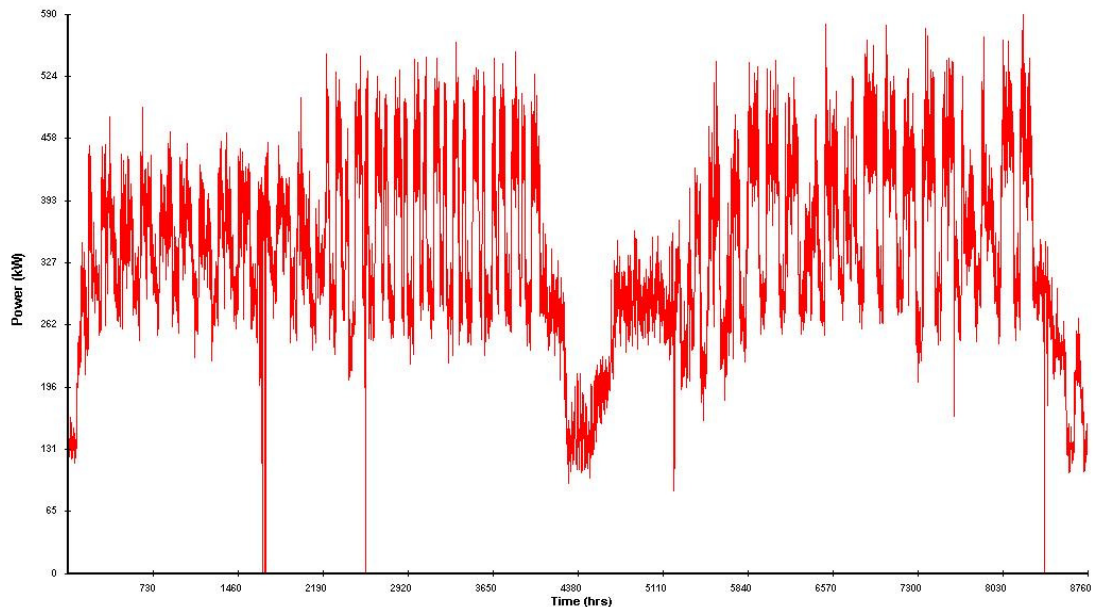


One extremely potent use of the output from an MCT farm could possibly be its use in meeting the demand of the many distilleries which make up the thriving whisky industry on the Island. These are small businesses which use fairly large amounts of energy per building in comparison to a domestic dwelling in the same area. Not only do they operate as distilleries, but many also have busy visitor centres on site which will further increase electrical demand. These types of industrial end-user on the island may be more open to Demand Side Management (DSM) or storage, especially where the most energy intensive of processes could perhaps be executed at a time which

would be favourable to the quality of supply/ demand matching of the MCT farm in terms of coinciding with a time of high output.

The use of preferential pricing of electricity could apply here, with industrial users such as the distilleries on the island being offered cheaper electricity at a time which suits the output of the MCT farm. Since the power excesses and deficits from the MCT farm occur at largely predictable intervals, such rates could be arranged well in advance and could tie in well with re-arrangement of production schedules for industrial users.

**Figure 57 Total Electrical Demand from all Distilleries on Islay**



There is a clear trough in the profile at around 4400 hours coinciding with early July. Considering that this is around the harvest time for the barley crops, this would coincide with a period of inactivity in terms of the kilning or fermentation processes, both of which require electrical power to perform.

To assess the potential for matching supply of an MCT farm with a combination of industrial demand profiles, a number of distilleries will be considered in more depth.

**Figure 58 Electrical Demand from Ardbeg Distillery**

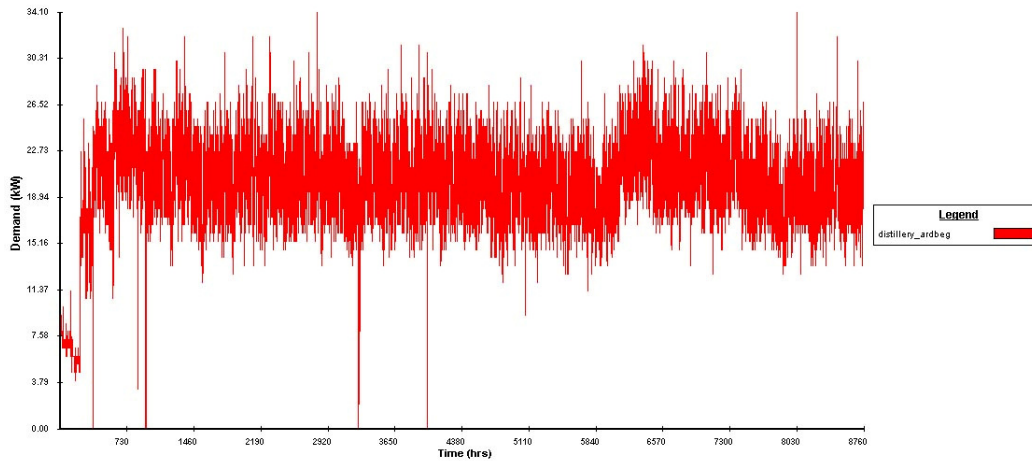
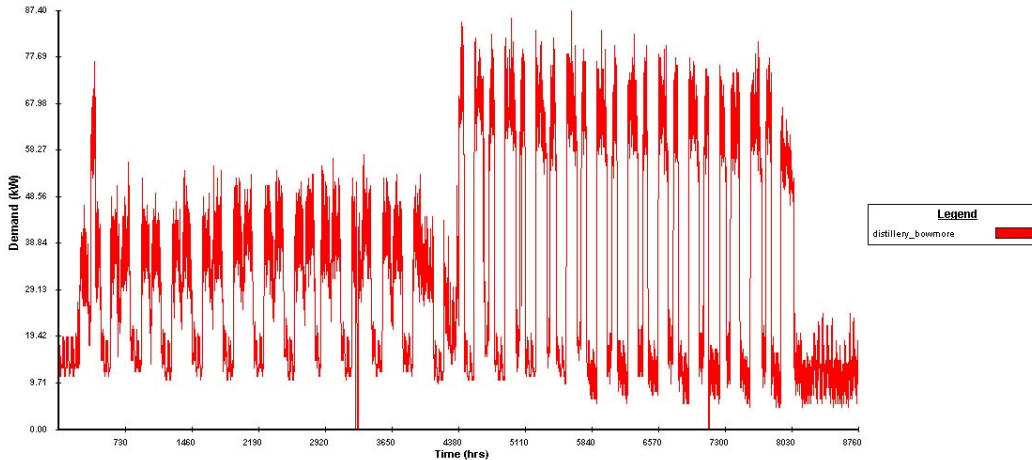


**Figure 59 Electrical Demand from Bowmore Distillery**



## ***4.5 Combining Supply Profiles to Improve Matching Capability***

It was unlikely that the supply profile from an MCT farm alone would provide a good match against each of the various demand profiles.

This is illustrated in figures 59 and 60, which show the output of a 60 unit MCT farm, of the size and rated power specified in Section 4.1, against a number of demand profiles for a 24 hour period and the same for Port Askaig and 10 unit MCT farm. Clearly, there are a number of periods where the size of the power supply falls short of the demand.

**Figure 60 Islay Total Electrical Demand against a 60 Unit MCT Farm Output**

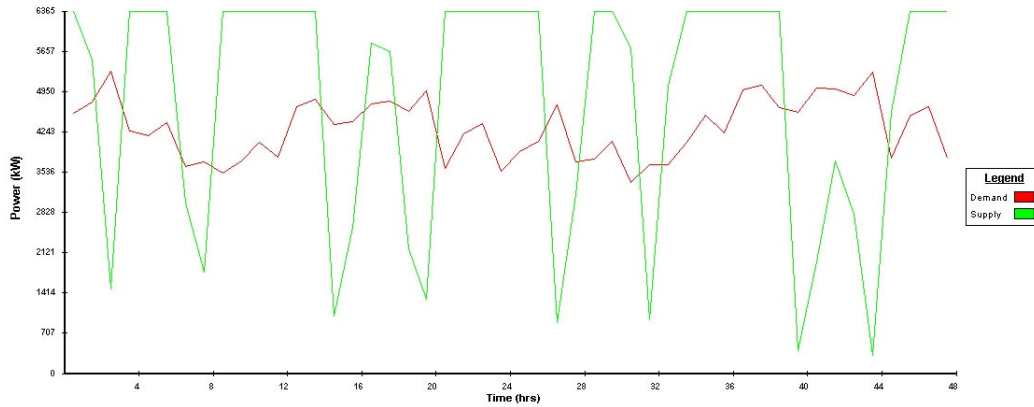
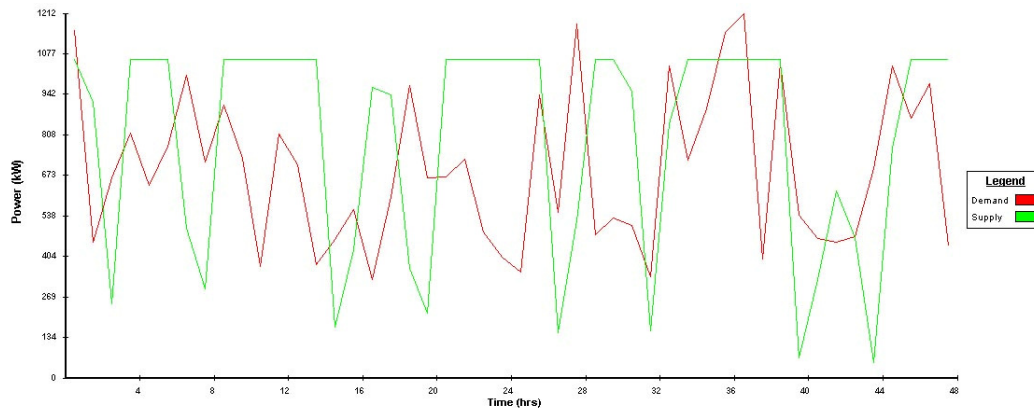


**Figure 61 Port Askaig Total Electrical Demand against a 10 Unit MCT Farm Output**



Therefore a sensible option available is to combine the output from the MCT farm with that of a number of other renewable options likely to be complementary when the aggregate is considered.

In this case study the scope for these other renewable options was limited to wind power and solar PV devices. Each combination was presented in a tabular format and listed the matching parameters from MERIT for each scenario, finally giving a conclusion on which combination of demand profiles

afforded the best matching performance and why this was the case. Table 6 shows this.

The intention for the climate dataset in this case study was to use the dataset for Glasgow as no actual dataset existed for Islay. Given that Glasgow is roughly on the same latitude as Islay, it was be expected that the climate data would provide reasonably accurate results for the wind turbine and PV supply profiles. Unfortunately, the Glasgow dataset was giving strange anomalies in the wind speed data and was also not available for an entire year so it was decided to use the climate dataset for Lerwick instead.

Table 8 shows the results for matching the demand profile for the entire island with 3 different supply option ensembles. The supply options chosen were selected based on

**Table 8 Daily Matching Analysis of Supply Option Ensemble**

	<b>Scenario 1</b>	<b>Scenario 2</b>	<b>Scenario 3</b>
<b>Demand profile</b>	Islay Total	Islay Total	Islay Total
<b>Supply Options</b>	6x 1.3MW Bonus Wind Turbines	6x 1.3MW Bonus Wind Turbines + 50,000 x (100W Poly Vert South) PV Panels	3x 1.3MW Bonus Wind Turbines + 30x 100kW MCT's
<b>Matching parameters from MERIT</b>	Demands:islay_total (real)	Demands:islay_total (real)	Demands:islay_total (real)
	Supplies:6WIND	Supplies:50000PV+6WIND	Supplies:3WIND+30MCT
	Number of DSM demands: 0	Number of DSM demands: 0	Number of DSM demands: 0
	Total Demand: 103.45 kWh	Total Demand: 103.45 kWh	Total Demand: 103.45 kWh
	Total Supply: 170.33 kWh	Total Supply: 170.76 kWh	Total Supply: 116.54 kWh
	Reasonable Match 6/10	Reasonable Match 6/10	Very Good Match 8/10
	Percentage Match: 69.90	Percentage Match: 69.94	Percentage Match: 84.82
	Inequality Coefficient:	Inequality Coefficient: 0.30	Inequality Coefficient: 0.15

	0.30		
	Correlation Coefficient: 0.04	Correlation Coefficient: 0.04	Correlation Coefficient: -0.23
	Residual Area:-63346.73	Residual Area:-63769.51	Residual Area:-11445.43
	Shared Area:90853.59	Shared Area:91062.77	Shared Area:90455.91

Looking at 24 hour matching statistics can provide an unrealistic snapshot of the quality of matching achievable by any one scenario. This is because, taking such a narrow period of sample climate data is not representative of the overall variation of that climate data over say a year or a month. For example, the wind from the Dundee data set for the first 24 hours of Jan 1<sup>st</sup> is maintained at high velocity for that 24 period. Conceivably the next 24 hour period could be much lower in wind velocity and so basing the quality of matching on just the first 24 hours is not representative.

For this reason the same scenarios must be assessed over larger periods of 1 month and 1 year to fully gauge the overall merits of each. This is achieved in tables 8 and 9 respectively.

**Table 9 Monthly Matching Analysis of Supply Option Ensemble**

	<b>Scenario 1</b>	<b>Scenario 2</b>	<b>Scenario 3</b>
<b>Demand profile</b>	Islay Total	Islay Total	Islay Total
<b>Supply Options</b>	6x 1.3MW Bonus Wind Turbines	6x 1.3MW Bonus Wind Turbines + 50,000 x 100W Poly South PV Panels	3x 1.3MW Bonus Wind Turbines + 30x 100kW MCT's
<b>Matching parameters from MERIT</b>	Demands:islay_total (real)	Demands:islay_total (real)	Demands:islay_total (real)
	Supplies:6WIND	Supplies:50000PV+6WIND	Supplies:3WIND+30MCT
	Number of DSM demands: 0	Number of DSM demands: 0	Number of DSM demands: 0

	Total Demand: 3.35 MWh	Total Demand: 3.35 MWh	Total Demand: 3.35 MWh
	Total Supply: 3.70 MWh	Total Supply: 3.72 MWh	Total Supply: 3.17 MWh
	Reasonable Match 6/10	Reasonable Match 6/10	Very Good Match 8/10
	Percentage Match: 69.32	Percentage Match: 69.45	Percentage Match: 82.82
	Inequality Coefficient: 0.31	Inequality Coefficient: 0.31	Inequality Coefficient: 0.17
	Correlation Coefficient: 0.03	Correlation Coefficient: 0.03	Correlation Coefficient: 0.03
	Residual Area:-343595.42	Residual Area:-371065.78	Residual Area:180691.85
	Shared Area:2414351.04	Shared Area:2430006.43	Shared Area:2787602.83

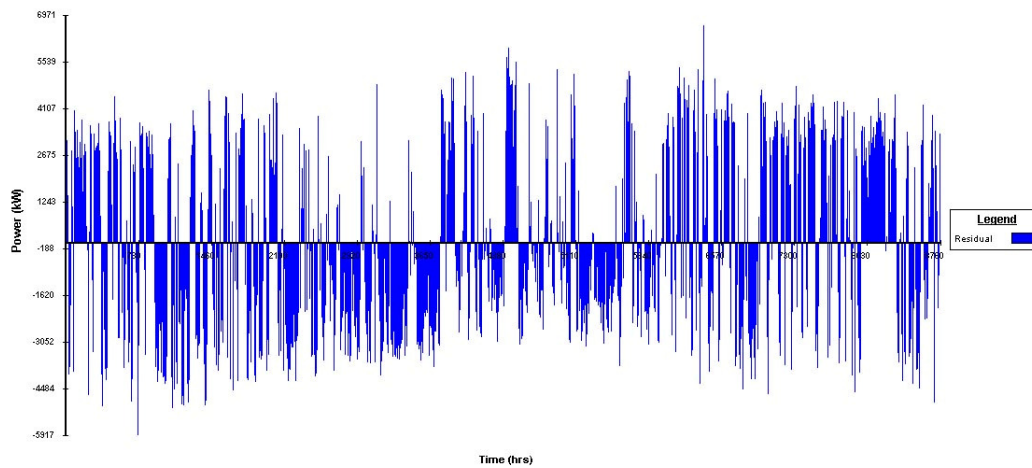
**Table 10 Yearly Matching Analysis of Supply Option Ensemble**

	Scenario 1	Scenario 2	Scenario 3
<b>Demand profile</b>	Islay Total	Islay Total	Islay Total
<b>Supply Options</b>	6x 1.3MW Bonus Wind Turbines	6x 1.3MW Bonus Wind Turbines + 50,000 x 100W Poly South PV Panels	3x 1.3MW Bonus Wind Turbines + 30x 100kW MCT's
<b>Matching parameters from MERIT</b>	Demands:islay_total (real)	Demands:islay_total (real)	Demands:islay_total (real)
	Supplies:6WIND	Supplies:50000PV+6WIND	Supplies:30WIND+30MCT
	Number of DSM demands: 0	Number of DSM demands: 0	Number of DSM demands: 0
	Total Demand: 31.53 MWh	Total Demand: 31.53 MWh	Total Demand: 31.53 MWh
	Total Supply: 31.25 MWh	Total Supply: 34.34 MWh	Total Supply: 33.25 MWh
	Reasonable Match 6/10	Reasonable Match 6/10	Good Match 7/10
	Percentage Match: 64.69	Percentage Match: 65.19	Percentage Match: 79.52
	Inequality Coefficient: 0.35	Inequality Coefficient: 0.35	Inequality Coefficient: 0.20
	Correlation Coefficient: 0.22	Correlation Coefficient: 0.20	Correlation Coefficient: 0.15
	Residual Area:287478.70	Residual Area:-2804653.08	Residual Area:-1719568.69
	Shared Area:19746063.28	Shared Area:21347553.25	Shared Area:26765119.37

### **Scenario 1**

Using 6 1.3MW wind turbines and no other renewable devices provided a reasonable match, but resulted in many periods of over-production and under production in terms of power supply against the demand. This is reflected in figure 62 which shows the residual.

**Figure 62 Residual from 6x 1.3MW Bonus Wind Turbines against Total Demand for Islay (1Year)**



### **Scenario 2**

The effect of adding even a considerable amount of solar PV panels (50,000 in this case) is insignificant to the quality of matching. Therefore a decision was made to concentrate the supply options combinations on wind and MCT, with the solar PV providing role of boosting the power output of the ensemble during daylight periods, should this prove to be beneficial.

### **Scenario 3**

The outcome from this approach of combining supply profiles was that ultimately the best matching performance was likely to come from a scenario based on scenario 3, in which the largest proportion of the power supply

comes from an equal share of wind and MCT, perhaps with solar PV providing a much smaller yet significant percentage.

This approach was further investigated in table which shows that by taking the yearly matching analysis of scenario 3, and adding 1,000 x 100W Poly South-facing PV Panels, actually only a marginally higher percentage match is achieved.

This is because the additional electrical power output from the panels during daylight hours each day will undoubtedly in some instances push the total aggregate of the power from the entire supply ensemble up to meet the demand, where previously the supply fell just short of matching it. However, equally, in other instances the additional power from the PV panels could be pushing the total aggregate power supply way beyond the demand and in doing so will degrade the quality of matching.

The balance of these effects on the aggregate supply profile against the demand profile will ultimately determine whether adding a large number of PV panels is worthwhile. In this case, it is not.

This is reflected in table 11 which shows only a marginal increase in percentage match after adding the 1, 000 solar panels of 100W rated power each, the quality of the match is not much better.

**Table 11 Minimal Benefit of adding 50,000 x 100W Poly South PV Panels to a combination of supply from 30 MCT's and 3 Wind Turbines**

<b>Demand profile</b>	Islay Total	Islay Total
<b>Supply Options</b>	3x 1.3MW Bonus Wind Turbines + 3x 100kW MCT's	3x 1.3MW Bonus Wind Turbines + 3x 100kW MCT's + 1000 x (100W Poly Vert South) Panels
<b>Matching parameters from MERIT</b>	Demands:islay_total (real)	Demands:islay_total (real)
	Supplies:3WIND+30MCT	Supplies:1000PV+3WIND+30 MCT
	Number of DSM demands: 0	Number of DSM demands: 0
	Total Demand: 31.53 MWh	Total Demand: 31.53 MWh
	Total Supply: 33.25 MWh	Total Supply: 33.32 MWh
	Good Match 7/10	Good Match 7/10
	Percentage Match: 79.52	Percentage Match: 79.53
	Inequality Coefficient: 0.20	Inequality Coefficient: 0.20
	Correlation Coefficient: 0.15	Correlation Coefficient: 0.15
	Residual Area:-1719568.69	Residual Area:-1785662.32
	Shared Area:26765119.37	Shared Area:26792414.59

The decision on whether such large scale use of solar PV would be feasible will be based on a cost/benefit approach. In other words, if a similar increase in percentage match can be achieved via other mean (e.g. storage or DSM) then it is unlikely that the costly option of solar PV would be pursued, especially with the large number of units required to provide the power output required in this case study.

Storage options will be discussed in Section 4.7.

Another interesting observation was a steady drop in the value of percentage match for each scenario as a progression was made from a simple 24-hour time period of climate data to a full year. This was entirely as expected, and the percentage match for one year is far more representative than the value for a 24-hour period.

**Table 12 Scenarios for Wind, MCT Combinations – Yearly Matching**

	Scenario 5	Scenario 6	Scenario 7	Scenario 8
<b>Demand profile</b>	Islay Total	Islay Total	Islay Total	Islay Total
<b>Supply Options</b>	2x 1.3MW Bonus Wind Turbines + 40X 100kW MCT's	4x 1.3MW Bonus Wind Turbines + 20 X 100kW MCT's	1x 1.3MW Bonus Wind Turbines + 50X 100kW MCT's	5x 1.3MW Bonus Wind Turbines + 10X 100kW MCT's
<b>Matching parameters from MERIT</b>	Demands:islay_total (real)	Demands:islay_total (real)	Demands:islay_total (real)	Demands:islay_total (real)
	Supplies:2WIND+40MCT	Supplies:4WIND+20MCT	Supplies:Bonus 1.3MW 68m +cost+50MCT	Supplies:5WIND+10MCT
	Number of DSM demands: 0	Number of DSM demands: 0	Number of DSM demands: 0	Number of DSM demands: 0
	Total Demand: 31.53 MWh	Total Demand: 31.53 MWh	Total Demand: 31.53 MWh	Total Demand: 31.53 MWh
	Total Supply: 40.86 MWh	Total Supply: 36.06 MWh	Total Supply: 43.27 MWh	Total Supply: 28.44 MWh
	<b>Good Match 7/10</b>	<b>Good Match 7/10</b>	<b>Good Match 7/10</b>	<b>Good Match 7/10</b>
	<b>Percentage Match: 75.64</b>	<b>Percentage Match: 73.58</b>	<b>Percentage Match: 73.63</b>	<b>Percentage Match: 72.43</b>
	Inequality Coefficient: 0.24	Inequality Coefficient: 0.26	Inequality Coefficient: 0.26	Inequality Coefficient: 0.28
	Correlation Coefficient: 0.12	Correlation Coefficient: 0.21	Correlation Coefficient: 0.05	Correlation Coefficient: 0.22
	Residual Area:-9330827.82	Residual Area:-4521674.52	Residual Area:-11735405.75	Residual Area:3089583.96
	Shared Area:28315349.57	Shared Area:25776482.93	Shared Area:28035770.15	Shared Area:22019683.26

From closer inspection of table 12 , it was clear that the best combination of supply profiles for over an entire year was a combination of 30 MCT's and 3 1.3MW Bonus Wind Turbines, with no contribution from solar PV, as it offered no significant benefit to the quality of matching. Indeed, from a renewable energy planner's perspective, the best combination of supply options is that which performs the best on average over the year. In summary, for the total

electrical demand for Islay the best percentage match of 79.52% is achieved by Scenario 3; comprising 30 MCT's, 3 Wind turbines and no solar PV.

30 (100kW MCT's) + 3(1.3 MW Wind Turbines) + 0 (Solar PV) = 79.52% match for 1 year

With use of storage and/or DSM this value could be improved yet further.

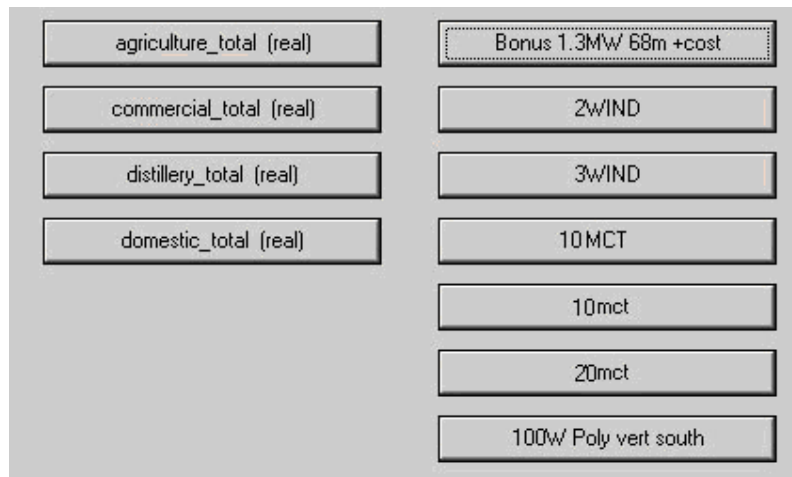
#### ***4.6 Combining Demand Profiles to Improve Matching Capability***

Rather than trying to match all of the island's electrical demand, it could prove more fruitful to attempt to match a combination of demand profiles from a number of different consumers on the island.

This could have the effect of producing an aggregate demand profile which is more suitable to matching against the ensemble of renewable supply profiles.

In turn, this could lead to the successful use of embedded generation, where the combined supply profile from wind, MCT and solar PV devices could meet most if not all of the demand from the combined profiles. Any shortfall could be supplied by the grid and any excess could be stored by batteries.

**Figure 63 Combinations of Demand Profiles**



- 1) First a number of demand profiles were selected; total agriculture, total commercial, total domestic and total from distilleries.
- 2) Next, a number of supply options were selected.
- 3) Matching was carried out

**Table 13 Best Results of Matching All Supply and Demand Combinations in Decreasing Matching Performance**

<b>Demand Combination</b>	<b>Supply Combination</b>	<b>% Match</b>
Distilleries + Agriculture + Domestic	1 wind + 20 mct + 15,000 PV	81.62
Distilleries + Domestic	1 wind + 20 mct + 15,000 PV	81.52
Distilleries + Agriculture + Domestic	1 wind + 20 mct	81.29
Distilleries + Agriculture + Domestic	1 wind + 20 mct + 15,000 PV	80.72
Distilleries + Agriculture + Domestic + Commercial	3 wind + 10 mct + 15,000 PV	80.67
Distilleries + Domestic + Commercial	2 wind + 10 mct + 15,000 PV	80.65

The result here is that the best matching results will not arise from combining demand profiles alone as there are insufficient complementary demand profiles. The best matching would be achieved by using DSM or storage.

#### ***4.7 The Use of Storage to Improve Matching Capability***

The smoothing effects of large amounts of battery storage for scenario 3 (3MCT's + 3 Wind Turbines against total demand for Islay) can be seen in table 12 below.

**Table 14 Storage Options for Scenario 3**

<b>No. of Batteries in Series</b>	500	1000	2000	3000	4000	5000
<b>% Match</b>	80.14	80.63	81.27	81.60	81.84	82.08

#### ***4.8 The Use of Demand Side Management (DSM) to Improve Quality of Matching***

The smoothing effects of DSM for scenario 3 (3MCT's + 3 Wind Turbines against total demand for Islay) can be seen in tables 15-18 below.

**Table 15 On/ off DSM for Scenario 3**

<b>DSM Restriction</b>	<b>No control</b>	<b>Low</b>	<b>Medium</b>	<b>High</b>
<b>(on/ off control)</b>				
<b>% Match</b>	79.52	67.15	67.15	67.15

**Table 16 Proportional DSM for Scenario 3**

<b>DSM Restriction</b>	<b>No control</b>	<b>Low</b>	<b>Medium</b>	<b>High</b>
<b>30 seconds duration</b>				
<b>% Match</b>	79.52	83.63	83.63	83.63

**Table 17 Proportional DSM for Scenario 3**

<b>DSM Restriction</b>	<b>No control</b>	<b>Low</b>	<b>Medium</b>	<b>High</b>
<b>1 mins duration</b>				

<b>% Match</b>	79.52	83.63	83.63	83.63
----------------	-------	-------	-------	-------

**Table 18 Proportional DSM for Scenario 3**

<b>DSM Restriction</b>	<b>No control</b>	<b>Low</b>	<b>Medium</b>	<b>High</b>
<b>5 mins duration</b>				
<b>% Match</b>	79.52	83.63	83.63	83.63

#### **4.9 Auto Search Facility on MERIT for Best Match Scenario**

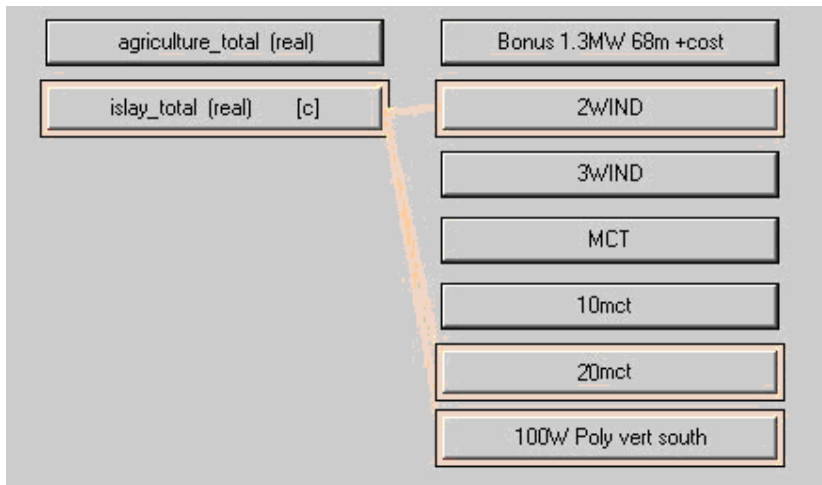
Using a facility in MERIT, which prompts the program to execute all the permutations and combinations of supply and demand matches, the following results for best matches between a number of supply and demand options were obtained.

**Table 19 Results of MERIT Auto Search Facility**

	<b>Best Match</b>	<b>2<sup>nd</sup> Best Match</b>	<b>3<sup>rd</sup> Best Match</b>	<b>4<sup>th</sup> Best Match</b>
<b>% Match</b>	87.11	86.88	86.87	86.6
<b>With DSM</b>	2 wind+ 20 MCT + 50,000 PV	3 wind + 10 MCT + 50,000 PV	3 wind + 20 MCT	3 wind + 10 MCT

The best match with DSM is shown in figure 64.

**Figure 64 Best Match from Auto Search Facility**



The best match To achieve a total 100% match would be possible by drawing the remaining electrical power from the grid. This could be proved in further work.

## 5 Conclusions

### ***5.1 Enhanced Channel Model***

The enhanced channel model has been developed to a level where it accounts for a number of the true facets to the behaviour of tidal currents in an open channel.

The model made use of a simple harmonic method for the influence of the tides to estimate the water heights in real time at either end of this idealised channel. Then making use of a basic hydrodynamic channel approach the velocity available to a “farm” of MCT devices situated in an open channel was calculated.

The model then improved on this available velocity by employing a number of empirical correction factors and improvements to encapsulate some of the reality behind the true behaviour of tidal current velocities in such a channel.

The model has succeeded in capturing

- Spring/ neap and equinox Variation in the tidal heights at each port
- Theoretically available velocity in a channel
- Frictional losses due to channel bathymetry
- Blockage effects due to placement on turbines in channel
- Effects of directionality
- Ebb and flood differences
- Depth velocity profile
- Power output of turbine including cut-in, rated velocity, power coefficient and the generator and gearbox efficiency of a MCT device

The model has failed to fully capture

- Slack Tides at the 1 hour resolution used in Merit

## **5.2 Autonomous Versus Network Grid Connected Strategy**

From the detailed case study of over a year of supply and demand profiles, it is clear that the island could not be completely autonomous based on the output of an MCT farm. However, by adding complementary renewable resources such as wind and solar PV and using DSM and/or energy storage the quality of supply/ demand matching does improve to a level which could account for a large proportion of the island electrical needs. If there was a facility for drawing from the grid to bridge the gaps and periods of low power output, then it would make for a viable argument for the pursuit of a supply strategy involving largely renewable forms of generation with minimal but timely back-up from the grid.

In general terms the potential for a fully autonomous island or coastal community based on output from a farm of MCT's alone would be greatly limited due to frequent periods of low or zero power output. To cope with this a number of other renewable resources could be used to bridge the gaps where there is zero power output and smooth the supply profile where there are periods of low power output.

So fully autonomy may not be possible, but a good degree of semi-autonomy could be readily achieved by clever complementary use of other renewable and conventional generation in tandem with the MCT farm, as long as the electricity grid was improved to accept distributed generation and to allow power to be drawn during deficits.

## **5.3 Conclusions from Case Study**

It was clear from the case study of the island of Islay on Scotland's West coast that despite the inherent variability from MCT farms, there is significant potential for combining output with that of other renewable devices to meet

some of the electrical demands of the local community through embedded generation.

With the additional use of storage and or DSM the quality of matching can be improved considerably. However with many storage options carrying a high capital cost for such large power ratings, the scope for storage seems fairly limited. This is especially true for the use of batteries.

A future option to bridge the gap could be hydrogen, although this needs to be developed further both in terms of a settled standard for the technology and the lack of a hydrogen infrastructure continues to be a barrier.

### Distilleries

A scenario was identified which would involve the distilleries (either as individual demands or collectively) employing a degree of demand side management with certain processes (i.e firing the kilns, heating water etc.) in order to better match the intermittent but largely predictable output from an MCT farm. Such a level of restriction would not necessarily suit a domestic consumer but with perhaps the added incentive of preferential pricing of electricity, industrial consumers such as distilleries may be tempted to tailor their production/ process schedules in order to meet times of cheaper electricity consumption.

## ***5.4 Replication of Channel Model to Other Locations***

The channel model can be easily replicated for almost any open channel which has two out of phase reservoirs at either end, as long as there is sufficient data available on the channel's dimensions and bathymetry for purposes of calculating the channel loss coefficient  $K_L$ .

Values have been calculated for the Pentland Firth and were intended to be used in an additional case study. However, due to the lack of electrical demand data for communities in that area, this was not possible. It could be included in further work. However, this demonstrates the ease at which the model can be replicated for another site of interest.

## 6 Recommendations & Further Work

Improvement of channel model interface in MERIT is a key priority given the impact of offering an added dimension to the supply options database which a complete and fully working interface would have. Also, the model could be further improved by increasing the resolution, by imposing time steps of shorter periods to fully capture slack tides. The case study could be developed further to include heating demands and the potential for distilleries on the island to tailor their production/ process schedules in order to meet times of cheaper electricity consumption, which could be imposed to coincide with times when the MCT farm is generating most power.

## Glossary of Terms

<b>A.C</b>	Alternating Current
<b>ATD</b>	Admiralty Tidal Diamond
<b>c.s.a</b>	Cross Sectional Area (of channel)
<b>CCGT</b>	Combined Cycle Gas Turbine
<b>CFD</b>	Computational Fluid Dynamics
<b>CHP</b>	Combined Heat & Power
<b>D.C</b>	Direct Current
<b>DG</b>	Distributed Generation
<b>DSM</b>	Demand Side Management
<b>EWTEC</b>	European Wave & Tidal Energy Conference
<b>FREDS</b>	Forum for Renewable Energy Development in Scotland
<b>GSP</b>	Grid Supply Point
<b>GSP</b>	Grid Supply Point
<b>HAWT</b>	Horizontal Axis Wind Turbine
<b>HV</b>	High Voltage
<b>HW</b>	High Water
<b>LV</b>	Low Voltage
<b>LW</b>	Low Water
<b>MCT</b>	Marine Current Turbine
<b>MEG</b>	Marine Energy Group
<b>MOD</b>	Ministry of Defence
<b>OWC</b>	Oscillating Water Column
<b>POL</b>	Proudman Laboratory Method
<b>PV</b>	Photo Voltaic
<b>RET's</b>	Renewable Energy Technologies
<b>RO</b>	Renewables Obligation
<b>ROC</b>	Renewables Obligations Certificate
<b>ROS</b>	Renewables Obligations Scotland
<b>SWAG</b>	Skye Windfarm Action Group

## References

1. FREDS. 2004, '2004 Harnessing Scotland's Marine Energy Potential', *Marine Energy Group (MEG) Report 2004*, pp.9
2. Sinden, G. 2005, 'Wave, wind, sun and tide is a powerful mix', *The Guardian*, Thursday 12<sup>th</sup> May
3. Department of Trade and Industry 2005,  
Available at: [http://www.dti.gov.uk/renewables/renew\\_1.1.htm](http://www.dti.gov.uk/renewables/renew_1.1.htm)
4. OECD IEA 2004, 'Renewable Energy and Electricity, Nuclear Energy Briefings Paper, Case Study; Denmark'  
Available at: <http://www.uic.com.au/nip38.htm>
5. BBC. 2005, 'Skye wind farm to be reconsidered',  
Available at:  
[http://news.bbc.co.uk/2/hi/uk\\_news/scotland/4577053.stm](http://news.bbc.co.uk/2/hi/uk_news/scotland/4577053.stm)
6. SWAG. 2005, 'The Benefits and Disadvantages'  
Available at: <http://www.sw-ag.org/the-pros-and-cons.html>
7. Scottish Parliament Business Committee, Enterprise and Culture Committee 2005 'Evidence Received for Renewable Energy in Scotland inquiry (10<sup>th</sup> Feb 2004)'  
Available at:  
<http://www.scottish.parliament.uk/business/committees/enterprise/inquiries/rei/ec04-reis-brown,mrwilliam.htm>
8. Dodge, DM. 1995, 'Illustrated History of Wind Power Development', Part 5 The Future of Wind Power  
Available at: <http://telosnet.com/wind/future.html>
9. The New Scientist. 16 May and 20 June 1998, Professional Engineering 10 June 1998, 'Renewable Energy, Sep-Dec 1996, vol. 9 No. 1-4, pp.870-874
10. Love, S., Agbeko, K., Fitzpatrick, S. 2004 'Marine Power Group Project 2004/05', PgDip., University of Strathclyde  
Available at:

[http://www.esru.strath.ac.uk/EandE/Web\\_sites/04-05/marine/index.html](http://www.esru.strath.ac.uk/EandE/Web_sites/04-05/marine/index.html)

11. University of St. Andrews. 2003, 'Awards for University's 'Ground-Breaking' Research'  
Available at:  
[http://calvin.standrews.ac.uk/external\\_relations/news\\_article.cfm?reference=428](http://calvin.standrews.ac.uk/external_relations/news_article.cfm?reference=428)
12. Scottish Executive 2002, Scottish Coastal forum Dec 2002, Section 2.2,  
Available at:  
<http://www.scotland.gov.uk/environment/coastalforum/powerpaper.pdf>
13. Scottish Executive. 2005, 'Marine Energy Group (MEG) Report'  
Available at:  
<http://www.scotland.gov.uk/Resource/Doc/1086/0006191.pdf>
14. EC Joule II. 1996, 'The Exploitation Of Tidal /Marine Currents'
15. Microhydropower. 2005, 'Micro hydro Definitions'  
Available at: <http://microhydropower.net/size.php>
16. IEE. 1996, 'AC & DC Power Transmission', Conference Publication no. 423
17. House of Commons Select Committee on Science and Technology. 2005
18. OFGEM. 2005,  
Available at:  
[http://www.ofgem.gov.uk/temp/ofgem/cache/cmsattach/41\\_27sep01\\_pub.pdf](http://www.ofgem.gov.uk/temp/ofgem/cache/cmsattach/41_27sep01_pub.pdf)
19. RETScreen International. 2005  
Available at: <http://www.retscreen.net/ang/default.asp>
20. NREL. 2005,  
Available at: <http://www.nrel.gov/homer/default.asp>
21. Energy Systems Research Unit, University of Strathclyde. 2005,  
Available at: <http://www.esru.strath.ac.uk>

22. Washington State Department of Ecology. 2005, 'Glossary of Coastal Terminology,  
Available at:  
[www.ecy.wa.gov/programs/sea/swces/products/publications/glossary/words/S\\_T.htm](http://www.ecy.wa.gov/programs/sea/swces/products/publications/glossary/words/S_T.htm)
23. British Wind Energy Association. 2005,  
Available at: <http://www.bwea.com/marine/devices.htm>
24. Johnstone, C M., Clarke J A., Grant A D 2005, 'Regulating the Output Characteristics of Tidal Current Power Stations to Facilitate Better Base Load Matching Over the Lunar Cycle', Renewable Energy, Vol 31, Issue 2, pp 173-180, Elsevier Science Ltd, February 2006. ISSN: 0960-1481.
25. Oceans Online. 2005,  
Available at: <http://www.oceansonline.com/tides.htm>
26. Proudman Oceanographic Laboratory. 2005, 'Insight into marine science',  
Available at: <http://www.pol.ac.uk/home/insight/tideinfo.html>
27. Supergen Marine Consortium. 2005, 'An Appraisal of a Range of Fluid Modelling Software'  
Available at:  
<http://www.supergen-marine.org.uk/download.php?view.12>
28. Proudman Oceanographic Laboratory. 2005, 'Tides questions and answers'  
Available at: <http://www.nbi.ac.uk/home/insight/tidefaq.html>
29. Admiralty Tide Tables NP 201-06 2001 and The Macmillan Reeds Nautical Almanac 2001.
30. Akwensivie, F., Chandra, P., McAlister, C., Murray, R., Sullivan, N., 2004, 'Marine Power Group Project 2003/04, PgDip., University of Strathclyde  
Available at:  
[http://www.esru.strath.ac.uk/EandE/Web\\_sites/03-04/marine/Resource\\_Map\\_2.htm](http://www.esru.strath.ac.uk/EandE/Web_sites/03-04/marine/Resource_Map_2.htm)
31. Fraenkel, P L. 2002, 'Power from Marine Currents'

Proceedings of the I MECH E Part A Journal of Power and Energy,  
Volume 216, Number 1, 1 February 2002

32. Napier University, Edinburgh. 2004 'Islay Case Study'  
Available from:  
[www.napier.ac.uk/depts/eri/Downloads/ArgApp7.pdf](http://www.napier.ac.uk/depts/eri/Downloads/ArgApp7.pdf))
33. Ileach, The Independent Newspaper for Islay and Jura. 2004,  
Available from: <http://www.ileach.co.uk/faq/>
34. Department of Trade & Industry. 2005, 'Review of State of the Art for Marine Renewables',  
Available from:  
[http://www.dti.gov.uk/NewReview/nr43/html/state\\_of\\_the\\_art.html](http://www.dti.gov.uk/NewReview/nr43/html/state_of_the_art.html)
35. Pugh, D T. 1987, Tides, Surges and Mean Sea-Level; A Handbook for Engineers and Scientists, Wiley, Chichester
36. Godin G. 1972, 'The Analysis of Tides', University of Toronto Press, Buffalo.
37. Couch, S., BRYDEN, I.G., 2004, 'The Impact of Energy Extraction on Tidal Flow Development.', Supergen Marine Marec Paper: 2004  
Available from:  
[http://www.supergen-marine.org.uk/documents/papers/Public/Resource%20Estimation/Marec\\_2004\\_Couch\\_Bryden.pdfv](http://www.supergen-marine.org.uk/documents/papers/Public/Resource%20Estimation/Marec_2004_Couch_Bryden.pdfv)
38. RSPB Energy. 2005, 'A quick guide to the Renewables Obligation',  
Available from:  
[www.rspbenergy.co.uk/popups/renewables\\_obligation.asp](http://www.rspbenergy.co.uk/popups/renewables_obligation.asp)
39. University of Michigan. 2005, 'Use of Manning's Equation for Measuring River Velocity',  
Available from:  
[http://www.cee.mtu.edu/peacecorps/resources/use\\_of\\_manning\\_equation\\_for\\_measuring\\_river\\_velocity.pdf#search=%22hydraulic%20radius%20manning%20coefficient%22](http://www.cee.mtu.edu/peacecorps/resources/use_of_manning_equation_for_measuring_river_velocity.pdf#search=%22hydraulic%20radius%20manning%20coefficient%22)
40. Larson, M. 2005 'Technical Data Sheet on Hydrodynamic Modelling', Available from:  
[http://homepage.mac.com/max.larson/Triton/download/TDS\\_Tide2D.pdf](http://homepage.mac.com/max.larson/Triton/download/TDS_Tide2D.pdf)